

The Pennsylvania State University  
The Graduate School

TOPICS IN BLACK HOLES AND QUANTUM COSMOLOGY

A Dissertation in  
Physics  
by  
Miguel Campiglia

© 2012 Miguel Campiglia

Submitted in Partial Fulfillment  
of the Requirements  
for the Degree of

Doctor of Philosophy

December 2012

The dissertation of Miguel Campiglia was reviewed and approved\* by the following:

Abhay Ashtekar  
Eberly Professor of Physics  
Dissertation Advisor, Chair of Committee

Martin Bojowald  
Professor of Physics

Murat Gunaydin  
Professor of Physics

Nigel Higson  
Professor of Mathematics

Richard Robinett  
Professor of Physics  
Director of Graduate Studies

\*Signatures are on file in the Graduate School.

# Abstract

Black holes and the big bang beginning of the universe are among the most spectacular predictions of general relativity, having a broad impact that ranges from observational astronomy to quantum gravity.

In this thesis we will focus on classical and quantum aspects of these subjects: In the first part we present a coordinate-free way of describing the approach to equilibrium of black holes within the framework of dynamical and isolated horizons. In the second part we focus on loop quantum cosmology. We present a uniqueness theorem of its kinematics, and explore the possible ways to implement its dynamics via path integrals.<sup>1</sup>

---

<sup>1</sup>The topics presented here form part of the research done during my PhD studies. See the Vita at the end of the Thesis for a complete list of my work during this period.

# Table of Contents

Acknowledgments	vi
<b>I Dynamical Horizons: Multipole Moments and Approach to Equilibrium</b>	<b>1</b>
<b>Chapter 1</b>	
<b>Introduction to quasi-local horizons</b>	<b>2</b>
1.1 Introduction . . . . .	2
1.2 Isolated and Dynamical Horizons . . . . .	5
1.2.1 Marginally trapped surfaces and tubes . . . . .	6
1.2.2 NEHs and IHs . . . . .	8
1.2.3 Dynamical Horizons . . . . .	12
<b>Chapter 2</b>	
<b>Multipole moments of DHs and Approach to equilibrium</b>	<b>16</b>
2.1 Dynamical to Isolated transition . . . . .	16
2.2 Multipole moments for Dynamical Horizons . . . . .	19
2.2.1 Balance laws for Multipole moments . . . . .	23
2.2.2 Relation with other approaches . . . . .	26
2.3 Discussion . . . . .	28
2.A Appendix: Limiting behavior at $S_0$ . . . . .	29
2.A.1 Limit to $S_0$ of the constraint equations . . . . .	31
2.A.2 Divergence of $K$ at $S_0$ . . . . .	35

<b>II Loop Quantum Cosmology</b>	<b>36</b>
<b>Chapter 3</b>	
<b>Introduction to loop quantum cosmology</b>	<b>37</b>
<b>Chapter 4</b>	
<b>Kinematics: A uniqueness result</b>	<b>44</b>
4.1 Introduction . . . . .	44
4.2 Weyl algebra, PLFs, and invariance. . . . .	46
4.3 Uniqueness . . . . .	48
4.4 Discussion . . . . .	50
<b>Chapter 5</b>	
<b>Dynamics: Path Integral formulations</b>	<b>52</b>
5.1 Configuration space path integral . . . . .	55
5.2 Phase space path integral . . . . .	58
5.3 Saddle point approximation . . . . .	61
5.3.1 The Hamilton-Jacobi function $S _0$ . . . . .	62
5.3.2 $\det \delta^2 S _0$ and the WKB approximation . . . . .	66
5.3.3 Comparison with exact solution . . . . .	68
5.4 Discussion . . . . .	70
5.A Appendix: Path integrals for polymerized free particle . . . . .	72
5.A.1 Configuration space path integral . . . . .	74
5.A.2 Phase space path integral . . . . .	78
5.A.3 Saddle point approximation . . . . .	80
5.B Appendix: WKB approximation for constrained systems . . . . .	84
5.C Appendix: Exact Amplitude . . . . .	86
<b>Bibliography</b>	<b>89</b>

# Acknowledgments

The work described in this dissertation was supported by the NSF grant PHY 0854743, the Eberly research funds of Penn State, the Frymoyer Honors Scholarship and the Duncan Fellowship.

I wish to thank Abhay Ashtekar, for all the support and patience he had with me. He will remain as a role model in my scientific career.

I would like to thank all the people from the Institute for Gravitation and the Cosmos and the Physics department for whom I benefited from their teaching, discussions, and friendship. In particular: Ivan Agullo, Jeffery Berger, Martin Bojowald, Alejandro Corichi, Sreejith Ganesh Jaya, Murat Gunaydin, Nigel Higson, Adam Henderson, Mikhail Kagan, Alok Laddha, Bruce Langford, Guoxing Liu, Diego Menendez, Przemyslaw Malkiewicz, Ross Martin, William Nelson, Phil Peterman, Juan Reyes, Radu Roiban, Samir Shah, David Simpson, David Sloan, Jorge Sofo, Victor Taveras, Casey Tomlin, Artur Tsobanjan, Edward Wilson-Ewing and Nicolas Yunes. Infinite thanks to Randi Neshteruk and Kathy Smith who filled the institute with positive energy.

I must also thank the many friends outside of physics that made my life better at Penn State: Alex, Arseny, Bernardo, Daniel, Pasha, Roberto, Roni, Vitaly and all the people from the Latin American Graduate Student Association. Finally and most importantly, I thank Grace and my family for all their love and support.

*To my parents*

## Part I

# Dynamical Horizons: Multipole Moments and Approach to Equilibrium



# Introduction to quasi-local horizons

## 1.1 Introduction

The first level understanding of black holes (BHs) comes from the study of the stationary solutions of vacuum general relativity (GR), the so-called Kerr family, describing a BH with given mass and angular momentum [1].

Going beyond the stationary case requires either perturbative schemes or numerical techniques. For instance, the study of the linearized Einstein's equations around the Kerr spacetime leads to the notion of ringdown modes and a first indication that this solution represents the final equilibrium state of a dynamical BH [2]. Fully dynamical situations are mostly accessible through numerical simulations. Of special interest, due to the potential detection of emitted gravitational waves, is the study of black hole mergers, a problem that has been fully addressed over the past decade [3, 4].

Part of the challenge in understanding the non-linear dynamics of BHs through numerical relativity comes from the well known fact that in GR there is no a priori background geometry or 'reference frame'. Thus, while in practice numerical simulations are performed in particular coordinate systems, one needs tools to extract meaningful invariant information. In this respect, dynamical and isolated horizons have proven to be powerful notions for the very basic task of identifying BHs with quasi-locally defined surfaces [5].

Numerical simulations show how these surfaces have a time-dependent shape that eventually settles down to a Kerr horizon, see for instance Refs. [6, 7, 8]. The

details of this process however remain poorly understood. One of the difficulties again lies on how to describe the phenomena in an invariant manner, thus distinguishing real physics from so-called coordinate or gauge effects. Our objective in this first part of the thesis will be to provide a framework that allows one to describe, in an invariant manner, how the geometry of these surfaces evolve to the final Kerr equilibrium.

We now introduce some of the concepts we will work with through what possibly is the simplest dynamical BH: The Vaidya spacetime. In terms of ingoing Eddington-Finkelstein coordinates, the Vaidya spacetime metric reads [9]:

$$ds^2 = - \left( 1 - \frac{2GM(v)}{r} \right) dv^2 + 2dvdr + r^2 d\Omega^2, \quad (1.1)$$

which for  $M(v) = \text{const.} > 0$ , reduces to the Schwarzschild spacetime (i.e., zero angular momentum Kerr). For general  $M(v)$ , Einstein's equations are satisfied provided the spacetime contains a stress-energy tensor given by

$$T_{ab} = \frac{\dot{M}(v)}{4\pi r^2} \nabla_a v \nabla_b v, \quad (1.2)$$

representing a spherical shell of null dust falling from infinity to the center. Positivity of the dust energy density imposes  $\dot{M} \geq 0$ . To make the following discussion concrete, consider a smooth  $M(v)$  such that  $\dot{M}$  vanishes everywhere except when  $v \in (0, v_0)$ , with,

$$M(v) = \begin{cases} 0 & \text{for } v < 0 \\ M_0 & \text{for } v > v_0. \end{cases} \quad (1.3)$$

Thus the metric represents an initially empty Minkowski space in which a BH is formed due to the gravitational collapse of infalling null dust, grows during  $v \in (0, v_0)$  reaching equilibrium at  $v = v_0$ , after which the spacetime is given by a Schwarzschild BH of mass  $M_0$ .

One of the characteristic signatures of BHs is the existence of an event horizon (EH): A three dimensional null surface enclosing the spacetime region from which no signal can ever escape. In the present example, the EH can be obtained by integrating backwards in time the family of null geodesics on the  $r = 2GM_0$ ,  $v > v_0$  null surface [9]. By its definition, the EH depends on the total spacetime

history, and thus may not reflect the local properties of the regions it goes through. For instance, in the example under discussion, the EH is present all the way to the  $v < 0$  Minkowski region [5] as illustrated in Fig. 1.1.

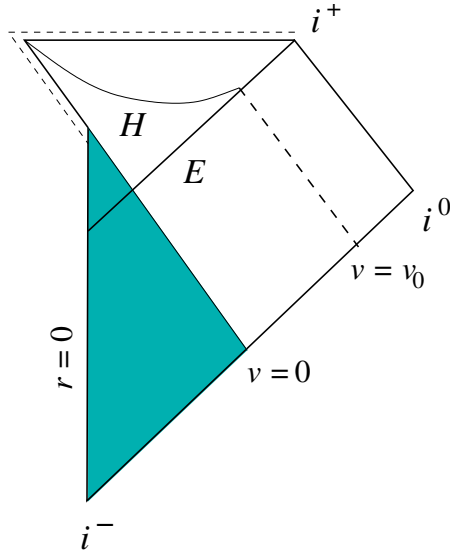


**Figure 1.1.** Penrose diagram of Vaidya metric (1.1) with mass function (1.3) [10]. The spacetime metric is flat in the shaded region. The event horizon is the 45 degree line indicated by  $E$ . It grows in the flat region in ‘anticipation’ of the collapse. The marginally trapped tube is denoted by  $H$ . It is space-like during the collapse, and after  $v_0$  becomes null and coincides with the event horizon. Figure taken from [5].

The alternative and quasi-local characterization of BHs is provided by marginally trapped tubes: Worldtubes of surfaces that represent a boundary between trapped and untrapped surfaces [11]. In stationary spacetimes, they coincide with the EH, but otherwise are distinct. In our example, this boundary is given by the surface  $C := M(v) - r/(2G) = 0$ , (denoted by  $H$  in the figure) thus representing the worldtube of ‘instantaneous’ Schwarzschild horizons. This surface is determined by the local geometry: It is formed at  $v = 0$  as the matter starts infalling, and grows until  $v = v_0$ , after which it coincides with the EH (see figure). The signature of this boundary, determined by,  $g^{ab}\nabla_a C \nabla_a C|_{C=0} = -\dot{M}$ , is either space-like ( $\dot{M} > 0$ ) or null ( $\dot{M} = 0$ ). Thus in the dynamical region the local boundary is a spatial hypersurface while it becomes null when equilibrium is reached.

This notion of local horizons extend to generic situations where no symmetries are present, sharing several of the features of our example. In particular, during the dynamical stages they are given by space-like hypersurface, whereas the

equilibrium stage is described by a null hypersurface. These are respectively the notions of dynamical and isolated horizons we will review in the next section.

Describing the local horizon beyond the spherically symmetric case is however more involved, as one needs to take into account all possible distortions on the MTSs, as well as its local rotation. Here is where the notion of multipole moments comes into picture.

Multipole moments for local horizons were introduced in the isolated case in [12]. They provide a diffeomorphism invariant characterization of the horizon geometry. Furthermore they have a physical interpretation of mass and angular momentum multipoles moments, in an analogy with charge and current multipole moments of classical electrodynamics. In the electrodynamics case, a localized charge and current distribution, can be characterized by its multipole moments. These description in turn facilitates the reconstruction of the electromagnetic field outside the source: The *source multipole moments* determine, via field equations, the *field multipole moments*, which characterize the  $1/r$  expansion of fields, where  $r$  is the distance to the source. Although such straightforward picture is not available in the non-linear regime of GR we are interested in, there exists numerical evidence for correlations between the horizon dynamics and the radiation at infinity [13, 14]. One of the ingredients needed to further explore such correlations is the availability of an unambiguous notion of multipole moments for dynamical horizons.

Our aim will be to extend the notion of multipole moments from isolated to dynamical horizons. This will provide a framework to invariantly describe the evolving geometry of dynamical horizons, and a tool for studying the physics of numerically evolved BHs.

## 1.2 Isolated and Dynamical Horizons

Isolated and Dynamical Horizons have quite distinct geometrical descriptions, as they involve null and space-like hypersurfaces respectively. A common feature however is that they are both foliated by marginally trapped surfaces. Since we will be eventually interested in the issue of the transition from a dynamical to isolated horizon, we will make use of a description in terms of these marginally trapped surfaces. Throughout our presentation, we will be dealing with submanifolds of

a four dimensional space time, on which Einstein's equations and the dominant energy condition hold. The discussion is mostly based on Refs. [5, 15, 16, 17].

*Notation:* Metric, connection, and curvature of spacetime:  $(g_{ab}, \nabla, R_{abcd})$ ; of three-dimensional space-like hyper surface:  $(h_{ab}, \mathcal{D}, {}^{(3)}\mathcal{R}_{abcd})$ ; of two-dimensional space-like surface:  $(q_{ab}, D, \mathcal{R})$ . Area radius  $R$  of a two-sphere  $S$  is defined by  $4\pi R^2 = \int_S d^2V$ . The action of a vector field  $X^a$  on a function  $f$  is denoted by  $X(f) = X^a \partial_a f$ .

### 1.2.1 Marginally trapped surfaces and tubes

Consider a closed space-like 2-surface  $S$ , with sphere topology, in four dimensional spacetime. We denote by  $q_{ab}$  and  $D$  the induced metric and its derivative operator on  $S$ .

The normal tangent space at each point of  $S$  is given by a Lorentzian two-dimensional plane. The extrinsic curvature of  $S$  refers to the change of this plane as we move along  $S$ . For our purposes it is useful to encode this information by referring to a null basis in the normal plane. Let  $\ell^a$  and  $n^a$  be future directed outgoing and ingoing normal null vectors such that  $\ell \cdot n = -2$ ,<sup>1</sup> and define the following fields on  $S$ :

$$\frac{1}{2}\theta_\ell q_{ab} + \sigma_{ab}^\ell := q_a^c q_b^d \nabla_c \ell_d \quad (1.4)$$

$$\frac{1}{2}\theta_n q_{ab} + \sigma_{ab}^n := q_a^c q_b^d \nabla_c n_d \quad (1.5)$$

$$\omega_a := -\frac{1}{2}q_a^b n_c \nabla_b \ell^c, \quad (1.6)$$

where the first two equations refer to a trace/trace-free part decomposition. The trace-free tensors  $\sigma_{ab}$ , referred to as shears, are symmetric by virtue of the surface forming property of the null normals. The traces  $\theta$  are referred to as expansions.  $\omega_a$  represents a connection one-form associated to the normal bundle of  $S$ . For simplicity, we will not display its dependence on the choice of null normals.

---

<sup>1</sup>This normalization, geared towards DHs and used in [17], differs from the  $\ell \cdot n = -1$  normalization used in [15, 16]. Our formulas will then have some different numerical factors with respect to these two references.

Given a different set of future directed null normals  $\ell'^a$  and  $n'^a$ , they will always be related to the first ones by a local boost:

$$\begin{aligned}\ell'^a &= f\ell^a \\ n'^a &= f^{-1}n^a,\end{aligned}\tag{1.7}$$

for some function  $f > 0$ . The expansions and shears relate to each other by the same multiplicative functions, whereas the normal connection transforms as

$$\omega'_a = \omega_a + D_a \ln f.\tag{1.8}$$

If we think of the surface  $S$  as an instantaneous shell of light, then  $n^a$  and  $\ell^a$  represent the direction of the light rays going inside and outside the surface. In regions of low curvature,  $\theta_n < 0$  and  $\theta_\ell > 0$ , meaning the light shells are respectively contracting and expanding, as one would normally envisage such situation. In strong curvature regimes however, it is possible for both expansions to be negative. Such is the situation inside BHs. The limit case when  $\theta_n < 0$  and  $\theta_\ell = 0$  is referred to as marginally trapped surface (MTS). The notions of BH boundary we will introduce refer to world tubes of these MTSs.

Consider then a three dimensional hypersurface  $H$ , of topology  $S^2 \times \mathbb{R}$ , such that it is foliated by MTSs. Let  $V^a$  be a vector tangent to  $H$  and orthogonal to the foliation. We will be interested in ‘future oriented tubes’ [15], for which  $V^a$  can be written as

$$V^a = \ell^a - B n^a\tag{1.9}$$

for some choice of null normals and some function  $B$ . Since  $\theta_\ell = 0$  everywhere on  $H$ , it follows that  $V(\theta_\ell) = 0$  so that

$$\ell(\theta_\ell) = B n(\theta_\ell).\tag{1.10}$$

Let us now extend  $\ell^a$  off  $H$  by a null geodesic congruence. The Raychaudhuri equation evaluated at a point in the MTS, where  $\theta_\ell = 0$ , becomes

$$\ell(\theta_\ell) = -|\sigma^\ell|^2 - R_{ab}\ell^a\ell^b.\tag{1.11}$$

Einstein's equations and the weak energy condition imply that the RHS of (1.11) is non-positive. Substituting the LHS by (1.10) we obtain the inequality

$$B n(\theta_\ell) \leq 0. \quad (1.12)$$

If the surfaces immediately inside  $S$  are trapped (this was the motivation for considering MTSs), then  $n(\theta_\ell) < 0$  which implies  $B \geq 0$ . Since  $V \cdot V = B$  we learn that  $H$  can be either space-like ( $B > 0$ ) or null ( $B = 0$ ). These are in fact the only two possibilities, as shown for instance in [15]. The first case corresponds to a DH, whereas the second to a non-expanding horizon (NEH). Finally, since  $\theta_{(V)} = -B\theta_n \geq 0$  we conclude that the area of the cross sections increases for DHs and remains constant for NEHs. In these considerations we have assumed the weak energy condition. If the energy condition were violated, as can be the case in the presence of quantum fields, the RHS of (1.11) could be positive leading to a time-like tube with decreasing area. This is what happens in the process of BH evaporation by Hawking radiation [18].

We will now discuss the null and space-like cases separately.

### 1.2.2 NEHs and IHs

The first thing to notice in the null case is that  $\ell(\theta_\ell) = 0$ , which by equation (1.11) implies  $\sigma_{ab}^\ell = 0$  and  $R_{ab}\ell^a\ell^b = 0$ . The vanishing of the expansion and shear of  $\ell^a$  is equivalent to

$$\mathcal{L}_\ell q_{ab} = 0 \quad (1.13)$$

and so the metric is 'time independent'.  $R_{ab}\ell^a\ell^b = 0$  implies, by Einstein's equations and the energy condition, that  $T_{ab}\ell^b = \propto \ell_a$ . This means that the matter energy flux associated to the vector field  $\ell^a$  is parallel to the horizon and so there is no energy flux going across the horizon.

From the fact that  $H$  is null, it follows that  $\ell$  is geodesic [1],

$$\ell^b \nabla_b \ell^a = \kappa_\ell \ell^a, \quad (1.14)$$

where  $\kappa_\ell$ , called surface gravity, plays the role of BH temperature in the thermodynamical interpretation [19]. So far nothing ensures that  $\kappa_\ell$  is a constant, and

so a general NEH will not represent a BH in equilibrium. Notice however that  $\kappa_\ell$  depends on the choice of null normal. Under the rescaling (1.7), it transforms as

$$\kappa_{\ell'} = f\kappa_\ell + \ell(f). \quad (1.15)$$

In particular one can choose the null normal so that  $\kappa_\ell$  is constant [16]. Incidentally, this implies that the normal connection is time-independent, as follows from the following identity of NEHs [16],

$$\mathcal{L}_\ell \omega_a = D_a \kappa_\ell. \quad (1.16)$$

The condition of  $\kappa_\ell$  being constant does not however uniquely fix  $\ell^a$ . In [16] it is shown that, on generic NEH,<sup>2</sup> the additional condition  $\ell(\theta_n) = 0$  uniquely fixes a preferred null normal (up to constant rescalings). Thus, under generic conditions, every NEH has a preferred null normal (up to a multiplicative constant) obeying  $\mathcal{L}_\ell \omega_a = 0$  and  $\ell(\theta_n) = 0$ . Such a horizon will have a ‘time independent’ geometry except possibly for the components of the extrinsic geometry encoded in  $\sigma_{ab}^n$  to which no condition has yet been imposed. When  $\sigma_{ab}^n$  is ‘time-independent’ the NEH is said to be an isolated horizon (IH). To summarize, an IH is a NEH with a preferred null normal  $\ell^a$  which Lie-drags *all* extrinsic curvature components (1.5,1.6).

*Note:* We have presented the concepts of NEH and IH using the auxiliary structure of a foliation, in order to ease the transition to the next section. The actual definitions of NEH and IH do not however refer to any foliation but directly deal with the geometry of the null hypersurface. There, the objects of relevance are, besides the null normal  $\ell^a$ , a degenerate metric of signature  $(0, +, +)$  and a connection  $\mathcal{D}^{\text{IH}}$  compatible with the metric (which is induced on the IH by the spacetime connection). The fields  $\omega_a$ ,  $\theta_n$  and  $\sigma_{ab}^n$  from our presentation encode the information of the connection  $\mathcal{D}^{\text{IH}}$ , and the IH requirement translates into the condition  $[\mathcal{L}_\ell, \mathcal{D}^{\text{IH}}] = 0$ .

Let us conclude by mentioning that IHs can be used as space-time boundaries in a canonical description of general relativity. Among other things, the framework allows for a derivation of the BH mechanics equations [20], extending the

---

<sup>2</sup>A generic NEH is one where the operator given in equation (2.57) is invertible, see [16].



classical results available for BH spacetimes. It also provides a classical setup for the construction of quantum black holes [21].

### 1.2.2.1 Geometric characterization of Isolated Horizons

Isolated horizons are fully characterized by: The preferred null normal  $\ell^a$  (up to constant rescaling), the null metric encoded in  $q_{ab}$ , and the compatible connection  $\mathcal{D}^{\text{IH}}$  encoded in  $\omega_a$ ,  $\theta_n$  and  $\sigma_{ab}^n$  (there can be in addition matter fields, but for simplicity we will restrict to the vacuum case). Einstein's equations imposes constraints among these fields and it is possible to isolate the free data that fully determines the horizon geometry [16]. The analysis is divided into extremal and non-extremal cases, defined by  $\kappa = 0$  and  $\kappa > 0$  respectively.<sup>3</sup> In what follows we focus on the non-extremal case.

When  $\kappa > 0$ , one can use Einstein's equations to express  $\sigma_{ab}^n$  and  $\theta_n$  in terms of  $q_{ab}$  and  $w_a$  [16]. Furthermore, the gauge invariant information of the 2-metric and the normal connection are encoded in the scalar curvature  $\mathcal{R}$  and in  $\epsilon^{ab}D_a\omega_b$  respectively. These two quantities in turn determine the so-called Newman-Penrose scalar  $\Psi_2$  at the horizon according to [16]:

$$\Psi_2 = \frac{\mathcal{R}}{4} + \frac{i}{2}\epsilon^{ab}D_a\omega_b. \quad (1.17)$$

In the next section we will define multipole moments for  $\Psi_2$ , providing a diff-invariant characterization of the IH geometry.

The situation in the extremal case is essentially the opposite: There,  $\sigma_{ab}^n$  and  $\theta_n$  are undetermined and thus constitute free data. In addition, there are constraints among the normal connection and the two dimensional geometry that, at least in the axisymmetric case, fully determines them [22].

### 1.2.2.2 Multipole moments for axisymmetric Isolated Horizons

In the presence of axisymmetry, it is possible to characterize the function  $\Psi_2$  in terms of diff-invariant multipole moments [12]. Let us briefly review the construc-

---

<sup>3</sup>Since on IHs there is no canonical normalization for  $\ell^a$ , the only invariant information contained in  $\kappa$  is its sign (either positive or zero). This should be contrasted with the situation on Killing horizons, where the vector field at infinity fixes the normalization and thus  $\kappa$  possess an invariant meaning.

tion.

Consider a cross section  $S$  of the IH. The axisymmetry of the IH implies the two dimensional metric  $q_{ab}$  posses a Killing vector field  $\varphi^a$ . The vector field in particular preserves the area two-form  $\epsilon_{ab}$  and so can be written as

$$\varphi^a = R^2 \epsilon^{ab} D_b z \quad (1.18)$$

for some function  $z : S \rightarrow \mathbb{R}$ . Equation (1.18) determines  $z$  up to an additive constant, which is fixed by requiring  $\int_S z d^2V = 0$ . One can further show that  $z$  is monotonically increasing from one pole to the other, and its range is  $[-1, 1]$ . Together with an affine parameter  $\phi$  of  $\varphi^a$ , one obtains a canonical (up to a global rotation) coordinate system  $(z, \phi)$  on  $S$ , in terms of which the metric takes the form

$$q_{ab} dx^a dx^b = R^2 (f^{-1} dz^2 + f d\phi^2), \quad (1.19)$$

with  $f = f(z)$  such that  $f(\pm 1) = 0$  and  $f'(\pm 1) = \mp 2$ . The scalar curvature is then given by

$$\mathcal{R}(z, \phi) = -\frac{f''(z)}{R^2}. \quad (1.20)$$

As an example and for later reference, for the Kerr horizon of parameters  $a$  and  $r$  (where the angular momentum is proportional to  $a \in [0, r]$ , and  $R^2 = r^2 + a^2$ ), the metric  $q_{ab}$  is given by the function

$$f_a(z) := \frac{(r^2 + a^2)}{r^2 + a^2 z^2} (1 - z^2). \quad (1.21)$$

In particular  $f_{a=0}(z) = (1 - z^2)$  represents the round sphere metric, where usual spherical coordinates are recovered by setting  $z = \cos \theta$ .

Given the axisymmetric metric  $q_{ab}$  on  $S$ , using  $z$  and  $\phi$  one can construct a canonical fiducial round metric by

$$\mathring{q}_{ab} dx^a dx^b := R^2 (f_0^{-1} dz^2 + f_0 d\phi^2). \quad (1.22)$$

Its corresponding spherical harmonics  $Y_{lm}$  are the ones used as weighting functions to define the multipole moments. Because of axisymmetry, only the  $m = 0$

moments are non-zero. They are defined as

$$\begin{aligned} I_l &:= \frac{1}{4} \int_S \mathcal{R} Y_{l0} d^2V = \int_S \text{Re} \Psi_2 Y_{l0} d^2V, \\ L_l &:= -\frac{1}{2} \int_S \omega_a \epsilon^{ab} D_b Y_{l0} d^2V = - \int_S \text{Im} \Psi_2 Y_{l0} d^2V, \end{aligned} \quad (1.23)$$

corresponding to the decomposition

$$\Psi_2 = \frac{1}{R^2} \sum_{l=0}^{\infty} (I_l - iL_l) Y_{l0}. \quad (1.24)$$

Summarizing, the geometric multipole moments (1.23) are constructed using the structure available from the axisymmetry, providing a set of diff-invariant quantities that fully characterize horizon geometry (see [12] for the explicit reconstruction of the IH geometry from a given set of multipole moments).

The geometric moments (1.23) can also be used to define ‘mass’ and ‘angular momentum’ multipoles in an analogy with charge and current multipoles of electromagnetism [12]:

$$\begin{aligned} J_l &= \sqrt{\frac{4\pi}{2l+1} \frac{R^{l+1}}{4\pi G}} L_l, \\ M_l &= \sqrt{\frac{4\pi}{2l+1} \frac{MR^l}{2\pi}} I_l. \end{aligned} \quad (1.25)$$

The normalizations are such that  $J_1$  agrees with the angular momentum as defined by either the Komar integral or the Hamiltonian framework, and

$$M_0 = M := \frac{1}{2GR} \sqrt{R^4 + 4G^2 J_1^2} \quad (1.26)$$

reproduces the mass of a Kerr black hole of radius  $R$  and angular momentum  $J_1$ .

From their definitions it follows that the angular momentum monopole  $J_0$ , as well as the mass dipole  $M_1$  vanish. The first property implies that the IH does not have NUT charge, while in a Newtonian interpretation, the second implies one is working in the center of mass frame.

### 1.2.3 Dynamical Horizons

The case when the worldtube  $H$  of MTSs is space-like is known as a dynamical horizon [17]. Since  $H$  is space-like, it has a unit time-like normal  $\tau^a$  and its geometry is encoded in the metric  $h_{ab} = g_{ab} + \tau_a \tau_b$ , of signature  $(+, +, +)$ , and

extrinsic curvature  $K_{ab} := h_a^c h_b^d \nabla_c \tau_d$ . Einstein equations impose the hypersurface constraints:

$$H := 2G_{ab}\tau^a\tau^b = {}^{(3)}\mathcal{R} + K^2 - K^{ab}K_{ab} = 16\pi GT_{ab}\tau^a\tau^b \quad (1.27)$$

$$H^a := G_{bc}\tau^b h^{ab} = \mathcal{D}_b (K^{ab} - Kh^{ab}) = 8\pi GT^{bc}\tau_c h^a_b, \quad (1.28)$$

where  $G_{ab} = R_{ab} - 1/2Rg_{ab}$ ,  $\mathcal{D}$  is the connection of  $h_{ab}$ ,  ${}^{(3)}\mathcal{R}$  its scalar curvature and  $T_{ab}$  the stress-energy tensor.

The foliation by MTSs induces a ‘2+1’ splitting of  $H$ . Let  $r^a$  be the unit vector tangent to  $H$  and orthogonal to the foliation. The two dimensional metric  $q_{ab}$  on  $S$  is then related to the three-metric by

$$h_{ab} = q_{ab} + r_a r_b. \quad (1.29)$$

We will denote by  $\tilde{K}_{ab} := q_a^c q_b^d \mathcal{D}_c r_d$  the extrinsic curvature of  $S$  within  $H$ . Finally, we decompose the extrinsic curvature of  $H$  as

$$K_{ab} = Aq_{ab} + S_{ab} + 2\omega_{(a}r_{b)} + Br_a r_b, \quad (1.30)$$

where  $S_{ab}$  is parallel to  $S$  and trace-free, and  $\omega_a$  is parallel to  $S$ . In the language of Section 1.2.1, the vector  $\omega_a$  corresponds to the connection one-form (1.6) associated to the null normals

$$\begin{aligned} \ell^a &:= \tau^a + r^a, \\ n^a &:= \tau^a - r^a. \end{aligned} \quad (1.31)$$

The expansion of  $\ell$  is given by  $\theta_\ell = 2A + \tilde{K}$  where  $\tilde{K} = q^{ab}\tilde{K}_{ab}$  and so the marginally trapped condition translates into

$$A = -\tilde{K}/2. \quad (1.32)$$

As shown in [17], condition (1.32) has the surprising consequence that one of the hypersurface constraints involves only derivatives along  $S$ , and thus provides an ‘instantaneous’ constraint for each leaf  $S$ . The fields featuring this constraint

are the shear of  $\ell^a$ , which we will call by  $\sigma_{ab}$ , and the vector field

$$\zeta^a := q^{ab} r^c \nabla_c \ell_b = \omega^a + D^a \ln |dR|, \quad (1.33)$$

Here  $|dR|$  is the norm of the three-dimensional gradient of the area radius  $R$ , viewed as a function  $R : H \rightarrow \mathbb{R}$ . The constraint in question is

$$2G_{ab} \tau^a \ell^b = H + 2r_a H^a = \mathcal{R} - |\sigma|^2 - 2|\zeta|^2 + 2D \cdot \zeta = 16\pi G T_{ab} \tau^a \ell^b. \quad (1.34)$$

One of the remarkable implications of this equation is that, upon integration over  $S$  and using the Gauss-Bonnet theorem  $\int_S \mathcal{R} d^2V = 8\pi$ , it leads to,

$$\frac{1}{2G} = \int_S \left[ \frac{1}{16\pi G} (|\sigma|^2 + 2|\zeta|^2) + T_{ab} \tau^a \ell^b \right] d^2V. \quad (1.35)$$

All three terms in the integral are non-negative (the matter one due to the energy condition), and so this equation puts a bound on the total integral of the each individual term. We will later make use of this property. For now let us show how this equation can be used to obtain certain balance laws on the horizon. To be specific, let us look at the balance law for the Hawking mass, which for DHs is given by  $M_H = R/(2G)$  [17]. Performing the integral  $\int_{R_1}^{R_2} dR$  on both sides of (1.35) and using the identity  $d^3V = d^2V dR/|dR|$  one obtains,

$$\frac{R_2 - R_1}{2G} = \int_{\Delta H} |dR| T_{ab} \tau^a \ell^b d^3V + \frac{1}{16\pi G} \int_{\Delta H} |dR| (|\sigma|^2 + 2|\zeta|^2) d^3V. \quad (1.36)$$

The two integral on the right hand side, which are explicitly non-negative, can be interpreted as matter and gravitational energy fluxes respectively [17]. Similar balance laws can be obtained for other quantities of interest. From their infinitesimal version one can recover the usual laws of BH mechanics. A key difference with IHs is that these are ‘physical process’ laws, relating the same horizon at different times, whereas in the IH case one is comparing different IHs with infinitesimally close parameters.<sup>4</sup>

---

<sup>4</sup>Recall from Section 1.2.2 that the mechanic laws IHs obey are derived from a Hamiltonian framework, and relate nearby points of the infinite dimensional phase space of spacetimes with an IH boundary.

We conclude the section by recalling the balance law for angular momentum. In general, the notion of angular momentum is associated to the presence of axisymmetry. One can however have a generalized notion of angular momentum associated to any vector field  $\varphi^a$  that is tangent to the cross sections  $S$  and divergence-free thereon. It is defined by the same expression one would get in the presence of axisymmetry:

$$J_S^\varphi := -\frac{1}{8\pi G} \int_S K_{ab} \varphi^a r^b d^2V \quad (1.37)$$

$$= -\frac{1}{8\pi G} \int_S \omega_a \varphi^a d^2V, \quad (1.38)$$

where the second equality follows from the decomposition of the extrinsic curvature (1.30). The balance law for  $\Delta J^\varphi$  is obtained by using i) Stokes theorem to express the difference as an integral over the bounded volume  $\Delta H$ , and ii) the momentum constraint (1.28). The result is

$$\Delta J^\varphi = - \int_{\Delta H} T_{ab} \tau^a \varphi^b d^3V - \frac{1}{16\pi G} \int_{\Delta H} P^{ab} \mathcal{L}_\varphi h_{ab} d^3V \quad (1.39)$$

where  $P_{ab} = K_{ab} - K h_{ab}$ . The two integrals are respectively interpreted as matter and gravitational angular momentum fluxes. In particular the gravitational angular momentum flux vanishes when  $\varphi^a$  is Killing vector field of the intrinsic metric  $h_{ab}$  on  $H$ .

# Multipole moments of DHs and Approach to equilibrium

Having introduced both isolated and dynamical horizons, we now focus on the interface between the two concepts. Specifically, we will explore the passage from dynamical to isolated horizon, and use the final equilibrium state as a ‘reference frame’ with respect to which the evolving geometry of the DH can be described.

As discussed in the first chapter, the final equilibrium of dynamical black holes is given by a Kerr BH. In the context of IHS however, the Kerr family is one in many possible horizons. Its special status only comes when one considers the whole spacetime, or at least some region enclosing the horizon.

Our strategy will be to include this additional information and thus focus on DHs that settle to a final Kerr horizon.

We will first discuss the general issue of passage from dynamical to isolated horizon and then present the construction of multipole moments, which provide an invariant characterization of the settling process.

## 2.1 Dynamical to Isolated transition

As mentioned at the end of Section 1.2.1, one of the properties of marginally trapped tubes is that they have definite signature along each cross section [15]. This implies the transition from dynamical to isolated horizon occurs at an ‘instant’ surface  $S_0$ . This transition can either happen at finite time or be asymptotic.

Most of what follows applies to both cases, but for concreteness we will center the discussion in the case where the transition happens at ‘finite time’. Consider then a worldtube of MTSs  $M := H \cup \Delta$  consisting of the union of a dynamical horizon  $H$  and a non-expanding horizon  $\Delta$ . We will eventually be interested in the case where  $\Delta$  is a Kerr horizon, but the following discussion applies to general NEHs.<sup>1</sup> We will assume  $M$  and the spacetime metric to be smooth.

We fix once and for all a null normal  $\bar{\ell}^a$  of the NEH  $\Delta$  (in the IH case we may chose it to belong to the preferred class, but otherwise we leave it general). NEHs do not have an a priori foliation. In the present setting however, the initial surface  $S_0$  induces a foliation given by  $\bar{v} : \Delta \rightarrow [0, \infty)$  such that  $\bar{\ell}(\bar{v}) = 1$  and  $\bar{v} = 0$  on  $S_0$ . We will denote by  $\bar{n}^a$  the ingoing null normal orthogonal to the foliation such that  $\bar{\ell} \cdot \bar{n} = -2$ .

To study the transition  $H \rightarrow \Delta$ , we introduce a smooth foliation function  $v : M \rightarrow \mathbb{R}$  on the total horizon  $M$  such that it agrees with  $\bar{v}$  for  $v > 0$ . Thus,  $v = \text{constant} < 0$  gives the leaves of the DH,  $v = \text{constant} > 0$  gives the leaves of the NEH, and  $v = 0$  represents the transition surface  $S_0$ . The freedom in the choice of such foliation function is given by ‘time reparametrizations’: Given another choice  $w$ , there exists a smooth function  $f$  such that  $w = f(v)$ , with  $f(v) = v$  for  $v \geq 0$ . Our construction of multipole moments of Section 2.2 will be independent of this reparametrization freedom.

A foliation  $v$  uniquely determines a vector field  $V^a$  satisfying: i)  $V^a$  is tangent to  $M$  and orthogonal to the cross sections, ii)  $V(v) = 1$ . These conditions imply that  $V^a$  coincides with  $\bar{\ell}^a$  on  $\Delta$ , and so it represents a smooth extension of this vector field to  $H$ . On  $H$ ,  $V^a$  is proportional to  $r^a$ :

$$V^a = |dv|^{-1} r^a =: 2b r^a, \quad (2.1)$$

where for later convenience  $b$  is defined by

$$2b = |dv|^{-1} = \dot{R} |dR|^{-1}; \quad \dot{R} \equiv \frac{dR}{dv}, \quad (2.2)$$

---

<sup>1</sup>There could in principle be a situation where the equilibrium is reached in stages: first DH to NEH and then NEH to IH.



or equivalently

$$V \cdot V = 4b^2. \quad (2.3)$$

This last equation tells us that  $b$  smoothly vanishes at  $S_0$ . If  $b$  is used to rescale the null normals (1.31) according to

$$\bar{\ell}_H^a := b \ell^a \quad (2.4)$$

$$\bar{n}_H^a := b^{-1} n^a, \quad (2.5)$$

one obtains smooth extensions of the NEH null normals. This is seen by writing  $b \ell^a = V^a + b n^a$  in (2.4), which becomes  $\bar{\ell}^a$  at  $S_0$ . The ingoing null normal is then uniquely determined by the normalization condition  $\bar{\ell}_H \cdot \bar{n}_H = -2$ . From now on we drop the subscript  $H$  and denote by  $\bar{\ell}^a$  and  $\bar{n}^a$  the total vector fields on  $M$ .

The condition that at  $S_0$  we have a given NEH determines the limiting value of the shears, expansions and normal connection (1.4,1.4,1.6) of the null normals (2.4), (2.5).

Some of the conclusions that can be obtained about the transition are:

- $|\sigma|^2$  and  $T_{ab}\tau^a\ell^b$ , featuring in the energy flux formula (1.36), have finite limits at  $S_0$ . Furthermore, for generic  $\Delta$ ,  $|\sigma|^2$  and  $T_{ab}\tau^a\ell^b$  cannot simultaneously vanish at  $S_0$ . The energy flux in (1.36) still vanishes at  $S_0$  due to the  $|dR|$  factor.
- $b^2$  vanishes as  $\dot{R}$ . That is,

$$b_0 := \frac{b}{\sqrt{\dot{R}}} \quad (2.6)$$

is a well defined function on  $H$  admitting a regular non-vanishing limit to  $S_0$ . Furthermore, the limiting value  $b_0|_{v=0}$  is related to the limiting value of the divergence of  $\zeta^a$ .

- The trace of the extrinsic curvature diverges at  $S_0$ . In particular, the ‘constant mean curvature’ strategy for solving the constraint equations [23] cannot be applied to DHs approaching equilibrium.

We leave the proof of these properties to the appendix. As an example for the first two points, in the Vaidya collapse one has  $b_0 = 1/\sqrt{2}$  (with respect to the coordinate  $v$  of (1.1)) and  $8\pi GT_{ab}\ell^a\tau^b = 1/R^2$  [17].

## 2.2 Multipole moments for Dynamical Horizons

We saw in Section 1.2.2.2 how multipole moments of IHs provide a diff-invariant characterization of the horizon geometry. We would like to extend this notion to DHs, in order to have a framework to describe the approach to equilibrium in an invariant manner.

Here is where we want to use the additional information that the final equilibrium is given by a Kerr horizon. The only property of the Kerr horizon we will actually need however is its axisymmetry. Thus our setup will be as in the previous section, with a total horizon of the form  $M = H \cup \Delta$ , with  $\Delta$  an axisymmetric IH.

Let us first consider the situation where  $H$  is also axisymmetric (and hence the total horizon  $M$  is axisymmetric). In this case it is straightforward to extend the definition of IH multipole moments to DHs [7]: On each DH cross section  $S$ , the multipole moments are simply defined to be

$$\begin{aligned} I_l(S) &:= \frac{1}{4} \int_S \mathcal{R} Y_{l0} d^2V \\ L_l(S) &:= -\frac{1}{2} \int_S \omega_a \epsilon^{ab} D_b Y_{l0} d^2V, \end{aligned} \tag{2.7}$$

where the spherical harmonics are defined by reproducing the construction of section 1.2.2.2 on each cross section  $S$ . These functions will be generically ‘time dependent’ in the sense that they will depend on the cross section, and will smoothly match with the multipole moments of the IH  $\Delta$  at  $S_0$ .

Let us now go to the general case where  $H$  is not necessarily axisymmetric, but still with final axisymmetric  $\Delta$ . Since now there is no intrinsic structure on  $S$  that can be used to define the spherical harmonics, the strategy will be to bring down to  $S$  the spherical harmonics available at  $\Delta$ . A satisfactory construction should be such that:

1. It is diff-invariant: It does not depend on choices of auxiliary structures
2. It should reduce to (2.7), when  $H$  is axisymmetric
3. The DH multipole moments should smoothly match the IH ones at  $S_0$

How can this be achieved? In the axisymmetric case, the weighting functions  $Y(z)_{l0}$  are defined in terms of the ‘potential’  $z$  of the Killing vector field  $\varphi^a$ , Eq.

(1.18). The idea is to repeat this construction with respect to a vector field  $\varphi_H^a$  on  $H$  which may not be Killing, but still of the form

$$R^2 \epsilon^{ab} D_b z = \varphi_H^a, \quad (2.8)$$

for some function  $z$ . This vector field should be uniquely determined by the available structure (a DH  $H$  ending in an axisymmetric IH  $\Delta$ ) and should reproduce the Killing vector field whenever  $H$  is axisymmetric.

We will seek such  $\varphi_H^a$  by transporting the axisymmetric vector field  $\varphi_\Delta^a$  on  $\Delta$  to  $H$ . A first guess is to define it by the following conditions:

$$\mathcal{L}_V \varphi_H^a = 0 \quad (\text{tentative}) \quad (2.9)$$

$$\varphi_H^a = \varphi_\Delta^a \quad \text{on } \Delta, \quad (2.10)$$

with  $V^a$  given by (2.1). This definition has the following desirable properties:

i)  $\varphi_H^a$  is tangent to  $H$  since (2.9) implies  $\varphi_H(v)$  is constant, and by (2.10) this constant is zero.

ii)  $\varphi_H^a$  is independent of the chosen parametrization: Given a different parametrization  $w = f(v)$ , the corresponding vector field is given by  $W^a = \dot{f}^{-1} V^a$ , which in turn implies  $\mathcal{L}_V \varphi_H^a = 0 \iff \mathcal{L}_W \varphi_H^a = 0$ .

iii) If  $H$  is axisymmetric,  $\varphi_H^a$  coincides with the Killing vector field  $\varphi^a$ : Axisymmetry implies  $\mathcal{L}_\varphi V = 0$ , and so  $\varphi^a$  obeys (2.9). Since it also obeys (2.10), it follows that  $\varphi_H^a = \varphi^a$ .

This construction however is not satisfactory as it fails in a fourth fundamental requirement: It does not guarantee that  $D \cdot \varphi_H = 0$ , the condition needed to have a ‘potential’  $z$  (1.18). This can be fixed by adding an appropriately ‘shift’ to the vector field  $V^a$  used to transport  $\varphi_H^a$  from  $\Delta$  to  $H$ . Thus consider a vector field of the form

$$X^a = V^a + N^a, \quad (2.11)$$

with  $N^a$  tangent to  $S$ , and consider now  $\varphi_H^a$  defined as before but with  $X^a$  in place of  $V^a$ . Clearly property i) above still holds. We then need to find  $N^a$  such that properties ii), iii) and the additional condition iv)  $D \cdot \varphi_H = 0$ , are satisfied.

Let us focus on the fourth property. Recall the notion of divergence does not require knowledge of the total metric but only of the area element:  $\mathcal{L}_{\varphi_H}\epsilon_{ab} = (D \cdot \varphi_H)\epsilon_{ab}$ . Furthermore, the notion of vanishing divergence makes use of the area element up to global rescalings. Thus, if the change of  $\epsilon_{ab}$  along  $X^a$  is of the form  $\mathcal{L}_X\epsilon_{ab} = a(v)\epsilon_{ab}$  for some function  $a(v)$ , the divergence of  $\varphi_H^a$  will remain constant and thus will be zero since it vanishes on  $\Delta$ . The condition that the total integral of  $\epsilon_{ab}/R^2$  is constant determines  $a = 2\dot{R}/R$ . The required vector field  $X^a$  should then satisfy:

$$\mathcal{L}_X\epsilon_{ab} = 2\dot{R}/R\epsilon_{ab}, \quad \text{or,} \quad \mathcal{L}_X(\epsilon_{ab}/R^2) = 0. \quad (2.12)$$

The change in the area element along a vector field of the form (2.11) is given by

$$\mathcal{L}_X\epsilon_{ab} = (2b\tilde{K} + D \cdot N)\epsilon_{ab}, \quad (2.13)$$

where we used (2.1) and  $\mathcal{L}_r\epsilon_{ab} = \tilde{K}\epsilon_{ab}$ , with  $\tilde{K}$  the trace of the extrinsic curvature of  $S \subset H$  (see Section 1.2.3). Thus, by taking

$$N^a = D^a g, \quad (2.14)$$

with  $g$  satisfying

$$-\Delta g = 2\dot{R}/R - 2b\tilde{K}, \quad (2.15)$$

one obtains a vector field obeying (2.12). Note that, given  $v$ , this  $N^a$  is unique and its construction is diffeomorphism invariant.

This prescription satisfies ii), since under reparametrization,  $N^a$  transforms as  $V^a$ :

$$v \rightarrow f(v) \Rightarrow N^a \rightarrow \dot{f}^{-1}N^a. \quad (2.16)$$

Finally, if  $H$  is axisymmetric, then we are guaranteed to have  $\mathcal{L}_\varphi N^a = 0$ , whence property iii) will be satisfied. We thus have a successful candidate for  $\varphi_H^a$ . Let us now explore further consequences. First, one can verify that the function  $z$  defined by

$$\mathcal{L}_X z = 0; \quad z|_{v=0} = \text{“axisymmetric } z\text{” at } S_0 \quad (2.17)$$

is a potential for  $\varphi_H^a$  in the sense of Eq. (2.8), and so has the same properties as in  $\Delta$ : Integrates to zero on  $S$  and its range is  $[-1, 1]$ . The  $m = 0$  spherical harmonics

can then be defined in terms of this function. Since  $H$  is not axisymmetric, we will also need  $m \neq 0$  spherical harmonics to have the full geometric information. For this we need an affine parameter  $\phi$  of  $\varphi^a$ . It can be defined similarly as for  $z$  by

$$\mathcal{L}_X \phi = 0; \quad \phi|_{v=0} = \text{“axisymmetric } \phi\text{” at } S_0. \quad (2.18)$$

It then follows that the  $(z, \phi, v)$  provides a coordinate system for  $H$  such that  $X^a = (\partial/\partial v)^a$  and  $\varphi_H^a = (\partial/\partial \phi)^a$ . The weighting functions are then taken to be  $Y_{lm}(z, \phi)$ . Alternatively, these weighting functions correspond to the Laplacian eigenfunctions of a fiducial round metric on  $S$ , that is defined by Lie dragging along  $X^a$  the fiducial round metric on  $S_0$  (see Section 1.2.2.2).

Let us now summarize the construction. First, we chose a parametrization  $v$  and corresponding vector field  $V^a$  as in Section 2.1. We then defined  $X^a$  by equations (2.11),(2.14) and (2.15). Finally,  $\varphi_H^a$  is defined by

$$\mathcal{L}_X \varphi_H^a = 0 \quad (2.19)$$

$$\varphi_H^a = \varphi_\Delta^a \quad \text{on } \Delta. \quad (2.20)$$

The vector field  $\varphi_H^a$  so constructed is such that: i) Is tangent to  $S$ , ii) is independent of the choice of parametrization  $v$ , iii) reduces to the Killing vector field when  $H$  is axisymmetric, and iv) is divergence-free. Furthermore, its potential  $z$  is Lie dragged by  $X^a$ . The spherical harmonics on  $S$  are then given by  $Y_{lm}(z, \phi)$ , with  $\phi$  an affine parameter of  $\varphi_H^a$  given by (2.18).

Having found the appropriate weighting functions, we define the multipole moments by

$$I_{lm}(S) := \frac{1}{4} \int_S \mathcal{R} Y_{lm} d^2V, \quad (2.21)$$

$$L_{lm}(S) := -\frac{1}{2} \int_S \omega_a \epsilon^{ab} D_b Y_{lm} d^2V. \quad (2.22)$$

The construction satisfies the three properties listed at the beginning of the section. In addition it shares with the IH moments the property that  $L_0 = 0$ . On the other hand,  $I_1$  does not need to vanish, and thus they do not represent a local rest frame, if one is to think of this quantity as being proportional to the deviation from the

center of mass (see Section 1.2.2.2). This is compatible with the the interpretation that these are the multipoles from the perspective of the final equilibrium state, whose center of mass may have shifted.

Note that the above represent the analogues of the isolated horizon geometric moments (1.23). The so-called physical moments can be obtained by appropriate constant rescaling as in (1.25).

We now discuss possible balance laws for these multipole moments, and compare our construction with others available in the literature.

### 2.2.1 Balance laws for Multipole moments

In Section 1.2.3, we mentioned certain balance laws that hold on DHs. In particular we looked at a ‘mass’ (1.36) and angular momentum (1.39) balance laws expressing the change of these quantities in terms of fluxes across the horizon. We now seek for similar balance laws for the multipole moments introduced before.

We will for simplicity focus on the geometric moments (2.21), (2.22), but similar balance laws can be obtained for the physical moments by including the appropriate factors.

Let us start with the angular moments. We observe that expression (2.22) has the same form as the generalized angular momentum (1.38), with respect to the vector field

$$\varphi_{lm}^a := \epsilon^{ab} D_b Y_{lm}, \quad (2.23)$$

namely

$$L_{lm}(S) = 4\pi G J_S^{\varphi_{lm}}, \quad (2.24)$$

with  $J_S$  as defined in (1.38). Thus, up to a proportionality factor, the multipole moments (2.22) can be thought of as giving the generalized angular momenta corresponding to the divergence-free (in  $S$ ) vector fields (2.23). In particular, we can repeat the analysis leading to angular momentum balance law (1.39). Using (2.24) and (1.39), we obtain

$$L_{lm}^{S_2} - L_{lm}^{S_1} = - \int_{\Delta H} \left( 4\pi G T_{ab} \tau^a \varphi_{lm}^b + \frac{1}{4} P^{ab} \mathcal{L}_{\varphi_{lm}} h_{ab} \right) d^3V, \quad (2.25)$$

where  $\Delta H$  is the portion of  $H$  bounded by the two surfaces. The interpretation of

this equation is as before: The angular moments change in response of matter and geometric fluxes across the horizon, given by the first and second terms in (2.25) respectively. The fluxes depend on the order of the moment, and in particular they vanish for  $l = 0$ , which is consistent with the fact that  $L_0 = 0$ .

We now turn to the  $I_{lm}$  moments. Here we would like to proceed in a similar spirit as for the DH ‘mass’ balance law (1.36). In particular, we will seek to express the change in moments in terms of the energy fluxes featuring (1.36). Notice however that we are dealing with the geometric (rather than ‘physical’) moments. In particular  $I_0 = \sqrt{\pi} = \text{constant}$ . We start by writing the difference as

$$I_{lm}^{S_2} - I_{lm}^{S_1} = \int dR \frac{dI_{lm}}{dR}. \quad (2.26)$$

Now, let  $(\partial/\partial R)^a = \dot{R}^{-1}X^a$  be the vector field associated to the coordinate system  $(R, z, \phi)$ . We then have

$$\frac{dI_{lm}}{dR} = \frac{1}{4} \int_S \mathcal{L}_{\partial/\partial R}(\mathcal{R}Y_{lm}\epsilon_{ab}) \quad (2.27)$$

$$= \frac{1}{4} \int_S \left( \frac{2}{R} \mathcal{R} + \partial_R \mathcal{R} \right) Y_{lm} d^2V, \quad (2.28)$$

where we used  $\mathcal{L}_{\partial/\partial R}\epsilon_{ab} = \frac{2}{R}\epsilon_{ab}$  and  $\partial Y_{lm}/\partial R = 0$ . In order to bring in the flux terms, we use Eq. (1.34), to express  $\mathcal{R}$  in terms of the radiative quantities. Doing so for the first term in (2.28) we obtain,

$$\frac{dI_{lm}}{dR} = \frac{1}{2R} \int_S Y_{lm} (|\sigma|^2 + 2|\zeta|^2 + 16\pi GT_{ab}\tau^a\ell^b - 2D \cdot \zeta) d^2V + \frac{1}{4} \int_S Y_{lm} \partial_R \mathcal{R} d^2V. \quad (2.29)$$

We finally integrate over  $R$  and rearrange terms to obtain:

$$I_{lm}^{S_2} - I_{lm}^{S_1} = \int_{\Delta H} \frac{|dR|}{2R} (|\sigma|^2 + 2|\zeta|^2 + 16\pi GT_{ab}\tau^a\ell^b) Y_{lm} d^3V \quad (2.30)$$

$$+ \int_{\Delta H} |dR| \left( \frac{1}{4} Y_{lm} \partial_R \mathcal{R} + \frac{1}{R} \zeta(Y_{lm}) \right) d^3V, \quad (2.31)$$

where we collected in the first integral the contribution from the gravitational and matter flux-like terms, weighted by the  $Y_{lm}$  factors. The remaining terms, collected in the second integral, have a less immediate interpretation. Their presence is

however necessary, as can be seen by looking at the  $l = 0$  case, where they must cancel the positive contribution of the flux integral (recall  $I_0 = \text{constant}$ ).

We conclude by exploring an alternative expression for the change of the multipole moments which exhibits certain symmetry between both sets of moments.

We begin with the angular moments. Recall from the earlier discussion that they can be thought of as generalized angular momentum with respect to the vector field (2.23):

$$L_{lm} = -\frac{1}{2} \int_S \omega_a \varphi_{lm}^a d^2V. \quad (2.32)$$

The vector fields  $\varphi_{lm}^a$  form a basis in the space of divergence-free vector fields of  $S$ , and thus from (2.32) one can reconstruct the generalized angular momentum with respect to any divergence-free vector field.

We now focus on the rate of change of  $L_{lm}$  with respect to the parameter  $v$  of the previous section and write

$$\frac{dL_{lm}}{dv} = -\frac{1}{2} \int_S \mathcal{L}_X(\omega_c \varphi_{lm}^c \epsilon_{ab}), \quad (2.33)$$

$$= -\frac{1}{2} \int_S \mathcal{L}_X(\omega_c) \varphi_{lm}^c \epsilon_{ab} - \frac{1}{2} \int_S \omega_c \mathcal{L}_X(\varphi_{lm}^c \epsilon_{ab}). \quad (2.34)$$

The second term is vanishing, since

$$\varphi_{lm}^c \epsilon_{ab} = \epsilon^{cd} D_d Y_{lm} \epsilon_{ab} = (R^2 \epsilon^{cd})(D_d Y_{lm})(R^{-2} \epsilon_{ab}), \quad (2.35)$$

and each term in parenthesis is Lie dragged by  $X^a$ . We thus conclude that

$$\frac{dL_{lm}}{dv} = -\frac{1}{2} \int_S \varphi_{lm}^a \mathcal{L}_X \omega_a d^2V. \quad (2.36)$$

Remarkably, a similar expression holds for the mass moments. This comes from the fact that one can locally write the scalar curvature as  $\mathcal{R} = 2\epsilon^{ab} D_a \Gamma_b$ , where  $\Gamma_a$  is the  $so(2)$  connection associated to an orthonormal dyad. In order to deal with the fact that  $\Gamma_a$  is not globally defined, consider the fiducial round round metric  $\hat{q}_{ab}$  on  $S$  (defined by Lie dragging along  $X^a$  the fiducial round metric at  $S_0$ , see Section 2.2). The multipole moments associated to the round metric are all



vanishing for  $l > 0$  [12]. We can thus write

$$I_{lm}(S) = \frac{1}{4} \int_S (\mathcal{R} - \mathring{\mathcal{R}}) Y_{lm} d^2V, \quad l > 0. \quad (2.37)$$

The advantage of this rewriting is that now there exist a globally defined one-form  $C_a$ , such that  $(\mathcal{R} - \mathring{\mathcal{R}}) = 2\epsilon^{ab} D_a C_b$  (roughly speaking,  $C_a$  is given by the difference between  $\Gamma_a$  and  $\mathring{\Gamma}_a$ ). The ‘mass’ moments then take the same form as the angular moments (2.32):

$$I_{lm} = \frac{1}{2} \int_S C_a \varphi_{lm}^a d^2V, \quad l > 0. \quad (2.38)$$

In particular, the moments do not depend on any gradient ambiguity in  $C_a$ . Proceeding as with the angular moments, we conclude that

$$\frac{dI_{lm}}{dv} = \frac{1}{2} \int_S \varphi_{lm}^a \mathcal{L}_X C_a d^2V, \quad (2.39)$$

where the equation is now valid for  $l \geq 0$ , for it gives the correct vanishing result for  $l = 0$ .

## 2.2.2 Relation with other approaches

Robert Owen [8] has defined multipole moments by expanding  $\mathcal{R}$  and  $\epsilon^{ab} D_a \omega_b$  with respect to a different set of basis functions. These are defined as eigenfunctions of a generalized Laplacian, with the property that, in the presence of axisymmetry, one recovers the potential  $z$  of the Killing field (1.18). In the axisymmetric case, the zeroth and first angular moments coincides with the ones defined here, but for higher multipoles, the moments will be related to ours by some time-dependent linear transformation.

The advantage of Owen’s approach is that moments are defined locally, and so there is no need to refer to the final equilibrium state. On the other hand the basis functions he uses are themselves time dependent. This makes it somewhat difficult to attribute direct physical meaning to the difference between moments evaluated at different times. This is to be contrasted to our approach where the basis functions are time-independent and refer to the final equilibrium state, making it clearer for the comparison of moments at different times.

Let us now bring to attention a subtle point we did not touch upon. The multipole moments for IHs are usually stated in terms of the real and imaginary parts of  $\Psi_2$ . For DHs however, these quantities are not simply given by  $\mathcal{R}$  and  $\epsilon^{ab}D_a\omega_b$ , but rather one has (vacuum case):

$$\text{Re}\Psi_2 = \frac{1}{4}(\mathcal{R} + q^{ab}q^{cd}\sigma_{ac}^\ell\sigma_{bd}^n) \quad (2.40)$$

$$\text{Im}\Psi_2 = \frac{1}{4}(2\epsilon^{ab}D_a\omega_b - \epsilon^{ab}q^{cd}\sigma_{ac}^\ell\sigma_{bd}^n). \quad (2.41)$$

When the DH becomes null, the shear terms vanish and one recovers the relation (1.17). But on the dynamical side, which quantity shall one use to define multipole moments? The choice we made puts emphasis on the geometry of the horizon itself, rather than in the Newman-Penrose components of the spacetime curvature. However, there is also the approach based on the use of ‘tendexes and vortexes lines’ to visualize spacetime curvature [24, 25]. There, curvature is represented through the integral lines of the eigendirections of the electric and magnetic Weyl curvature tensors,

$$E_{ab} = C_{abcd}\tilde{\tau}^c\tilde{\tau}^d, \quad (2.42)$$

$$B_{ab} = \star C_{abcd}\tilde{\tau}^c\tilde{\tau}^d = \frac{1}{2}\epsilon_{ac}{}^{pq}C_{pqbd}\tilde{\tau}^c\tilde{\tau}^d, \quad (2.43)$$

in a given 3+1 foliation of spacetime ( $C_{abcd}$  is the Weyl tensor and  $\tilde{\tau}^a$  refer to the unit time-like normal to the foliation hypersurfaces  $\Sigma$ ). In the presence of a BH, these lines cross the MTS. At this surface, the normal components of the electric and magnetic tensors act as sources for these lines, providing a qualitative picture for the interaction of the BH with gravitational radiation [24]. These normal components are nothing but the real and imaginary part of  $\Psi_2$ ,

$$\Psi_2 = \frac{1}{2}(E_{ab}\tilde{\tau}^a\tilde{\tau}^b + iB_{ab}\tilde{\tau}^a\tilde{\tau}^b), \quad (2.44)$$

where  $\tilde{\tau}^a$  denotes the space-like unit normal of the MTS in  $\Sigma$ . Note however that this  $\Psi_2$  refers to the choice of foliation  $\Sigma$  which is quite arbitrary in dynamical situations. Therefore, beyond the Kerr solution on which much of the intuition is based in this approach, the invariant significance of the approach to equilibrium

via dynamics of tendexes and vortexes remains illusive.

## 2.3 Discussion

There is both theoretical and numerical evidence that the final equilibrium state of dynamical BHs is given by the Kerr solution. This result cannot be derived purely within the framework of local horizons, since the Kerr horizon is just a two-parameter family in an infinite-dimensional space of possible IHs. However, as we have shown, if this information is fed into the local description, one can obtain a very detailed, diffeomorphism invariant description of the approach to equilibrium, which has remained poorly understood thus far.

The Kerr horizon is well understood from the perspective of isolated horizons: It posses an intrinsic characterization [26], and can be represented in terms of specific multipole moments [12]. As a BH is formed by a gravitational collapse or a merger of two BHs, the question then is: How is the final equilibrium state reached?

To address this issue we constructed an analytical framework to extract the strong field physics of the approach to equilibrium. We presented a way to invariantly describe the DH evolving geometry by extending the notion of multipole moments of IHs to DHs. The constraint equations then imply certain balance laws these moments obey. In the process, we also analyzed the conceptually subtle transition from the space-like dynamical horizon to the null isolated horizon, finding the asymptotic behavior of fields as the transition surface is approached. In particular, our dynamical horizon multipole moments were shown to tend to those of the isolated horizon, i.e., the Kerr horizon multipoles in situations of astrophysical interest.

There are several phenomena associated to BHs that have been discovered through numerical relativity. These include, the critical behavior in gravitational collapse [27], and the occurrence of so-called kicks in the collision of BHs [28]. Our framework provides the tools to formulate new questions in numerical relativity: How do the multipole moments settle to the final Kerr value as a function of the horizon radius? Are there universal features in such process? The number of numerical simulations of BH merges is growing very rapidly and our framework

can be readily used to extract the coordinate independent physical information from the last stages of these numerical evolutions. It is possible an interplay between our analytical methods and numerics will shed new light on how diverse dynamical horizon geometries finally settle down to the same geometry, given by the Kerr isolated horizon. Finally, the balance law identities provide non-trivial checks for the numerical simulations.

Our results also open new avenues for further theoretical investigations. We conclude with two examples.

Part of the motivation in studying dynamical BHs is given by the prospects of measuring their emitted gravitational waves. However, the relation between DHs and gravitational waves is more subtle than one's initial picture. For, DHs lie inside the EH and thus cannot be the source of the gravitational radiation at infinity. Nevertheless there do exist correlations between the evolution of the DH and the gravitational radiation at infinity. In particular, a research program aimed at understanding and exploiting these correlations is currently being pursued by Jaramillo et.al. [14]. Our framework provides a more complete conceptual arena for such analyses. Among other things, our results are likely to reduce the gauge ambiguities that are present in this and related investigations.

Finally, in Section 1.2.2.1 we discussed the free data of IHs, and later show how the multipole moments encode such information. The analogue of this problem for DH remains open:<sup>2</sup> Find a set of freely specifiable data which, through the DH equations, allow one to reconstruct the full horizon geometry. The multipole moments of DHs could offer a new perspective to this problem.

## 2.A Appendix: Limiting behavior at $S_0$

In this appendix, we show the properties enunciated in Section 2.1 and discuss the limit to  $S_0$  of the constraint equations.

Equation (1.35), tell us that  $|\sigma|^2$ ,  $|\zeta|^2$  and  $T_{ab}\tau^a\ell^b$  (which is positive due to the energy condition) remain bounded as we approach  $S_0$ , and so we conclude that  $\sigma_{ab}$ ,  $\zeta_a$  and  $T_{ab}\tau^a\ell^b$  have well defined limits at  $S_0$ . While analyzing the constraint at  $S_0$  we will see that for generic NEHs these two quantities cannot vanish

---

<sup>2</sup>Except in the special case of spherically symmetric DHs [29].

simultaneously.

To show the relation between  $b$  and  $\dot{R}$ , we start by expressing the rate of change in the area  $\dot{A} \equiv dA/dv$  as

$$\dot{A} = \int_{S_v} \mathcal{L}_V (\epsilon_{ab}). \quad (2.45)$$

Writing the RHS integrand as  $\mathcal{L}_V \epsilon_{ab} = -b^2 \theta_{\bar{n}} \epsilon_{ab}$ , and expressing  $\dot{A}$  in terms of  $\dot{R}$ , equation (2.45) takes the form  $8\pi R \dot{R} = -\int_{S_v} b^2 \theta_{\bar{n}} d^2V$ , from which we obtain,

$$\lim_{v \rightarrow 0} \int_{S_v} \frac{b^2}{\dot{R}} \theta_{\bar{n}} d^2V = -8\pi R_0, \quad (2.46)$$

with  $R_0$  is the areal radius of  $S_0$ . Since the integrand in (2.46) is strictly negative and  $\theta_{\bar{n}} \rightarrow \theta_{\bar{n}}^{(0)}$  has a well defined limit, it follows that

$$b_0 = \frac{b}{\sqrt{\dot{R}}} \quad (2.47)$$

is a well defined function on  $H$  admitting a regular non vanishing limit to  $S_0$ . We thus conclude that  $b^2$  vanishes at the same rate as  $\dot{R}$  does:

$$b^2 \sim \dot{R} b_0^2, \quad \text{for } v \rightarrow 0. \quad (2.48)$$

To show the relation of the limiting values of  $b_0$  and  $\zeta^a$ , we decompose the vector into its curl/divergence free components:

$$\zeta^a = -D^a(\ln u) + s^a, \quad (2.49)$$

where  $u > 0$  is unique up to a multiplicative constant and  $D \cdot s = 0$ . Recall this vector differs with the normal connection  $\omega_a$  by a gradient term, Eq. (1.33). Using

$$|dR| = \frac{\dot{R}}{2b} = \frac{\sqrt{\dot{R}}}{2b_0} \quad (2.50)$$

we can rewrite the gradient term as

$$D_a \ln |dR| = -D_a \ln b_0 \quad (2.51)$$

since  $D_a f(v) = 0$  for any function that is constant along the cross sections ( $D_a$  is the derivative operator tangential to  $S$ ). Finally, the normal connection  $\omega_a$  defined in terms of the null normals (1.31), is related to the normal connection  $\bar{\omega}_a$  of the barred null normals (2.4), (2.5) according to (1.8), with  $b$  playing the role of  $f$ :

$$\bar{\omega}_a = \omega_a + D_a \ln b = \omega_a + D_a \ln b_0, \quad (2.52)$$

where again we made use of the fact that  $D_a$  is the derivative tangential to  $S$ . Combining (1.33), (2.49), (2.50) and (2.52) we obtain

$$\bar{\omega}_a = D_a \left( \ln \frac{b_0^2}{u} \right) + s_a. \quad (2.53)$$

Since  $u$  has a well defined limit (because  $\zeta_a$  does) and  $u > 0$ , the ratio  $b_0^2/u$  has a well defined limit and gives the gradient part of the NEH normal connection at  $S_0$ . Thus, if we know the geometry of  $\Delta$ , we can determine  $b_0|_{v=0}$  in terms of  $u|_{v=0}$  or vice versa. Notice that the relation is up to a multiplicative constant. But an overall multiplicative constant of  $b_0|_{v=0}$  can be fixed by the condition

$$- \int_{S_0} b_0^2 \theta_{\bar{n}} d^2V = 8\pi R_0, \quad (2.54)$$

that follows from Eqs. (2.46) and (2.47).

## 2.A.1 Limit to $S_0$ of the constraint equations

Let us now discuss the limit to  $S_0$  of the hypersurface constraints (1.27), (1.28). As noted before, it is convenient to combine the scalar and ‘radial’ momentum constraints according to the  $\ell^a$  and  $n^a$  directions. The remaining constraints are then the momentum along the directions tangential to  $S$ .

### 2.A.1.1 $2G_{ab}\tau^a\ell^b = 16\pi GT_{ab}\tau^a\ell^b$ constraint

Let us start with the combination  $H + 2r_a H^a$  already discussed in (1.34). It turns out that if the decomposition (2.49) is used for  $\zeta_a$ , the constraint becomes

equivalent to a linear operator equation in  $u$ :

$$\mathbf{M}^{\text{DH}}u := -\Delta u + 2s^a D_a u + (\mathcal{R}/2 - |\sigma|^2/2 - |s|^2 - 8\pi GT_{ab}\tau^a \ell^b)u = 0. \quad (2.55)$$

Since  $u > 0$ , the equation tell us that the operator  $\mathbf{M}^{\text{DH}}$  has to admit a non-trivial kernel. Let us write the operator as a geometrical piece we call  $\mathbf{M}$  plus ‘radiative’ terms:

$$\mathbf{M}^{\text{DH}} = \mathbf{M} - |\sigma|^2/2 - 4\pi GT_{ab}\ell^a \ell^b, \quad (2.56)$$

with

$$\mathbf{M} = -\Delta + 2s^a D_a + \mathcal{R}/2 - R_{ab}q^{ab}, \quad (2.57)$$

where we used  $8\pi GT_{ab}\tau^a \ell^b = 4\pi GT_{ab}\ell^a \ell^b + R_{ab}q^{ab}$ , which follows from Einstein’s equations and equation (1.31). Let us now restrict attention to the transition surface  $S_0$ . The ‘geometric’ piece  $\mathbf{M}$  is closely related to an operator that features the discussion of NEHs. In particular, it encodes the notion of ‘genericity’: The NEH is generic if  $\mathbf{M}|_{v=0}$  has trivial kernel.<sup>3</sup> Thus, the constraint equation (2.55) implies that  $|\sigma|^2/2 + 4\pi GT_{ab}\ell^a \ell^b \neq 0$  at  $S_0$  for generic NEHs. From the energy condition, this imply that both terms cannot vanish simultaneously. Furthermore, by writing  $2T_{ab}\tau^a \ell^b = T_{ab}\ell^a \ell^b + T_{ab}\bar{n}^a \bar{\ell}^b$  and using that  $T_{ab}\bar{n}^a \bar{\ell}^b \geq 0$ , we conclude that  $|\sigma|^2$  and  $T_{ab}\tau^a \ell^b$  cannot vanish simultaneously, as claimed in Section 2.1.

We will now show two examples of the features above, corresponding to a spherically symmetric and an extremal IH.

Consider the case where  $\Delta$  is given by a spherically symmetric vacuum horizon (corresponding to a final equilibrium state given by a Schwarzschild black hole). The operator  $\mathbf{M}|_{v=0}$  is then given by the standard Laplacian on the sphere plus a constant curvature term. Its eigenfunctions are the spherical harmonics,

$$\mathbf{M}|_{v=0} Y_{lm} = R^{-2}(l^2 + l + 1)Y_{lm}, \quad (2.58)$$

and one verifies that it has no non-trivial kernel and so the horizon is generic.

---

<sup>3</sup>We recall this condition for NEHs guarantees the existence of null normals such that  $\kappa$  is constant and  $\theta_n$  is time-independent [16]. The operator featuring in the NEH discussion is given by  $\tilde{\mathbf{M}} = -\Delta - 2\bar{\omega}^a D_a - D \cdot \bar{\omega} - |\bar{\omega}|^2 + \mathcal{R}/2 - R_{ab}q^{ab}$ . The two are related by a simple transformation:  $g\tilde{\mathbf{M}}(g^{-1}u) = \mathbf{M}^\dagger u$ , where  $g$  is the gradient part of  $\bar{\omega}$ . In particular they have the same kernel dimensionality.

Thus, a DH approaching this  $\Delta$  must have non-vanishing radiative terms at  $S_0$ . For instance, in the case of the Vaidya collapse discussed before, one has  $\sigma_{ab} = 0$  and  $4\pi GT_{ab}\ell^a\ell^b|_{v=0} = 1/R_0^2$ , and so the kernel of the corresponding operator  $\mathbf{M}^{\text{DH}}|_{v=0}$  is given by  $u = \text{constant}$ . On the other hand, in the case of a DH in vacuum with final equilibrium state given by the Schwarzschild black hole, we must have  $\sigma_{ab} \neq 0$  at  $S_0$ . This in turn implies the DH is not spherically symmetric, in agreement with the fact that there are no dynamical space times in spherically symmetric vacuum GR. Thus, at  $S_0$  the horizon transits from no spherical symmetry to spherical symmetry. An example of this situation is provided by the DH formed after coalescence in a head-on collision of non-rotating BHs [7].

Let us now consider the other extreme where  $\Delta$  is an extremal Kerr horizon. Extremal horizons are examples of non-generic horizons [16], and so this represents a complementary situation of the previous case. One of the properties of extremal horizons is that  $\bar{n}(\theta_{\bar{\ell}}) = 0$  (generically this quantity is negative as discussed in Section 1.2.1), which implies that on  $H$ ,  $n(\theta_{\ell}) \rightarrow 0$  as we approach  $S_0$ . Using that  $n(\theta_{\ell}) = -\ell(\theta_{\ell})$ , we learn from the Raychaudhuri equation (1.11) that  $\sigma_{ab}$  and  $T_{ab}\ell^a\ell^b$  vanish at  $S_0$ , in contrast with the situation for generic horizons. Thus, in this case the operator  $\mathbf{M}^{\text{DH}}|_{v=0}$  has no ‘radiative’ components, and its purely determined by the geometric piece  $\mathbf{M}$ . The constraint equation (2.55) assures it has non-trivial kernel, showing again its non-generic character. Explicit expressions for the extremal Kerr geometry, in term of the axisymmetric coordinates discussed in Section 1.2.2.2, are

$$q_{ab} = R^2(f^{-1}dz^2 + fd\phi^2), \quad f = 2(1 - z^2)/(1 + z^2), \quad (2.59)$$

$$s_a = -2(1 - z^2)/(1 + z^2)^2 d\phi, \quad (2.60)$$

from which one can construct the operator  $\mathbf{M}$  and verify that  $u_0 = \sqrt{1 + z^2}$  is its (unique) null eigenfunction.



### 2.A.1.2 Remaining constraints

Let us now discuss the behavior of the remaining hypersurface constraints as we approach  $S_0$ . The complementary constraint of the previous one is given by

$$2G_{ab}\tau^a n^b = -b^2\theta_{\bar{n}}^2/2 + V(\theta_{\bar{n}}) + \kappa_V\theta_{\bar{n}} - b^2|\sigma^{\bar{n}}|^2 - 2D_a\bar{\omega}^a - 2|\bar{\omega}|^2 + \mathcal{R} = 16\pi GT_{ab}\tau^a n^b, \quad (2.61)$$

which we wrote in terms of quantities that have well defined limit as we approach  $\Delta$ . At  $S_0$  this expression becomes,

$$\bar{\ell}(\theta_{\bar{n}}) + \kappa_{\bar{\ell}}\theta_{\bar{n}} - 2D_a\bar{\omega}^a - 2|\bar{\omega}|^2 + \mathcal{R} = 8\pi GT_{ab}\bar{\ell}^a \bar{n}^a, \quad (2.62)$$

where all fields are evaluated at  $S_0$ . This reproduces one of the NEHs equations [16], and so no new information is gained.

The remaining equations are the ones given by the momentum constraint along the directions parallel to  $S$ . Written in terms of quantities with known limit, it reads,

$$-D_a(b^2\theta_{\bar{n}})/(4b) - b\theta_{\bar{n}}\zeta_a/2 + D^c(bS_{ac})/b + (\mathcal{L}_V\bar{\omega}_a - D_a\kappa_V)/(2b) = 8\pi GT_{bc}\tau^c q_a^c. \quad (2.63)$$

The limit of this equation is more involved as it contains quotient of vanishing quantities. Moving those terms to the RHS, the limiting expression is

$$D^c(b_0\sigma_{ac})/b_0|_{v=0} = \lim_{v \rightarrow 0} \{ [8\pi GT_{bc}\bar{\ell}^c q_a^c - (\mathcal{L}_V\bar{\omega}_a - D_a\kappa_V)] / b \}. \quad (2.64)$$

The equations tell us that the numerator on the RHS vanishes at  $S_0$ . This is a condition already present on the NEH, where  $T_{bc}\bar{\ell}^c q_a^c$ , and  $(\mathcal{L}_{\bar{\ell}}\bar{\omega}_a - D_a\kappa_{\bar{\ell}})$  vanish separately (see Section 1.2.2). Equation (2.64) however tell us these term vanish at a rate equal or faster than  $b$ . We will conclude with a small observation regarding this point.

Consider the case where  $\Delta$  is a generic vacuum IH. From our previous discussion,  $\sigma_{ab} \neq 0$  at  $S_0$ . This in turn implies that the LHS of (2.64) is nonzero,<sup>4</sup> and

<sup>4</sup>For symmetric trace-free tensors  $A_{ab}$  on  $S$ ,  $D^b A_{ab} = 0 \Rightarrow A_{ab} = 0$ . This follows from the fact that there are no harmonic one-forms on  $S$  [30]. Writing the tensor as  $A_{ab} = D_a X_b + D_b X_a - D \cdot X q_{ab}$ , one has  $D^b A_{ab} = (d + d^\dagger)^2 X_a = 0$ , implying  $X_a$  (and so  $A_{ab}$ ) vanishes.

so we conclude that  $(\mathcal{L}_V \bar{\omega}_a - D_a \kappa_V)$  goes to zero as  $\sqrt{\dot{R}}$ . Consider now the case of a finite-time  $C^k$  transitions, that is  $M$  is  $C^k$  and the spacetime metric is  $C^{k+1}$ . The vector field  $\bar{\ell}^a$  on  $M$  is  $C^k$ , which implies that  $(\mathcal{L}_V \bar{\omega}_a - D_a \kappa_V)$  vanishes in a  $C^{k-1}$  way, or in local coordinates, it vanishes as  $\sim v^k$  or faster. Similarly,  $b^2$  is  $C^k$  and so  $\dot{R} \sim v^n$  with  $n \geq k - 1$ . But the condition that the ratio in (2.64) is finite, implies that actually  $n \geq 2k$ , thus  $b$  and  $R$  are smoother than one's initial guess.

## 2.A.2 Divergence of $K$ at $S_0$

In terms of the decomposition (1.30), the trace of the extrinsic curvature is given by  $K = 2A + B$ , where

$$A = q^{ab} \nabla_a \tau_b / 2 \quad (2.65)$$

and

$$B = r^a r^b \nabla_a \tau_b. \quad (2.66)$$

Writing  $\tau^a$  in terms of the null normals, we have that  $A = \theta_n/4 = b\theta_{\bar{n}}/4$ , and so  $A \rightarrow 0$  as  $v \rightarrow 0$ . The second term can be written as

$$B = \frac{1}{2b} (\kappa_V - V(\ln b)), \quad (2.67)$$

where

$$\kappa_V := -\frac{1}{2} \bar{n}_b V^a \nabla_a V^b \quad (2.68)$$

is an extension of the notion of surface gravity to DHs [15, 17]. In particular at  $S_0$  it becomes the surface gravity of the NEH and thus has a well defined limit.

Let us now assume that the null normal  $\bar{\ell}$  in  $\Delta$  is such that  $\kappa_{\bar{\ell}}$  is constant (there is always such null normal as discussed in Section 1.2.2). In a coordinate system of the type discussed in Section 2.2,  $V(\ln b) \rightarrow \dot{b}/b$  plus higher order terms as we approach  $S_0$ . Thus, in order for  $B$  to remain finite, we would need  $\dot{b}/b \rightarrow \kappa_{\bar{\ell}}$ , implying  $b \sim e^{\kappa_{\bar{\ell}} v}$ . But since  $\kappa_{\bar{\ell}} > 0$ , such  $b$  cannot be approaching 0. We thus conclude that  $B$  and hence  $K$  diverge at  $S_0$ .

## Part II

# Loop Quantum Cosmology

# Introduction to loop quantum cosmology

The big bang beginning of our universe predicted by GR provides one of the principal motivations for the necessity of an underlying quantum theory of gravity. Quantum cosmology aims at obtaining a quantum description of the homogenous sector of GR. Within the loop quantum gravity (LQG) framework, this leads to a resolution of the big bang singularity, which is replaced by a bounce [31, 32].

In the second part of this thesis we present two contributions in loop quantum cosmology (LQC). The first is a kinematical result, and establishes, under certain hypothesis, the uniqueness of the so-called ‘polymer’ quantization used in LQC. This is analogue to the uniqueness theorems of the full theory. The second one explores the possible ways dynamics in LQC can be implemented via path integrals.

Before going to these two main topics, we give a brief introduction in LQC, focusing on the background needed for the later chapters.

The starting point in LQG is a recasting of general relativity in terms of a  $SU(2)$  Yang-Mills phase space [33]. The fundamental variables are a  $SU(2)$  connection  $A_a^i$  and its conjugate momenta, a densitized triad  $E_i^a$ . These fields are related to

the standard ADM variables by

$$q^{ab} = \sum_{i=1}^3 |\det E|^{-1} E_i^a E_i^b, \quad (3.1)$$

$$K_a{}^b = \frac{1}{\gamma} \sum_{i=1}^3 |\det E|^{-1/2} E_i^b (A_a^i - \Gamma_a^i), \quad (3.2)$$

where  $q^{ab}$  and  $K_a{}^b$  are the metric and extrinsic curvature of the constant-time hypersurface on which the canonical data lives,  $\Gamma_a^i$  is the spin connection, and  $\gamma > 0$  is the so-called Barbero-Immirzi parameter, see for instance [33, 34].

In LQC, one restricts attention to configurations which are homogenous and isotropic. Here we will focus on the spatially flat case, where the spatial metric can be written in the form,

$$ds^2 = a^2 \mathring{q}_{ab} dx^a dx^b = a^2 (dx_1^2 + dx_2^2 + dx_3^2), \quad (3.3)$$

with respect to cartesian coordinates  $x^a$ . To parametrize the homogenous, isotropic sector of the full phase space, it is convenient to introduce a fiducial orthonormal triad  $\mathring{e}_i^a$  and co-triad  $\mathring{\omega}_a^i$  compatible with the fixed reference metric  $\mathring{q}_{ab}$ . Then, one can show that from each gauge<sup>1</sup> equivalence class  $[(A_a^i, E_i^a)]$  of homogenous and isotropic phase space variables, one can pick one given by [35]:<sup>2</sup>

$$A_a^i = c \mathring{\omega}_a^i, \quad E_i^a = p (\mathring{q})^{\frac{1}{2}} \mathring{e}_i^a, \quad (3.4)$$

for some real numbers  $c$  and  $p$ . In this description the local rotations and spatial diffeomorphisms are frozen, except, as was realized only recently, for a 4-parameter family of rigid translations and dilatations. This remaining freedom will play a key role in our analysis but we postpone this issue till Chapter 4.

The phase space of homogenous and isotropic configurations is thus described by the pair of real numbers  $(c, p)$ , where  $a^2 = |p|$ , and  $c$  carries information of the time derivative of  $a$ . In order to find their Poisson bracket one needs to refer to

<sup>1</sup>By gauge we refer to standard  $SU(2)$  gauge transformations (local rotations) as well as spatial diffeomorphisms.

<sup>2</sup>Our notation differs from the standard in the literature. Our  $c$  and  $p$  correspond to the usual  $\tilde{c}$  and  $\tilde{p}$ . In the literature  $c$  and  $p$  are then given by the combination  $c = V_0^{1/3} \tilde{c}$  and  $p = V_0^{2/3} \tilde{p}$ .

the original infinite dimensional symplectic structure of the phase space of general relativity. This involves an integration over the  $\mathbb{R}^3$  spatial manifold, which diverges for the homogenous configurations (3.4). One instead restricts the integral to a cell of finite volume  $V_0$  (with respect to the fiducial metric  $q_{ab}$ ). One can regard this cell as an infra-red cutoff, which is to be eventually removed upon computing the observables of the theory. The resulting Poisson bracket is then given by [35]:

$$\{c, p\} = \frac{8\pi G\gamma}{3V_o} := \frac{\kappa}{\hbar}. \quad (3.5)$$

The passage from the classical to quantum theory involves the choice of a set of ‘elementary’ phase space functions which is sufficiently large to separate point in phase space, and such that it is closed under Poisson brackets. These elementary functions are to be unambiguously promoted to quantum operators, with commutators reproducing the Poisson brackets relations (times  $i\hbar$ ). In LQG, these functions are the fluxes of the electric field  $E_i^a$  through arbitrary two-surfaces, and holonomies of the connection  $A_a^i$  along arbitrary curves. In the present homogenous and isotropic setting, it is sufficient to consider a subset of these function. For instance, one can consider holonomies along the  $x_3$  axis, and fluxes along the transversal  $x_1-x_2$  plane. This selects  $p$  and  $e^{i\mu c}$ ,  $\mu \in \mathbb{R}$  as the elementary functions to be unambiguously promoted to quantum operators.

In LQG, diffeomorphism invariance singles out a unique kinematical Hilbert space [36, 37]. The Hilbert space of LQC is constructed by reproducing the structure of the LQG Hilbert space in the homogenous and isotropic context. In a ‘connection’ representation  $\psi(c)$ , this leads to the space of almost periodic functions [35], given by functions of the form

$$\psi(c) = \sum_j \alpha_j e^{i\mu_j c}, \quad \alpha_j \in \mathbb{C}, \mu_j \in \mathbb{R}, \quad (3.6)$$

with inner product given by

$$\langle e^{i\mu c} | e^{i\mu' c} \rangle = \delta_{\mu\mu'}, \quad (3.7)$$

or equivalently by,

$$\|\psi\|^2 := \lim_{L \rightarrow \infty} \frac{1}{2L} \int_{-L}^L |\psi(c)|^2 dc. \quad (3.8)$$

The fundamental operators act then in the standard fashion:

$$(\widehat{e^{i\mu c}} \psi)(c) = e^{i\mu c} \psi(c) \quad (3.9)$$

$$(\widehat{p} \psi)(c) = -i\kappa \frac{d}{dc} \psi(c). \quad (3.10)$$

Even though this space is constructed in close analogy with the LQG space, so far it has not been systematically derived by imposing diffeomorphism invariance as in the full theory. In fact, one did not expect this to be the case, as it was believed that the diffeomorphisms are completely frozen in the homogenous and isotropic setting. However, as mentioned below equation (3.4), in fact there exists a remanent subgroup of diffeomorphisms. This has changed the perspective and, as we will see in Chapter 4, the LQC representation does follow from an invariance requirement.

So far we have only discussed kinematical aspects. Our second main result refers to dynamics. Therefore we will conclude this introduction by summarizing LQC dynamics. Recall first that in canonical GR, dynamics is encoded in the so-called Hamiltonian constraint, which in the present homogenous and isotropic case reduces to a single phase space function  $C$ . In order to have non-trivial dynamics one needs to consider additional degrees of freedom. We will focus in the case of gravity coupled to a massless scalar field. This introduces a new pair of canonical variables,  $\{\phi, p_\phi\} = 1$ , and the Hamiltonian constraint (in harmonic gauge, see [38]) takes the form

$$C = p_\phi^2 - \frac{3V_0}{4\pi G \gamma^2} c^2 p^2 =: C_{\text{matt}} + C_{\text{grav}}. \quad (3.11)$$

In the quantum theory, one considers a kinematical Hilbert space of the form  $\mathcal{H}_{\text{kin}} = \mathcal{H}_{\text{kin}}^{\text{grav}} \oplus \mathcal{H}_{\text{kin}}^{\text{matt}}$ , where  $\mathcal{H}_{\text{kin}}^{\text{grav}}$  is the LQC Hilbert space introduced before and  $\mathcal{H}_{\text{kin}}^{\text{matt}} = L^2(\mathbb{R}, d\phi)$  is the standard Schroedinger quantization, with  $\widehat{p}_\phi = -i\hbar \partial_\phi$  and  $\widehat{\phi}$  acting by multiplication. Quantum dynamics is encoded in the solutions to

the constraint equation

$$\widehat{C}|\Psi_{\text{kin}}\rangle = 0, \quad (3.12)$$

as we will further explain at the end of this section. The matter part of the constraint is given by  $\widehat{C}_{\text{matt}} = \widehat{p}_\phi^2$ , whereas the construction of  $\widehat{C}_{\text{grav}}$  is more involved and requires additional input from the full theory.<sup>3</sup> It turns out the resulting operator takes a simple form when expressed in a ‘volume’ representation as we now proceed to describe.

From the definition of  $p$  (3.4) it follows that the volume of the cell as measured by the physical metric (3.3) is given by  $V = V_0|p|^{3/2}$ . To express this quantity in the quantum theory, we look at the eigenvectors of the  $\widehat{p}$  operator. These are given by  $\psi(c) = e^{ipc/\kappa}$ , with eigenvalue  $p \in \mathbb{R}$ . The action of the volume operator is then defined by  $\widehat{V}e^{ipc/\kappa} = V_0|p|^{3/2}e^{ipc/\kappa}$ . The volume representation is given by ‘wave functions’  $\psi(\nu)$  that specify the coefficients in this  $\widehat{p}$  eigenbasis, with

$$\nu := \frac{V_0}{2\pi G} \text{sign}(p) |p|^{3/2}, \quad (3.13)$$

so that

$$\widehat{V}\psi(\nu) = 2\pi G|\nu|\psi(\nu). \quad (3.14)$$

In this representation, the operator  $\widehat{C}_{\text{grav}}$  takes a simple form involving uniform steps in  $\nu$ . Introducing the notation,

$$(\widehat{e^{i\lambda b}\psi})(\nu) := \psi(\nu + 2\lambda\hbar), \quad \lambda \in \mathbb{R}, \quad (3.15)$$

for the operators implementing shifts in  $\nu$ , the gravitational constraint takes the form [39, 38]:

$$\widehat{C}_{\text{grav}} = -\frac{3\pi G}{\ell_o^2} \left( \sqrt{|\widehat{\nu}|} \widehat{\sin \ell_o b} \sqrt{|\widehat{\nu}|} \right)^2 =: -\Theta, \quad (3.16)$$

where  $\ell_o$  is related to the LQG ‘area gap’  $\Delta = 4\sqrt{3}\pi\gamma\ell_{\text{Pl}}^2$  via  $\ell_o^2 = \gamma^2\Delta$  and  $\widehat{\nu}$  acts by multiplication. The notation  $\Theta$  for this operator is introduced for later convenience.

---

<sup>3</sup>Due to the inner product (3.7), the operator  $\widehat{e^{i\mu c}}$  is not continuous in  $\mu$ , and the classical function  $c$  has no quantum counterpart. One then needs to express the ‘connection’  $c$  as a limit of ‘holonomies’  $e^{i\mu c}$ . Upon quantization, however, this limit cannot be taken and one instead has to use results from quantum geometry from the full theory [39].



*Remark:* Mathematically, (3.16) can be thought of as the quantization of a regularized version of  $C_{\text{grav}}$ . In terms of the canonical pair  $(\nu, b)$ , with  $\nu$  given in (3.13) and  $b := \frac{c}{\gamma\sqrt{|p|}}$  (with Poisson brackets  $\{\nu, b\} = -2$ ), the classical gravitational constraint takes the form  $C_{\text{grav}} = -3\pi G\nu^2 b^2$ . Upon a ‘regularization’  $b \rightarrow \frac{\sin \ell_o b}{\ell_o}$ , one recovers a ‘classical’ version of (3.16). Such interpretation is however physically misleading, since what plays the role of regularization parameter  $\ell_o$  depends on  $\hbar$ , and so it cannot be dissociated from the quantization procedure.

To summarize, the constraint equation is given by

$$\widehat{C}|\Psi_{\text{kin}}\rangle \equiv (\widehat{p}_\phi^2 - \Theta)|\Psi_{\text{kin}}\rangle = 0, \quad (3.17)$$

where  $\widehat{p}_\phi^2 = -\hbar^2 \partial_\phi^2$  is the matter contribution and  $\Theta$  defined in (3.16) the gravitational part.

Solutions to the constraint equation, as well as their inner product, can be obtained through the group averaging procedure [40]. Given a state  $|\Psi_{\text{kin}}\rangle$  in the kinematical space  $\mathcal{H}_{\text{kin}}$ , a physical state  $|\Psi_{\text{phys}}\rangle$  (i.e. a solution to the constraint equation) is given by:

$$|\Psi_{\text{phys}}\rangle = \int d\alpha e^{\frac{i}{\hbar}\alpha\widehat{C}}|\Psi_{\text{kin}}\rangle \quad (3.18)$$

(see, e.g., [41]). In terms of the (generalized) orthonormal basis in  $\mathcal{H}_{\text{kin}}$  given by  $|\nu, \phi\rangle$  with

$$\langle \nu', \phi' | \nu, \phi \rangle = \delta_{\nu'\nu} \delta(\phi', \phi), \quad (3.19)$$

the mapping (3.18) is encoded in the Green’s function [42, 41]:

$$A(\nu_f, \phi_f; \nu_i, \phi_i) := \int d\alpha \langle \nu_f, \phi_f | e^{\frac{i}{\hbar}\alpha\widehat{C}} | \nu_i, \phi_i \rangle, \quad (3.20)$$

and Eq. (3.18) takes the form,

$$\Psi_{\text{phys}}(\nu, \phi) = \sum_{\nu'} \int d\phi' A(\nu, \phi; \nu', \phi') \Psi_{\text{kin}}(\nu', \phi'). \quad (3.21)$$

In other words,  $A(\nu_f, \phi_f; \nu_i, \phi_i)$  gives the matrix elements of the ‘extractor’ that extracts a physical state from every (suitably regular) kinematical one. Therefore, it will be referred to as the *extraction amplitude*.

The inner product between two physical states  $|\Phi_{\text{phys}}\rangle$  and  $|\Psi_{\text{phys}}\rangle$  is defined as

follows. Let  $|\Phi_{\text{kin}}\rangle$  and  $|\Psi_{\text{kin}}\rangle$  be kinematical states such that under the extraction map defined by Eq. (3.18) they get mapped to the given physical states. The physical inner product is then defined by the action of the ‘bra’  $\langle\Phi_{\text{phys}}|$  on the ‘ket’  $|\Psi_{\text{kin}}\rangle$ , or equivalently,

$$\begin{aligned} (\Phi_{\text{phys}}, \Psi_{\text{phys}}) &:= \langle\Phi_{\text{kin}}|\int d\alpha e^{\frac{i}{\hbar}\alpha\widehat{C}}|\Psi_{\text{kin}}\rangle \\ &= \sum_{\nu,\nu'} \int d\phi d\phi' \bar{\Phi}_{\text{kin}}(\nu,\phi) A(\nu,\phi;\nu',\phi') \Psi_{\text{kin}}(\nu',\phi'). \end{aligned} \quad (3.22)$$

We thus see that all the information of the quantum dynamics is encoded in the extraction amplitude  $A(\nu_f, \phi_f; \nu_i, \phi_i)$ . This quantity will play a central role in Chapter 5, as it represents the object one should be able to recover in a path integral formulation. Taking the present canonical quantum theory as the starting point, we will derive the path integrals that reproduce the extraction amplitude  $A(\nu_f, \phi_f; \nu_i, \phi_i)$ , thus learning how the features of LQC manifest in the language of path integrals.

# Kinematics: A uniqueness result

## 4.1 Introduction

Recall from the previous chapter that in order to construct the phase space of homogenous and isotropic configurations, one introduces certain fiducial structures, namely a triad  $\hat{e}_i^a$ , a co-triad  $\hat{\omega}_a^i$ , and a cell of fiducial volume  $V_0$ . Given these structures, that we fix once and for all, one can parametrize the homogenous and isotropic configurations  $(A, E)$  by the pair  $(c, p)$  according to equation (3.4), with Poisson brackets given by Eq. (3.5). In this reduction one freezes gauge (local rotations and diffeomorphism) transformations that change the form of (3.4). This fixes all gauge transformations except for a four dimensional subgroup of diffeomorphisms generated by vector fields

$$\xi := x^a \frac{\partial}{\partial x^a} ; \quad \frac{\partial}{\partial x^i}, \quad i = 1, 2, 3. \quad (4.1)$$

Out of these, the translations  $\frac{\partial}{\partial x^i}$  act trivially on the pairs  $(c, p)$  whereas the dilatation  $\xi$  has a finite  $e^{s\mathcal{L}_\xi}$  action:

$$(A_a^i, E_i^a) \rightarrow (e^s A_a^i, e^{2s} E_i^a), \quad (4.2)$$

which translates into the transformation

$$(c, p) \rightarrow (e^s c, e^{2s} p). \quad (4.3)$$

Even though (4.2) represent a gauge symmetry from the space-time viewpoint, from the phase space perspective Eq. (4.3) cannot be regarded as a symmetry transformation in the sense of Dirac, since it does not preserve the Poisson brackets (3.5). It nevertheless represents a genuine symmetry of the system, and, as we will show, when this condition is fed into the quantization process one recovers the LQC Hilbert space.

Let us now delineate the strategy we will follow, and leave for the next section a more precise formulation of the problem.

As briefly discussed in Chapter 3, the elementary functions that are to be promoted to quantum operators are given by  $p$  and  $e^{i\mu c}$ ,  $\mu \in \mathbb{R}$ , corresponding to fluxes and holonomies used in the full theory. One then requires the quantum operators to obey commutation relations dictated by the Poisson brackets, namely:

$$[\widehat{e^{i\mu c}}, \widehat{p}] = -\kappa \mu \widehat{e^{i\mu c}}. \quad (4.4)$$

These relations lead to an abstract operator algebra, and represent a symmetry reduced version of the holonomy-flux algebra of the full theory [33]. The strategy followed in LQG is to construct representations of the algebra out of positive linear functional (PLFs) via the so-called GNS construction [43]. In order to ensure that the symmetry group of the system (local rotations and diffeomorphisms) is properly lifted to the quantum theory, one seeks PLFs that are invariant under these symmetry transformations. One of the celebrated results in LQG is the uniqueness of such PLF [36], providing an unambiguous quantization of the phase space. The same result can also be obtained by studying the exponentiated version of the algebra [37], and this is the strategy we will follow here as it is mathematically simpler. In the present case, the exponentiated version of relations (4.4) is given by

$$\widehat{e^{i\mu c}} \widehat{e^{i\nu p}} = e^{-i\kappa\mu\nu} \widehat{e^{i\nu p}} \widehat{e^{i\mu c}}, \quad (4.5)$$

and defines the so-called Weyl algebra. Following the LQG strategy, we will seek for PLFs that are invariant under the symmetry transformation (4.3), and show it leads to the LQC one. We now proceed to make these ideas more precise.

## 4.2 Weyl algebra, PLFs, and invariance.

Let us start by defining the Weyl algebra in detail. The idea is to start with a vector space  $\mathcal{W}$  generated by linear combinations  $a$  of abstract elements  $W(\mu, \eta) = e^{i(\mu c + \eta p)}$ :

$$a = \sum_n \lambda_n W(\mu_n, \eta_n) \in \mathcal{W} \quad (4.6)$$

On this vector space, one defines a  $\star$  operation by:

$$a^\star := \sum_n \bar{\lambda}_n W(-\mu_n, -\eta_n), \quad (4.7)$$

where  $\bar{\lambda}_n$  denotes the complex conjugate of  $\lambda_n$ . One finally introduces a product  $\mathcal{W} \times \mathcal{W} \rightarrow \mathcal{W}$  defined by

$$W(\mu_1, \eta_1) \circ W(\mu_2, \eta_2) := e^{-i\frac{\kappa}{2}(\mu_1\eta_2 - \mu_2\eta_1)} W(\mu_1 + \mu_2, \eta_1 + \eta_2), \quad (4.8)$$

and extended by linearity to arbitrary elements in  $\mathcal{W}$ . This gives  $\mathcal{W}$  the structure of a  $\star$ -algebra which we denote by  $\mathfrak{W}$ . A key feature of the Weyl algebra is that, since the product of two  $W$ s is again a  $W$ , as a vector space  $\mathfrak{W}$  is simply  $\mathcal{W}$ . This greatly simplifies the task of finding representations of  $\mathfrak{W}$ .

In the GNS approach [19, 44], unitary representations of the Weyl algebra  $\mathfrak{W}$  are constructed starting from a linear functional  $\mathcal{F} : \mathcal{W} \rightarrow \mathbb{C}$  that is positive with respect to the product structure:

$$\mathcal{F}(a^\star \circ a) \geq 0 \quad \forall a \in \mathcal{W}, \quad (4.9)$$

and such that  $\mathcal{F}(\mathbf{1}) = 1$ , where  $\mathbf{1} \equiv W(0, 0)$  represents the unit element on the algebra. Upon constructing the representations, this positive linear functional will correspond to expectation values of operators on a preferred state associated to  $\mathcal{F}$ .

Since the underlying vector space of  $\mathfrak{W}$  is simply  $\mathcal{W}$ , because of the linearity property,  $\mathcal{F}$  is determined by its value on the algebra basis elements

$$F(\mu, \eta) := \mathcal{F}(W(\mu, \eta)) , \quad (4.10)$$

and so in practice we will be dealing with a function of two variables, rather than a functional on the infinite dimensional space  $\mathfrak{W}$ . In particular, the representation used in LQC corresponds to the function

$$F^{\text{LQC}}(\mu, \eta) = \begin{cases} 1 & \text{if } \mu = 0 \\ 0 & \text{otherwise} \end{cases}, \quad (4.11)$$

which, in the description of Chapter 3, represents the expectation value of the Weyl operator  $W(\mu, \eta)$  in the state  $\psi(c) = 1$  [45].

Once the the PLF is selected, the GNS construction will provide a representation of the Weyl algebra by operators  $\widehat{W(\mu, \eta)}$  acting unitarily on a Hilbert space. Recall however that we are interested in representations of the holonomy-flux algebra (4.4). Whereas the ‘holonomy’ operator  $\widehat{e^{i\mu c}}$  operator is recovered from the operator corresponding to  $W(\mu, 0)$ , to obtain the flux operator  $\widehat{p}$  one needs to take the derivative of  $\widehat{W(0, \eta)}$  with respect to  $\eta$ . By Stone’s theorem, this is possible if and only if the operator associated to  $W(0, \eta)$  is continuous in  $\eta$ . This in turn is possible if and only if  $F(0, \eta)$  is continuous in  $\eta$ .

We now discuss the issue of the invariance requirement. The transformation (4.3) induces a linear transformation  $\alpha : \mathcal{W} \rightarrow \mathcal{W}$  defined by

$$\alpha W(\mu, \eta) := W(\alpha\mu, \alpha^2\eta), \quad (4.12)$$

where  $\alpha = e^s$ . In analogy with the full theory, we will seek for linear functionals that are invariant under this transformation, namely:

$$\mathcal{F}(\alpha a) = \mathcal{F}(a) \quad (4.13)$$

for all elements in the algebra and for all  $\alpha > 0$  transformations (4.12). Notice however, that there is an important difference with the situation in the full theory, namely, that the transformation  $\alpha$  is not an automorphism of  $\mathfrak{W}$ . This traces back to the fact that the transformation (4.3) does not preserve the Poisson brackets. Nevertheless, the invariance condition (4.13) is a well defined requirement. The fact that  $\alpha$  does not preserve the product structure makes it a stronger condition than otherwise, and this is ultimately the reason it is able to single out the LQC

representation.

### 4.3 Uniqueness

Let us summarize the required properties from the previous discussion. We are looking for a linear functional  $\mathcal{F} : \mathcal{W} \rightarrow \mathbb{C}$  with the properties:

- 1)  $\mathcal{F}(\mathbf{1}) = 1$
- 2)  $\mathcal{F}(a^* \circ a) \geq 0 \quad \forall a \in \mathcal{W}$
- 3)  $\alpha \mathcal{F} = \mathcal{F}$
- 4)  $F(0, \eta) = \mathcal{F}(W(0, \eta))$  is continuous in  $\eta$ .

Properties 1) and 2) say  $\mathcal{F}$  is a PLF of  $\mathfrak{W}$ ; property 3) is the invariance requirement (4.13), and property 4) ensures we can recover a representation of the original algebra (4.4). The LQC PLF defined by (4.11) obeys the invariance and continuity requirement. We will now show how this is the only PLF satisfying these properties. For simplicity in the following we omit the  $\circ$  symbol in the product of two elements.

The invariance requirement 3) translates into the property

$$F(\alpha\mu, \alpha^2\eta) = F(\mu, \eta) \tag{4.14}$$

for the function  $F$ . In other words,  $F$  is constant along half-parabolas where  $\eta \propto \mu^2$  and  $\mu$  is either positive or negative. This in particular tell us that

$$F(0, \eta) = k_+ \quad \text{for } \eta > 0, \tag{4.15}$$

$$F(0, \eta) = k_- \quad \text{for } \eta < 0, \tag{4.16}$$

for some constants  $k_{\pm}$ . Conditions 1) and 4) imply then that  $k_{\pm} = 1$  and so

$$F(0, \eta) = 1. \tag{4.17}$$

We now need to prove that  $F$  vanishes elsewhere. For that we will need to refer to condition 2). If  $a = W(\mu, \eta)$ , then 2) is automatically satisfied because

$W(\mu, \eta)^*W(\mu, \eta) = \mathbf{1}$ . In order to gain non-trivial information from this property, we need to consider linear combinations of the algebra generators. We start by constructing a particular linear combination that due to (4.17) saturates the inequality 2). For given  $\mu$  and  $\eta$  define the following algebra element

$$a(\mu, \eta) := e^{-i\frac{\kappa}{2}\mu\eta}W(\mu, \eta) - W(\mu, 0). \quad (4.18)$$

Direct computation shows that

$$\mathcal{F}(a^*(\mu, \eta)a(\mu, \eta)) = 2F(0, 0) - F(0, \eta) - F(0, -\eta) = 0 \quad (4.19)$$

where in the last equality we used (4.17). Let

$$a_1 := a(\mu_1, \eta_1), \quad (4.20)$$

$$a_2 := a(\mu_2, \eta_2), \quad (4.21)$$

be two algebra elements of this type, and consider an arbitrary linear combination of them:

$$a := \lambda_1 a_1 + \lambda_2 a_2. \quad (4.22)$$

From (4.19), we have,

$$\mathcal{F}(a^*a) = \bar{\lambda}_1 \lambda_2 \mathcal{F}(a_1^* a_2) + \lambda_1 \bar{\lambda}_2 \mathcal{F}(a_1 a_2^*), \quad (4.23)$$

or, in matrix notation, letting  $\lambda = (\lambda_1, \lambda_2)$  and  $\mathbf{M}$  the Hermitian matrix

$$\mathbf{M} = \begin{pmatrix} 0 & \mathcal{F}(a_1^* a_2) \\ \bar{\mathcal{F}}(a_1^* a_2) & 0 \end{pmatrix} \quad (4.24)$$

equation (4.23) takes the form

$$\mathcal{F}(a^*a) = \bar{\lambda}^t \mathbf{M} \lambda. \quad (4.25)$$

The positivity condition says this quantity is non-negative for any  $\lambda$ . This implies that the eigenvalues of the matrix  $\mathbf{M}$  are non-negative. But the eigenvalues of  $\mathbf{M}$  are given by  $\pm |\mathcal{F}(a_1^* a_2)|$ , and so we conclude they must vanish. Hence  $\mathbf{M} = 0$  and



therefore

$$\mathcal{F}(a^*(\mu_1, \eta_1)a(\mu_2, \eta_2)) = 0 \quad (4.26)$$

for any quadruple  $(\mu_1, \eta_1, \mu_2, \eta_2)$ .

Consider now the particular case  $\mu_1 = 0, \mu_2 = \tilde{\mu} = \alpha\mu, \eta_1 = -\tilde{\eta} = -\alpha\eta = \eta_2$ . Direct computation shows,

$$0 = \mathcal{F}(a^*(0, -\tilde{\eta})a(\tilde{\mu}, \tilde{\eta})) \quad (4.27)$$

$$= F(\tilde{\mu}, 0) + F(\tilde{\mu}, 2\tilde{\eta}) - 2 \cos(\kappa\tilde{\mu}\tilde{\eta}/2) F(\tilde{\mu}, \tilde{\eta}) \quad (4.28)$$

$$= F(\mu, 0) + F(\mu, 2\eta) - 2 \cos(\kappa\alpha^3\mu\eta/2) F(\mu, \eta) , \quad (4.29)$$

where in the last equality we used the invariance property (4.14). Equation (4.29) is valid for any pair  $\mu, \eta$  and for any positive  $\alpha$ . Consider the case where  $\mu\eta \neq 0$ . Then, equation (4.29) is of the form  $A + B \cos(\omega t) = 0, \forall t > 0$  (with  $\omega = \kappa\mu\eta/2 \neq 0$  and  $t = \alpha^3$ ), which implies  $A$  and  $B$  must vanish. This in turn implies that  $F(\mu, \eta) = 0$  for  $\mu\eta \neq 0$ , and  $F(\mu, 0) = 0$  for  $\mu \neq 0$ . Finally, note that when  $\mu = 0$ , equation (4.29) reproduces Eq. (4.17), and so there are no further restrictions on  $F$ . Thus, (4.17) and (4.29) imply that  $\mathcal{F}$  is the LQC positive linear functional defined by (4.11).

## 4.4 Discussion

One of the remarkable results in full LQG is the uniqueness of its kinematical structure: The requirement of diffeomorphism invariance is strong enough to select a unique quantization of the phase space [36, 37]. In LQC, quantum kinematics was constructed in two steps. The first —construction of the kinematical algebra of operators— has been systematic in that the ‘elementary’ phase space functions that have unambiguous quantum analogs are simply restrictions of the holonomy and flux variables of the full theory to homogeneous and isotropic configurations. The second —selecting the appropriate representation of this algebra— on the other hand has not been as systematic. Here the required positive linear functional was obtained by ‘mimicking’ the definition of the one used in the full theory. It is then natural to ask if one could make the second step also systematic by proving

an uniqueness result analogous to that in full LQG [36, 37]. For some time, this was thought not to be possible because, while that result makes a crucial use of the requirement that the action of diffeomorphism symmetries be represented by unitary transformations on the kinematical Hilbert space, it was believed that all the diffeomorphisms are gauge fixed in the homogeneous isotropic example of LQC. However, as we have shown, in the spatially flat case, there does exist a remanent non-trivial symmetry, namely dilatations. One thus has a candidate symmetry for the invariance requirement. Our main result is that this requirement again suffices to select a unique representation of the kinematic operator algebra. Thus, the entire LQC kinematics can be constructed in a systematic fashion, once one recognizes the ‘left over’ diffeomorphism symmetry: As far as quantum kinematics is concerned the situation in LQC is the same as in full LQG.

## Dynamics: Path Integral formulations

In non-relativistic quantum mechanics or quantum field theory, there exist two frameworks to describe the quantum theory: The canonical and the path integral one. Consider for instance the case of a non-relativistic particle in one spatial dimension. In the canonical framework, the central object is the Hamiltonian operator  $\hat{H}$ , and its associated evolution operator  $\hat{U}(t) = e^{-\frac{i}{\hbar}t\hat{H}}$ . From the transition amplitudes  $U(x_f, x_i; t) := \langle x_f | \hat{U}(t) | x_i \rangle$ , one can calculate the probability for the system to transit from any initial state to any final one in a given time  $t$ . In the path integral approach, the transition amplitude  $U(x_f, x_i; t)$  is obtained as ‘a sum over all possible paths from  $x_i$  to  $x_f$ ’, each of them weighted with an amplitude proportional to the exponential of  $\frac{i}{\hbar}$  times the classical action evaluated along the path [46]:

$$U(x_f, x_i; t) = \sum_{\substack{\text{all paths from } x_i \text{ to } x_f \\ \text{with total time } t}} e^{\frac{i}{\hbar}S[x(t)]}. \quad (5.1)$$

As originally shown by Feynman [47], the equivalence with the canonical framework follows from the fact that (5.1) can be interpreted as the  $N \rightarrow \infty$  limit of the well-defined composition of  $N$  infinitesimal-time amplitudes:

$$U(x_f, x_i; t) = \lim_{N \rightarrow \infty} \int dx_{N-1} \dots dx_1 U(x_f, x_{N-1}; \frac{t}{N}) \dots U(x_1, x_i; \frac{t}{N}). \quad (5.2)$$

The explicit connection between (5.1) and (5.2) follows from the particular form of the matrix elements  $U(x_{n+1}, x_n; \frac{t}{N})$  as  $N \rightarrow \infty$ , see for instance [46].

The canonical and path integral approaches can be seen as complementary frameworks, and different problems are easier to tackle with one or the other. Since LQC is by construction a canonical theory, it is of interest to obtain its path integral description. In particular this can provide insights into semiclassicality issues, as well as establishing contact with the path integral approach to full LQG, the so-called spinfoams [34].

Our objective in this chapter will be to cast LQC into a path integral form by following Feynman's original strategy for obtaining the path integral from the canonical theory.<sup>1</sup> There are however two main differences with the non-relativistic particle example that we will have to take care of:

1. Dynamics in LQC is not given by an evolution operator but rather is encoded in the solutions of a constraint equation.
2. The non-standard 'polymer'-like Hilbert space.

Thus, we will have to adapt Feynman's strategy to incorporate these two novel features.

The first point is common with other constrained systems like the relativistic particle [48], or Wheeler-DeWitt quantum cosmology [49, 50]. In all these cases, the role of transition amplitude in the path integral (5.1) is replaced by an 'extraction amplitude'. We introduced this quantity in equation (3.20) for the LQC case. Recall from Chapter 3 that this object contains all the dynamical information of the quantum theory, as it allows to reconstruct the physical Hilbert space, see equations (3.21) and (3.22). Thus the extraction amplitude will be the quantity we will seek to express as a path integral.

The second point, proper of LQC (and LQG), can be regarded as conceptually separate from the first one. In particular, it would be present in a situation of a system described by what is often referred to as a 'polymer' Hilbert space with true Hamiltonian and evolution operator. For this reason we devote Appendix 5.A to analyze in detail the path integral of a toy-model system given by a 'polymerized'

---

<sup>1</sup>This chapter is based on paper number 8 from the list in the Vita. Therefore, there will be some inevitable overlap with that publication.

non-relativistic free particle. The advantage of such analysis will be twofold. First it will allow us to focus on the issue of ‘polymer’ spaces in path integrals without worrying about constraint equations, and second it will provide an example where all relevant quantities can be computed in closed and simple form.

In order to describe the content of this chapter, we need to return for a moment to the non-relativistic particle example. Observe that (5.1), represents a *configuration space* path integral, where one sums over paths in the configuration space of the system, which in this case is the real line. There also exist a similar *phase space* path integral, where one sums over paths in phase-space, that is the  $(x, p)$  plane. In this sum  $x_i$  and  $x_f$  are fixed, but  $p_i$  and  $p_f$  are unrestricted. The amplitude of each path is again given by the exponential of  $\frac{i}{\hbar}$  times the (phase-space) action,  $S[x(t'), p(t')] = \int dt' [p \dot{x} - H(x, p)]$ . In the non-relativistic particle case, the integral over the paths in  $p$  is an infinite dimensional Gaussian integral that can be explicitly performed and yields the configuration space path integral [46].

In LQC one again finds two types of path integrals, taking place in configuration and phase space. They are however qualitatively different between each other. The configuration-space path integral was extensively analyzed in Henderson’s PhD thesis [51], and here we will only discuss it briefly for completeness (Section 5.1). One of its prominent features is that the resulting sum is over discontinuous paths which can be interpreted as describing quantum spacetimes, in close analogy with the spinfoam path integral formulation of full LQG.

Our focus here will be on the phase-space path integral, which we present in Section 5.2. In this case, the sum is over continuous phase-space paths, with amplitudes determined by an action, much like in the non-relativistic particle example. However, we will find that this action is not just the classical one but has quantum geometry corrections that are responsible for the particular features of LQC, as for instance the replacement of the big bang by a big bounce. This form of the path integral will allow us for a saddle point evaluation, which we perform in Section 5.3. Here we will make use of WKB techniques, which we summarize in Appendix 5.B. Among other things, this will provide a physical understanding of the properties of the extraction amplitude, as will be explicitly seen by comparison with the exact amplitude (given in Appendix 5.C).

We conclude this introduction by delineating the strategy we will follow in the

construction of the path integrals. As discussed above in reference to the first point, we will seek to express the extraction amplitude in the path integral form. Our point of departure will be its defining equation (3.20):

$$A(\nu_f, \phi_f; \nu_i, \phi_i) := \int d\alpha \langle \nu_f, \phi_f | e^{\frac{i}{\hbar}\alpha\widehat{C}} | \nu_i, \phi_i \rangle . \quad (5.3)$$

The strategy in the constructions will be as follows: We will first regard the integrand in (5.3) as the matrix elements of a fictitious evolution operator; then seek for a path integral representation of that fictitious transition amplitude; and finally carry out the  $\alpha$  integral.

## 5.1 Configuration space path integral

As described above, we start by focusing on the integrand of equation (5.3), namely:

$$A(\nu_f, \phi_f; \nu_i, \phi_i; \alpha) := \langle \nu_f, \phi_f | e^{\frac{i}{\hbar}\alpha\widehat{C}} | \nu_i, \phi_i \rangle . \quad (5.4)$$

Mathematically one can regard  $\alpha\widehat{C}$  as a (fictitious) Hamiltonian operator. Then  $A(\nu_f, \phi_f; \nu_i, \phi_i; \alpha)$  can be interpreted as the transition amplitude for an initial kinematic state  $|\nu_i, \phi_i\rangle$  to evolve to a final kinematic state  $|\nu_f, \phi_f\rangle$  in a unit ‘time interval’  $\tau = 1$  and we can follow Feynman’s procedure [47] to express it as a sum over histories. Technically, a key simplification comes from the fact that the constraint  $\widehat{C}$  is a sum of two commuting pieces that act separately on  $\mathcal{H}_{\text{kin}}^{\text{matt}}$  and  $\mathcal{H}_{\text{kin}}^{\text{grav}}$ . Consequently, the amplitude (5.4) factorizes as

$$A(\nu_f, \phi_f; \nu_i, \phi_i; \alpha) = A_\phi(\phi_f, \phi_i; \alpha) A_G(\nu_f, \nu_i; \alpha) \quad (5.5)$$

with

$$A_\phi(\phi_f, \phi_i; \alpha) = \langle \phi_f | e^{\frac{i}{\hbar}\alpha p_\phi^2} | \phi_i \rangle \quad (5.6)$$

$$A_G(\nu_f, \nu_i; \alpha) = \langle \nu_f | e^{-\frac{i}{\hbar}\alpha\widehat{\Theta}} | \nu_i \rangle . \quad (5.7)$$

It is easy to cast the first amplitude,  $A_\phi$ , in the desired form using either a standard Feynman expansion or simply evaluating it by inserting a complete eigen-basis of

$p_\phi$ . The result is:

$$A_\phi(\phi_f, \phi_i; \alpha) = \frac{1}{2\pi\hbar} \int dp_\phi e^{\frac{i}{\hbar}\alpha p_\phi^2} e^{\frac{i}{\hbar}p_\phi(\phi_f - \phi_i)}. \quad (5.8)$$

The non-trivial piece lies in the gravitational amplitude  $A_G$ . Here is where the non-standard LQC inner product comes into play. In Section 5.6 we show how the path integral construction for matrix elements of the form (5.7) involves paths that are given by volume sequences  $(\nu_i, \nu_1, \dots, \nu_f)$  such that consecutive volumes are different. The paths are such that volume transitions  $\nu_m \rightarrow \nu_{m+1}$  can occur at any ‘time’  $\tau_m$  with  $\tau_m \leq \tau = 1$ . The sum over all such paths takes the form:

$$A_G(\nu_f, \nu_i; \alpha) = \sum_{M=0}^{\infty} \int_{1 > \tau_M > \dots > \tau_1 > 0} d\tau_M \dots d\tau_1 \sum_{\substack{\nu_{M-1}, \dots, \nu_1 \\ \nu_m \neq \nu_{m+1}}} A(\nu_M, \dots, \nu_0; \tau_M, \dots, \tau_1; \alpha) \quad (5.9)$$

where the amplitude of each path is given by

$$\begin{aligned} A(\nu_M, \dots, \nu_0; \tau_M, \dots, \tau_1; \alpha) &= e^{-\frac{i}{\hbar}(1-\tau_M)\alpha \Theta_{\nu_M \nu_M}} \left(-\frac{i}{\hbar}\alpha \Theta_{\nu_M \nu_{M-1}}\right) \times \\ &\dots e^{-\frac{i}{\hbar}(\tau_2 - \tau_1)\alpha \Theta_{\nu_1 \nu_1}} \left(-\frac{i}{\hbar}\alpha \Theta_{\nu_1 \nu_0}\right) e^{-\frac{i}{\hbar}\tau_1 \alpha \Theta_{\nu_0 \nu_0}}, \end{aligned} \quad (5.10)$$

where

$$\Theta_{\nu' \nu} \equiv \langle \nu' | \Theta | \nu \rangle. \quad (5.11)$$

Although in principle each  $\nu$ -sum ranges over all Reals, only a countably number of paths give non-vanishing amplitudes. From the form of the  $\Theta$  operator (3.16), those non-trivial paths are simple to identify: They should have support on lattices of the form  $4\ell_o \hbar \mathbb{Z} \subset \mathbb{R} + \epsilon$ . For concreteness we will focus on the  $\epsilon = 0$  lattice.

Now, in the present situation the ‘times’  $\tau_m$  are pure gauge and have no physical meaning. The actual paths of interest are given by the volume sequences  $(\nu_i, \nu_1, \dots, \nu_f)$  regardless of the transition ‘times’  $\tau_m$ . The amplitude for such paths will be given by

$$A(\nu_M, \dots, \nu_0; \alpha) := \int_{1 > \tau_M > \dots > \tau_1 > 0} d\tau_M \dots d\tau_1 A(\nu_M, \dots, \nu_0; \tau_M, \dots, \tau_1; \alpha). \quad (5.12)$$

And so we end up with the following expansion for (5.7):

$$A_G(\nu_f, \nu_i; \alpha) = \sum_{M=0}^{\infty} \sum_{\substack{\nu_{M-1}, \dots, \nu_1 \\ \nu_m \neq \nu_{m+1}}} A(\nu_M, \dots, \nu_0; \alpha). \quad (5.13)$$

The strategy now is to insert this expansion in (5.3), and perform the  $\alpha$  integral over each path separately. That is, we want to define a ‘gauge invariant’ amplitude for each path as

$$A(\nu_M, \dots, \nu_0; \phi_f, \phi_i) := \int d\alpha \langle \phi_f | e^{\frac{i}{\hbar} \alpha p_\phi^2} | \phi_i \rangle A(\nu_M, \dots, \nu_0; \alpha), \quad (5.14)$$

leading to a final expansion of the form

$$A(\nu_f, \phi_f; \nu_i, \phi_i) = \sum_{M=0}^{\infty} \left[ \sum_{\substack{\nu_{M-1}, \dots, \nu_1 \\ \nu_m \neq \nu_{m+1}}} A(\nu_M, \dots, \nu_0; \phi_f, \phi_i) \right]. \quad (5.15)$$

This step is potentially problematic since permuting the  $\alpha$  integral with the sum over  $M$  may lead to ill-defined expressions. In the present case however, the amplitudes (5.14) are well defined. Let us illustrate the situation with the simple case of a constant volume path ( $M = 0$ ), where the amplitude takes the form

$$A(\nu; \alpha) = e^{-\frac{i}{\hbar} \alpha \Theta_{\nu\nu}}. \quad (5.16)$$

Using (5.8) we obtain

$$A(\nu; \phi_f, \phi_i) = \frac{1}{2\pi\hbar} \int d\alpha \int dp_\phi e^{\frac{i}{\hbar} \alpha p_\phi^2} e^{\frac{i}{\hbar} p_\phi (\phi_f - \phi_i)} e^{-\frac{i}{\hbar} \alpha \Theta_{\nu\nu}} \quad (5.17)$$

$$= \frac{1}{2\pi\sqrt{\Theta_{\nu\nu}}} \cos\left(\sqrt{\Theta_{\nu\nu}}(\phi_f - \phi_i)/\hbar\right). \quad (5.18)$$

This computation can be generalized to arbitrary paths, showing the amplitudes (5.14) are well defined [41, 51]. Issues of convergence of series of the type (5.15) were investigated in [51].

The expansion (5.14) provides a concrete instance of a spinfoam like expansion strictly derived from the canonical theory. This has provided valuable insights into several aspects of spinfoams in LQG, where, even though the original idea comes



from the canonical theory [52], there does not yet exist a systematic derivation. However, because the sum is over discrete ‘quantum’ paths, this representation of the extraction amplitude is not so well suited for analyzing semi-classical issues. Therefore we will now introduce a representation in terms of phase space path integrals.

## 5.2 Phase space path integral

The starting point is again given by expressions (5.3), (5.4) and (5.5). Focusing in the gravitational amplitude (5.7), we start by expressing it as a sum over ‘discrete-time’ configuration space paths,

$$A_G(\nu_f, \nu_i; \alpha) = \sum_{\nu_{N-1}, \dots, \nu_1} \langle \nu_f | e^{-\frac{i}{\hbar} \epsilon \Theta} | \nu_{N-1} \rangle \langle \nu_{N-1} | e^{-\frac{i}{\hbar} \epsilon \Theta} | \nu_{N-2} \rangle \dots \langle \nu_1 | e^{-\frac{i}{\hbar} \epsilon \Theta} | \nu_i \rangle, \quad (5.19)$$

where each sequence  $(\nu_f, \nu_{N-1}, \dots, \nu_1, \nu_i)$  in the sum is regarded as a discrete-time path. For small  $\epsilon$ , the terms appearing in (5.19) can be written as

$$\langle \nu_{n+1} | e^{-\frac{i}{\hbar} \epsilon \alpha \Theta} | \nu_n \rangle = \delta_{\nu_{n+1}, \nu_n} - \frac{i}{\hbar} \epsilon \alpha \langle \nu_{n+1} | \Theta | \nu_n \rangle + \mathcal{O}(\epsilon^2). \quad (5.20)$$

As discussed below Eq. (5.11), the amplitudes above vanish unless the volume are supported in a lattice which we take to be

$$\nu \in 4\ell_o \hbar \mathbb{Z}. \quad (5.21)$$

The matrix elements of  $\Theta$  can be obtained from Eq. (3.16) and are given by

$$\langle \nu_{n+1} | \Theta | \nu_n \rangle = -\frac{3\pi G}{4\ell_o^2} \sqrt{|\nu_n \nu_{n+1}|} \frac{(\nu_n + \nu_{n+1})}{2} (\delta_{\nu_{n+1}, \nu_n + 4\ell_o \hbar} - 2\delta_{\nu_{n+1}, \nu_n} + \delta_{\nu_{n+1}, \nu_n - 4\ell_o \hbar}). \quad (5.22)$$

As in usual path integral constructions, we now bring-in  $b$ , the momentum variable conjugate to  $\nu$ . Thanks to (5.21), this can be readily done in the present case, through the identity

$$\delta_{\nu', \nu} = \frac{\ell_o}{\pi} \int_0^{\pi/\ell_o} db e^{-\frac{i}{2\hbar} b(\nu' - \nu)}, \quad (5.23)$$

which, when used to rewrite the Kronecker deltas appearing in Eqs. (5.20) and (5.22), leads to the following expression for (5.20):

$$\begin{aligned} \langle \nu_{n+1} | e^{-\frac{i}{\hbar} \epsilon \alpha \widehat{\Theta}} | \nu_n \rangle &= \frac{\ell_o}{\pi} \int_0^{\pi/\ell_o} db_{n+1} e^{-\frac{i}{\hbar} b_{n+1} (\nu_{n+1} - \nu_n)/2} \left[ 1 + \frac{i}{\hbar} \epsilon \alpha C_G^n \right] + \mathcal{O}(\epsilon^2) \\ &= \frac{\ell_o}{\pi} \int_0^{\pi/\ell_o} db_{n+1} e^{-\frac{i}{\hbar} b_{n+1} (\nu_{n+1} - \nu_n)/2 + \frac{i}{\hbar} \epsilon \alpha C_G^n} + \mathcal{O}(\epsilon^2), \end{aligned} \quad (5.24)$$

where

$$C_G^n = -\frac{3\pi G}{\ell_o^2} \sqrt{\nu_n \nu_{n+1}} \frac{\nu_n + \nu_{n+1}}{2} \sin^2(\ell_o b_{n+1}). \quad (5.25)$$

The amplitude (5.7) then takes the form of a ‘discrete-time’ phase space path integral

$$A_G(\nu_f, \nu_i; \alpha) = \left(\frac{\ell_o}{\pi}\right)^N \sum_{\nu_{N-1}, \dots, \nu_1} \int db_N \dots db_1 e^{i S_G^N}, \quad (5.26)$$

where

$$S_G^N = \epsilon \sum_{n=0}^{N-1} \left[ -\frac{b_{n+1} \nu_{n+1} - \nu_n}{2\epsilon} + \alpha C_G^n \right]. \quad (5.27)$$

There is a final subtlety to complete the path integral for the gravitational factor, which is that the paths under consideration do not cover the full phase space, since  $\nu_n$  takes values on the the lattice (5.21) and  $b_n \in [0, \pi/\ell_o)$ . As discussed in Section 5.A.2, one can perform the substitution

$$\frac{\pi}{\ell_o} \sum_{\nu_n} \int_0^{\pi/\ell_o} db_n \dots \rightarrow \int_{-\infty}^{\infty} d\nu_n \int_{-\infty}^{\infty} db_n \dots, \quad (5.28)$$

and upon taking the formal  $N \rightarrow \infty$  limit obtain a phase space path integral of the form

$$A_G(\nu_f, \nu_i; \alpha) = \int [\mathcal{D}\nu(\tau)] [\mathcal{D}b(\tau)] e^{i S_G}, \quad (5.29)$$

with

$$S_G = \int_0^1 d\tau \left( -\frac{1}{2} b \dot{\nu} - \alpha 3\pi G \nu^2 \frac{\sin^2 \ell_o b}{\ell_o^2} \right). \quad (5.30)$$

Finally, combining this result with the usual path integral for the matter factor, and bringing in the  $\alpha$  integral, we obtain<sup>2</sup> the expression for the total extraction

---

<sup>2</sup>Note that the integral over  $\alpha$  is an ordinary one-variable integral. It can nevertheless be reinterpreted as an integral over *all* possible values  $\alpha(\tau)$  together with the a gauge fixing condition

amplitude as a formal path integral:

$$A(\nu_f, \phi_f; \nu_i, \phi_i) = \int d\alpha \int [\mathcal{D}\nu(\tau)] [\mathcal{D}b(\tau)] [\mathcal{D}p_\phi(\tau)] [\mathcal{D}\phi(\tau)] e^{\frac{i}{\hbar}S}, \quad (5.31)$$

with

$$S = \int_0^1 d\tau \left( p_\phi \dot{\phi} - \frac{1}{2} b \dot{\nu} - \alpha \left( p_\phi^2 - 3\pi G \nu^2 \frac{\sin^2 \ell_o b}{\ell_o^2} \right) \right), \quad (5.32)$$

and the integral is over all trajectories *in the classical phase space* as in usual path integrals. This expression is only formal but enable us to use the standard techniques such as the saddle point approximation.

Since we now integrate over all paths in the classical phase space, in particular, the paths are allowed to go through points with  $\nu = 0$  which represent the classical singularity. How can then we see the singularity resolution in this setting? The answer is that the paths are not weighted by the standard FRW action but by a ‘polymerized’ version of it which still retains the memory of the quantum geometry underlying the Hamiltonian theory. As we will see, this action is such that a path going through the classical singularity has negligible contribution whereas bouncing trajectories give the dominant contribution.

*Remark:* There are other systems in which the passage from the Hamiltonian quantum theory to a path integral results in an action that has  $\hbar$ -corrections. Perhaps the simplest example is that of a non-relativistic particle on a curved Riemannian manifold for which the standard Hamiltonian operator is simply  $\hat{H} = -(\hbar^2/2m)g^{ab}\nabla_a\nabla_b$ . Quantum dynamics generated by this  $\hat{H}$  can be recast in the path integral form following the Feynman procedure [47]. The transition amplitude is then given by [53]

$$\langle q, t | q', t' \rangle = \int \mathcal{D}[q(\tau)] e^{\frac{i}{\hbar}S} \quad (5.33)$$

with

$$S = \int d\tau \left( \frac{m}{2} g_{ab} \dot{q}^a \dot{q}^b + \frac{\hbar^2}{12m} R \right) \quad (5.34)$$

where  $R$  is the scalar curvature of the metric  $g_{ab}$ . Extrema of this action are not the geodesics one obtains in the classical theory but rather particle trajectories in a  $\hbar$ -dependent potential. The two sets of trajectories can be qualitative different.

---

$d\alpha/d\tau = 0$ . Doing so allows one to rewrite the path integral with any other gauge fixing condition; see for instance [50].

### 5.3 Saddle point approximation

In quantum mechanics and quantum field theory the steepest descent approximation is a powerful practical tool to calculate leading contributions to the transition amplitude in an  $\hbar$  expansion. In particular, this approximation provides the much needed intuition on when quantum corrections are dynamically important and when they are not. In Section 5.B we recast this  $\hbar$  expansion in a form suitable for the extraction amplitude of constrained systems. We will now use those results to obtain the leading term using a saddle point approximation.

In this approximation, the extraction amplitude (5.31) is given by

$$A(\nu_f, \phi_f; \nu_i, \phi_i) \sim (\det \delta^2 S|_0)^{-1/2} e^{\frac{i}{\hbar} S|_0}. \quad (5.35)$$

Here  $S|_0$  is the action evaluated along the trajectory extremizing the action with initial and final configuration points fixed. For given initial and final points, there exist in general two trajectories joining them, one with positive and the other with negative  $p_\phi$  values. The positive and negative  $p_\phi$  sectors are however decoupled and can be studied separately [41]. For concreteness we restrict ourselves to the ‘positive frequency’ branch, and so only the  $p_\phi > 0$  trajectory gets picked. We will evaluate the phase factor in Sec.5.3.1. The prefactor  $(\det \delta^2 S|_0)^{-1/2}$  represents a formal infinite dimensional determinant which we will evaluate in Sec.5.3.2. In Sec.5.3.3 we compare the resulting approximate amplitude to the exact one, computed numerically.

Before proceeding with these calculations, we would like to point out a conceptual subtlety. In ordinary quantum mechanics, the steepest descent approximation provides the leading term in the transition amplitude in an  $\hbar$  expansion. In our case, the action  $S$  that features in the path integral (5.31) itself depends on  $\hbar$  through  $\ell_o \sim \sqrt{\gamma^3 \hbar G}$ , while the  $\hbar$  expansion of Section 5.B assumes that the action does not change as  $\hbar$  tends to zero. Therefore, to directly apply the result of Section 5.B, now we have to take the limit  $\hbar \rightarrow 0$  while keeping  $\ell_o$  fixed. Hence we will obtain the leading term in the extraction amplitude in the approximation  $\hbar \rightarrow 0$ ,  $\gamma \rightarrow \infty$  keeping  $\gamma^3 \hbar$  fixed. To emphasize this subtlety, *we will use inverted commas, as in ‘classical limit’ and ‘semi-classical approximation’ while referring to this limit.* Let us briefly explore the meaning of this limit. In classical general

relativity,  $\gamma \rightarrow \infty$  corresponds to ignoring the new term in the Holst action for general relativity, in comparison with the standard Palatini term. What about the ‘semi-classical’ approximation? Eigenvalues of the volume operator are given by  $(8\pi G\ell_o\hbar)n$  where  $n$  is a non-negative integer. Therefore, in the ‘semi-classical limit’ the spacing between consecutive eigenvalues goes to zero and  $\nu$  effectively becomes continuous as one would expect. Finally, states that are relevant in this limit have large  $n$ , just as quantum states of a rigid rotor that are relevant in the semi-classical limit have large  $j$ .

### 5.3.1 The Hamilton-Jacobi function $S|_0$

To calculate the  $S|_0$  term, we need to solve the equations of motion obtained from the action (5.32), then evaluate the action along those trajectories, and finally express the result in terms of the given initial and final points. The (positive frequency) trajectories which solve the equations of motion can be written in terms of two integration constants,  $\nu_B$  and  $\phi_B$ , as

$$\nu(\phi) = \nu_B \cosh(\sqrt{12\pi G}(\phi - \phi_B)), \quad (5.36)$$

$$b(\phi) = \frac{2 \operatorname{sign}(\nu_B)}{\ell_o} \tan^{-1}(e^{-\sqrt{12\pi G}(\phi - \phi_B)}). \quad (5.37)$$

These solutions have several interesting features.

(i) As seen from the cosh dependence of the volume, these trajectories represent bouncing universes, with  $\phi_B$  and  $\nu_B$  giving the scalar field and volume values at the bounce point. The minimum volume  $\nu_B$  is related with the scalar field momentum  $p_\phi$  by  $|\nu_B| = 2\ell_o p_\phi / \sqrt{12\pi G}$ . Note that if  $\nu_B$  is positive (resp. negative), then  $\nu(\phi)$  remains positive (resp. negative) for all  $\phi$ . For concreteness we will focus on trajectories with positive  $\nu_B$ .

(ii)  $\nu(\phi)$  can vanish only on the trajectory with  $\nu_B = 0$  i.e.,  $\nu(\phi) = 0$  for all  $\phi$ . Thus if we begin with the initial state  $\nu_i \neq 0, \phi_i$ , there is no (real) ‘classical’ trajectory at all with  $\nu_f = 0$  for any value of  $\phi_f$ .

(iii) Whereas in general relativity *all* trajectories begin at the big-bang—they all tend to  $\nu = 0$  as  $\phi \rightarrow -\infty$ —it is obvious from (5.36) that all our trajectories tend to  $\nu \rightarrow \infty$  in this limit (except for the trajectory  $\nu(\phi) = 0 \forall \phi$ ).

(iv) Recall that in full LQC, states which are sharply peaked at a low curvature configuration for large values of  $\phi$  remain sharply peaked on certain ‘effective trajectories’ for all  $\phi$  [39]. These are among solutions (5.37).

(v) The relation between  $\nu$  and  $\phi$  given in Eq. (5.36) coincides with the expression for the expectation value of the volume operator at a given scalar field value  $\phi$  in *any* quantum state of LQC [38].

Evaluation of the action along these solutions can be greatly simplified if one integrates by parts the term  $-\int_0^1 d\tau \frac{1}{2} b \dot{\nu}$  in (5.32). Then, using the equations of motion, the terms  $\frac{1}{2} \dot{b} \nu$  and  $p_\phi \dot{\phi}$  cancel each other and the action evaluated along the solutions is just given by only the boundary term,

$$S|_0 = \frac{1}{2} (\nu_i b_i - \nu_f b_f). \quad (5.38)$$

To express  $S|_0$  in terms of initial and final configuration variables, we need to solve for the constants  $\nu_B$  and  $\phi_B$  in terms of  $\nu_f, \phi_f; \nu_i, \phi_i$ . Without loss of generality we can take  $\phi_i = 0$  and  $\phi_f = \varphi$  (by setting  $\varphi = \phi_f - \phi_i$  at the end, one recovers the general case). Then we are led to solve the equations

$$\nu_i = \nu_B \cosh(-\sqrt{12\pi G} \phi_B) \quad (5.39)$$

$$\nu_f = \nu_B \cosh(\sqrt{12\pi G}(\varphi - \phi_B)), \quad (5.40)$$

for  $\nu_B$  and  $\phi_B$  in terms of the initial and final data:

$$e^{\sqrt{12\pi G} \phi_B} = \sqrt{\frac{e^{\sqrt{12\pi G} \varphi} - \nu_f / \nu_i}{-e^{-\sqrt{12\pi G} \varphi} + \nu_f / \nu_i}} \quad (5.41)$$

$$\nu_B = \frac{\nu_i}{|\sinh(\sqrt{12\pi G} \varphi)|} \sqrt{\left( e^{\sqrt{12\pi G} \varphi} - \frac{\nu_f}{\nu_i} \right) \left( -e^{-\sqrt{12\pi G} \varphi} + \frac{\nu_f}{\nu_i} \right)} \quad (5.42)$$

Clearly,  $\nu_B, \phi_B$  are real for any given initial configuration  $(\nu_i, \phi_i)$  if and only if the final configuration satisfies

$$e^{-\sqrt{12\pi G} |\varphi|} < \frac{\nu_f}{\nu_i} < e^{\sqrt{12\pi G} |\varphi|}. \quad (5.43)$$

This is the necessary and sufficient condition for the existence of real trajectories.

Let us first focus on the ‘classically’ allowed region (5.43). Using (5.37) to express  $b_i$  and  $b_f$  appearing in (5.38) in terms of the initial and final data  $(\nu_f, \phi_f; \nu_i, \phi_i)$  we obtain the desired expression of the Hamilton-Jacobi function:

$$S|_0 = \frac{\nu_i}{\ell_o} \tan^{-1} \left( \sqrt{\frac{e^{\sqrt{12\pi G}\varphi} - \nu_f/\nu_i}{-e^{-\sqrt{12\pi G}\varphi} + \nu_f/\nu_i}} \right) - \frac{\nu_f}{\ell_o} \tan^{-1} \left( e^{-\sqrt{12\pi G}\varphi} \sqrt{\frac{e^{\sqrt{12\pi G}\varphi} - \nu_f/\nu_i}{-e^{-\sqrt{12\pi G}\varphi} + \nu_f/\nu_i}} \right), \quad (5.44)$$

where  $\varphi = \phi_f - \phi_i$ . The ‘classically’ allowed region consists of the upper and lower quarters in Fig. 5.1. For  $\nu_f, \phi_f$  in these two quarters,  $S_0$  is real and thus the amplitude (5.35) has an oscillatory behavior. Outside these regions the action becomes imaginary and one gets an exponentially suppressed amplitude. Thus, the situation is analogous to that in quantum mechanics.

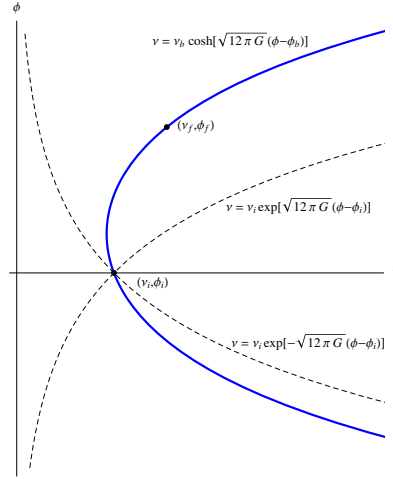


**Figure 5.1.** For fixed  $(\nu_i, \phi_i)$ , the (dashed) curves  $\nu_f = \nu_i e^{\pm\sqrt{12\pi G}(\phi_f - \phi_i)}$  divide the  $(\nu_f, \phi_f)$  plane into four regions. For a final point in the upper or lower quarter, there always exists a real trajectory joining the given initial and final points (as exemplified by the thick line). If the final point lies on the left or right quarter, there is no real solution matching the two points. The action becomes imaginary and one gets an exponentially suppressed amplitude.

For completeness, let us now discuss the case where the final point lies in the ‘classically’ forbidden region, this is to say the situation where the boundary data satisfy

$$\frac{\nu_f}{\nu_i} < e^{-\sqrt{12\pi G}|\varphi|} \quad \text{or} \quad \frac{\nu_f}{\nu_i} > e^{\sqrt{12\pi G}|\varphi|}. \quad (5.45)$$

For concreteness let  $\nu_i$  be positive as in Fig.5.1 but now there is no restriction on the sign of  $\nu_f$ . To find extrema of the action that join the initial and final configurations satisfying (5.45), we can follow the semi-classical procedure used to calculate tunneling amplitudes in familiar systems and allow paths with imaginary momenta. Let us define

$$\tilde{b} = ib, \quad \tilde{p} = ip, \quad \tilde{\alpha} = i\alpha, \quad \tilde{S} = iS. \quad (5.46)$$

Eq. (5.32) then implies

$$\tilde{S} = \int d\tau \left( \tilde{p}\dot{\phi} - \frac{1}{2}\tilde{b}\dot{\nu} + \tilde{\alpha} \left( \tilde{p}^2 - 3\pi G\nu^2 \frac{\sinh^2 \ell_o \tilde{b}}{\ell_o^2} \right) \right). \quad (5.47)$$

We now consider the case when the tilde quantities are real and compute the stationary trajectories of  $\tilde{S}$ . The ‘positive frequency’ (i.e.  $\tilde{p} > 0$ ) trajectories are parameterized by two integration constants,  $\nu_o$  and  $\phi_o$ , and take the form

$$\nu(\phi) = \nu_o \sinh(\sqrt{12\pi G}(\phi - \phi_o)), \quad (5.48)$$

$$\tilde{b}(\phi) = \frac{2 \operatorname{sign}(\nu_o)}{\ell_o} \tanh^{-1}(e^{-\sqrt{12\pi G}|\phi - \phi_o|}). \quad (5.49)$$

They represent universes that go through a singularity at  $\phi = \phi_o$ , where the volume vanishes and  $\tilde{b}$  diverges. As in the ‘classically’ allowed region we have  $|\nu_o| = 2\ell_o\tilde{p}/\sqrt{12\pi G}$ . In terms of the initial and final data, the integration constants are

$$e^{\sqrt{12\pi G}\phi_o} = \sqrt{\frac{e^{\sqrt{12\pi G}\varphi} - \nu_f/\nu_i}{e^{-\sqrt{12\pi G}\varphi} - \nu_f/\nu_i}} \quad (5.50)$$

$$\nu_o = \frac{|\nu_i| \operatorname{sign}(\nu_f - \nu_i)}{\sinh(\sqrt{12\pi G}\varphi)} \sqrt{\left( e^{\sqrt{12\pi G}\varphi} - \frac{\nu_f}{\nu_i} \right) \left( e^{-\sqrt{12\pi G}\varphi} - \frac{\nu_f}{\nu_i} \right)}, \quad (5.51)$$

which, as expected, take real values in the ‘forbidden’ region (5.45). The action can then be evaluated as before. Although now the paths encounter a divergence in  $\tilde{b}$ , the integral (5.47) is convergent and given by the tilde version of (5.38). (Moreover, the product  $\nu(\phi)\tilde{b}(\phi)$  is always finite and vanishes at  $\phi = \phi_o$ .) For the



case when  $\varphi > 0$  and  $\nu_f/\nu_i < e^{-\sqrt{12\pi G}\varphi}$  the result is

$$\begin{aligned} \tilde{S}|_0 = & \frac{\nu_i}{\ell_o} \tanh^{-1} \left( \sqrt{\frac{e^{-\sqrt{12\pi G}\varphi} - \nu_f/\nu_i}{e^{\sqrt{12\pi G}\varphi} - \nu_f/\nu_i}} \right) \\ & - \frac{\nu_f}{\ell_o} \tanh^{-1} \left( e^{\sqrt{12\pi G}\varphi} \sqrt{\frac{e^{-\sqrt{12\pi G}\varphi} - \nu_f/\nu_i}{e^{\sqrt{12\pi G}\varphi} - \nu_f/\nu_i}} \right). \end{aligned} \quad (5.52)$$

Similar expressions hold for other regions. For instance, in the  $\varphi > 0$ ,  $\nu_f/\nu_i > e^{\sqrt{12\pi G}\varphi}$  case the action takes the same form, except that the arguments of the  $\tanh^{-1}$  functions are the reciprocals of the ones appearing in (5.52).

In all cases,  $\tilde{S}|_0$  is negative; the extraction amplitude is exponentially suppressed for paths in the ‘classically forbidden’ regions. But as we approach the dashed curves marking the boundary of the ‘classically’ allowed and forbidden regions, the action  $\tilde{S}$  goes to zero. In particular then, from Fig.5.1 it may appear that for any given  $\nu_i$  there is a significant probability of reaching the singularity  $\nu_f = 0$  for large  $\varphi = \phi_f - \phi_i$ . However, as is common in more familiar systems, the steepest descent approximation also becomes poor in a neighborhood of the dashed curves! Indeed, we know from full LQC that (in the deparameterized framework) the expectation value of  $|\widehat{\nu}|$  tends to *infinity* for large  $\varphi$ . More generally, plots of the exact extraction amplitudes in Sec.5.3.3 will show that the amplitude is always suppressed in the classically forbidden regions. Thus, while the steepest descent approximation provides much physical insight, it is by no means a substitute for the full quantum theory.

### 5.3.2 $\det \delta^2 S|_0$ and the WKB approximation

To compute the amplitude  $(\det \delta^2 S|_0)^{-1/2}$ , one would need a suitable regularization in order to deal with the infinite dimensional determinant. This can be done in ordinary quantum mechanics or field theory, and should as well be doable here. We will however take a different route and calculate this factor by means of the WKB approximation [54, 55].

Note that the extraction amplitude  $A(\nu_f, \phi_f; \nu_i, \phi_i)$  can be thought of as a physical state if one takes the initial data as fixed parameters and the final data

as arguments of the wavefunction: the family of states

$$\Psi_{\nu_i, \phi_i}(\nu_f, \phi_f) := A(\nu_f, \phi_f; \nu_i, \phi_i), \quad (5.53)$$

parameterized by  $\nu_i$  and  $\phi_i$  satisfy the constraint equation

$$\widehat{C} \Psi_{\nu_i, \phi_i} = 0. \quad (5.54)$$

The  $\hbar$  expansions underlying the desired WKB approximation are discussed in Appendix 5.B. We begin with the ansatz for the physical state:

$$\Psi_{\nu_i, \phi_i}(\nu_f, \phi_f) = a(\nu_f, \phi_f; \nu_i, \phi_i) e^{\frac{i}{\hbar} W(\nu_f, \phi_f; \nu_i, \phi_i) + \mathcal{O}(\hbar)}. \quad (5.55)$$

Following the procedure of Appendix 5.B, the imposition of the constraint equation (5.54) to zeroth and first order in  $\hbar$  leads to the following equations for  $a$  and  $W$ :

$$C(\nu_f, \phi_f, \partial_{\nu_f} W, \partial_{\phi_f} W) = 0, \quad \text{and} \quad \mathcal{L}_X a = 0 \quad (5.56)$$

where

$$C(\nu, \phi, b, p_\phi) = p_\phi^2 - 3\pi G \frac{\sin^2 \ell_o b}{\ell_o^2} \nu^2$$

is the ‘effective constraint’, and

$$X = \left. \frac{\partial C}{\partial p_\phi} \right|_{p_\phi = \partial_{q_f} W} \frac{\partial}{\partial q_f}$$

is the vector field on configuration space  $q_f = (\nu_f, \phi_f)$  obtained from the Hamiltonian vector field of the constraint.

The first equation is the Hamilton-Jacobi equation and, as expected, one can check that  $S|_0$  given by (5.44) solves it. The amplitude  $a$  is determined by the second equation together with the condition

$$a(\nu_i, \phi_i; \nu_f, \phi_f) = a(\nu_f, \phi_f; \nu_i, \phi_i) \quad (5.57)$$

which follows from the fact that  $\bar{\Psi}_{\nu_i, \phi_i}(\nu_f, \phi_f) = \Psi_{\nu_f, \phi_f}(\nu_i, \phi_i)$ :

$$a = |\nu_i^2 (e^{\sqrt{12\pi G}\varphi} - \frac{\nu_f}{\nu_i}) (-e^{-\sqrt{12\pi G}\varphi} + \frac{\nu_f}{\nu_i})|^{-1/4}. \quad (5.58)$$

This is the factor we identify with  $(\det \delta^2 S|_0)^{-1/2}$ . Note that this quantity diverges at  $\nu_f = \nu_i e^{\pm\sqrt{12\pi G}\varphi}$  (dashed lines in Fig. 5.1) where the amplitude goes from oscillatory to exponential decay behavior. Thus, the WKB approximation can be valid only away from the dashed lines. This simply mirrors what happens in the WKB approximation in ordinary quantum mechanics.

To summarize, we have succeeded in finding a saddle point approximation of the path integral as in equation (5.35). The determinant factor was not calculated directly but by matching with the terms of a WKB expansion. Therefore, we will call the resulting approximate extraction amplitude  $A^{\text{WKB}}$ :

$$A^{\text{WKB}}(\nu_f, \phi_f; \nu_i, \phi_i) := a e^{\frac{i}{\hbar} S|_0}, \quad (5.59)$$

where  $a$  is given by Eq. (5.58),  $S|_0$  by Eq. (5.44) and as before  $\varphi = \phi_f - \phi_i$ . We now proceed to numerically compare this approximate amplitude with the exact one.

### 5.3.3 Comparison with exact solution

One of the advantages of the model under study is its solvability [38]. In particular, it is possible to obtain a closed form expression of the extraction amplitude  $A(\nu_f, \phi_f; \nu_i, \phi_i)$  [41]. This is displayed in Section 5.C. We calculated the exact solution numerically and compared it with the saddle point approximation obtained in Sec.5.3.2. We found that there is a good agreement away from the dashed lines of Fig. 5.1 which mark the transition between the ‘classically’ allowed region to the ‘classically’ forbidden one. Along the dashed line, however, the WKB amplitude diverges and the approximation fails badly just as in ordinary quantum mechanics.

We illustrate these results in figures 5.2, 5.3 and 5.4. In the first two figures we plot of the real parts of the exact and WKB amplitudes as a function of  $\nu_f$  and  $\phi_f$  respectively, for fixed values of the remaining variables. The exact amplitude shows a sudden transition from oscillatory to decaying behavior. If one had access

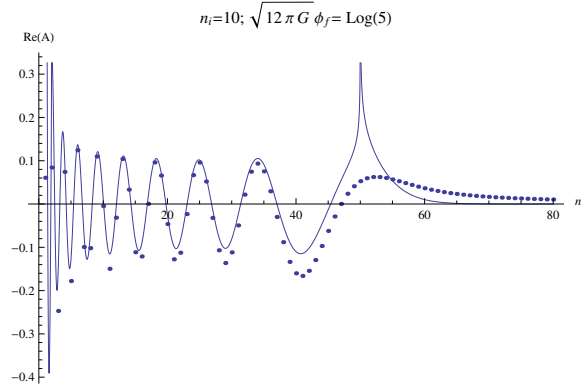


**Figure 5.2.** Real parts of the exact and WKB amplitudes are plotted as a function of the final volume  $n_f := \nu_f/4\ell_o\hbar$ . The exact amplitude (dots) has support on the ‘lattice’  $(\nu_f - \nu_i)/4\ell_o\hbar \in \mathbb{Z}$ . At  $n_f = n_i e^{\sqrt{12\pi G}(\phi_f - \phi_i)} = 50$  there is the transition from oscillatory to exponential behavior, and the WKB amplitude (solid line) diverges. (It also diverges at  $n_f = n_i e^{-\sqrt{12\pi G}(\phi_f - \phi_i)} = 2$ .) Here,  $\phi_i, \nu_i$  and  $\phi_f$  are kept fixed:  $\phi_i = 0$ ,  $n_i := \nu_i/4\ell_o\hbar = 10$  and  $\sqrt{12\pi G}\phi_f = \log 5$ .

only to the exact result, this behavior would have seemed rather puzzling. The WKB approximation provides a physical understanding of this behavior. Thus, not only does the WKB approximation reproduce the qualitative behavior of the exact extraction amplitude away from the dashed lines of Fig.5.1, but it anticipates that the dashed lines mark a boundary between two quite different behaviors of the exact answer and provides a physical understanding of this difference.

What can we say regarding the regime of validity of the saddle point approximation? From the path integral perspective, we expect it to be valid whenever  $S/\hbar \gg 1$ . From Eq. (5.44), we see that  $S|_0$  scales with the volume times a coefficient which can be interpreted as measuring the departure from the dashed lines  $\nu_f = \nu_i e^{\pm\sqrt{12\pi G}|\varphi|}$ . At these lines  $S|_0 = 0$  and, as we have just seen, the approximation totally breaks down. As we depart from these lines,  $S|_0$  takes a nonzero value, and its scale is given by the initial and final volume. For instance, if we keep the ratio  $\nu_f/\nu_i$  fixed, the action grows linearly with  $\nu_i$  and we expect the approximation to improve as  $\nu_i$  increases. This behavior is indeed observed, an example of which is display in Figure 5.4. Thus, the standard expectations on the validity of the WKB approximation are all borne out.

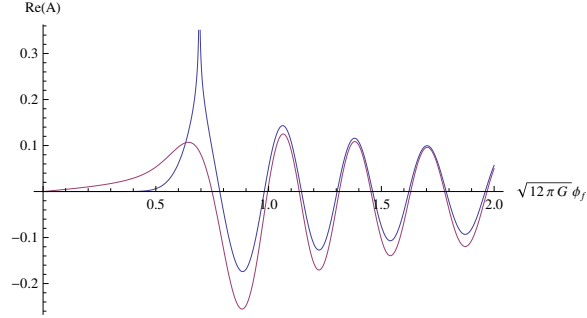


**Figure 5.3.** Real parts of the exact and WKB amplitudes are plotted as a function of the final scalar field  $\phi_f$ . Here  $\phi_i, \nu_i$  and  $\nu_f$  are kept fixed:  $\phi_i = 0, n_i := \nu_i/4\ell_o\hbar = 10$  and  $n_f := \nu_f/4\ell_o\hbar = 20$ . The WKB solution is the curve diverging at  $\sqrt{12\pi G}\phi_f = \log(\nu_f/\nu_i) = \log 2$ .

## 5.4 Discussion

Loop quantum cosmology is a canonical quantization of the homogenous sector of GR which incorporates key ingredients from full loop quantum gravity. Here we explored the ways this theory could be described from the perspective of path integrals.

We first outlined how a configuration-space ‘path-integral’ can be constructed. The non-standard inner product  $\langle \nu' | \nu \rangle = \delta_{\nu'\nu}$  manifests in that the resulting expansion takes the form of a sum over ‘quantum paths’ rather than over classical configuration-space trajectories. The structure is reminiscent of spinfoams, a framework that aims at constructing the path integral for LQG [34]. We did not touch upon many aspects of this construction, such as convergence, the role of the scalar field as regulator, and a more detailed comparison with spinfoams, which have been analyzed in detail in [51].

Rather, we focused on a second path integral construction. As opposed to the first example, here one integrates over classical (phase-space) trajectories, whose weights take the standard form of an exponential of  $\frac{i}{\hbar}$  times an action. This action, obtained as the result of a systematic derivation from the canonical theory, is not the classical Einstein-Hilbert action but a modified version that includes quantum geometry corrections. Note that such a change of action in the transition from the Hamiltonian quantum theory to a path integral can occur already in much simpler systems. For example, for a particle moving on a Riemannian manifold, dynam-

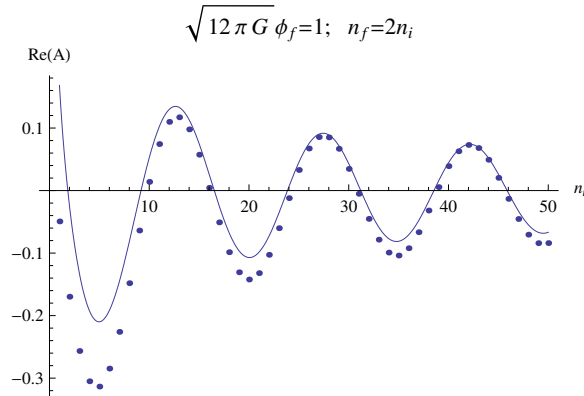


**Figure 5.4.** Comparison of the exact and WKB amplitudes for initial and final configurations with  $\nu_f = 2\nu_i$  as a function of  $n_i := \nu_i/4\ell_o\hbar$ . As  $n_i$  increases, the WKB solution (continuous line) becomes closer to the exact solution (dots). (The distance between the amplitudes oscillates, but overall it decreases.) This calculation was done for  $\phi_i = 0$  and  $\phi_f = 1/\sqrt{12\pi G}$ .

ics generated by the *standard* Hamiltonian operator,  $\hat{H} = -(\hbar^2/2m) g^{ab} \nabla_a \nabla_b$ , is correctly captured in the path integral framework only if one adds to the classical action an  $\hbar$  dependent term that depends on the scalar curvature of the Riemannian metric [53].

Our discussion resolves an apparent tension regarding the singularity resolution in LQC: From a naive path integral perspective, quantum effects near the classical singularity should be negligible, since there the Einstein-Hilbert action becomes very large as compared to  $\hbar$ . How could then there be large quantum effects producing a bounce? Such reasoning does not take into account possible quantum correction to the action itself. And as we have seen, these corrections are crucial. Indeed, in this case the equations of motion of the corrected action can be obtained explicitly. These equations and their solutions describe bouncing cosmologies which are characteristic of the singularity resolution in LQC. Thus the exact results on singularity resolution in LQC are in complete harmony with the path integral intuition, once one realizes that the action that descends from the Hamiltonian theory includes quantum geometry corrections. Furthermore, because we have an additional constant in the theory—the Barbero-Immirzi parameter—it is meaningful to consider  $\hbar$  expansions while retaining quantum geometry effects. This is achieved by sharpening the precise manner in which the limit is taken:

$\hbar \rightarrow 0$ ,  $\gamma \rightarrow \infty$  such that  $\hbar\gamma^3 = \text{const.}$  This  $\hbar$  expansion enables us to introduce the WKB approximation which helps one understand features of the exact amplitude, e.g., the oscillatory versus damping behavior that occurs as one varies the final configuration  $(\nu_f, \phi_f)$  keeping the initial configuration  $(\nu_i, \phi_i)$  fixed. It also provides an ‘explanation’ of the surprising effectiveness of the effective equations [56] in LQC from a path integral framework.

Thus, from the LQC perspective, it would be incorrect to simply define the theory starting with smooth metrics and matter fields and assigning to each path the weight that comes from the Einstein Hilbert action because this procedure completely ignores the quantum nature of the underlying Riemannian geometry. For a satisfactory treatment of ultraviolet issues such as the singularity resolution, it is crucial that the calculation retains appropriate memory of this quantum nature. This viewpoint can be traced back to full LQG and spinfoam models. In full LQG, quantum geometry is an essential feature already of *kinematics*. It is then not surprising that in spinfoams the histories that one sums over are *quantum* geometries. This situation is parallel to the configuration space path integral discussed in Section 5.1. In LQC we were fortunate in that the integral over quantum paths could be recast into an integral over all paths in the classical phase space. This enabled us to carry out the steepest descent approximation and develop physical intuition for the qualitative properties of the exact extraction amplitude. A similar reformulation of spinfoams of the full theory appears to be difficult. But if it could somehow be achieved, one would have a powerful tool both to probe semi-classical aspects of full quantum gravity and to develop valuable intuition for the ultraviolet properties of the theory. In particular, the resulting quantum geometry corrections to the full Einstein-Hilbert action would bring the difference between spin foams and perturbative path integrals into sharp focus.

## 5.A Appendix: Path integrals for polymerized free particle

This appendix parallels the analysis of the chapter, but with the system under study being a ‘polymerized’ free particle [45, 57]. In particular we will be dealing

with a true Hamiltonian and evolution operator rather than with a constraint equation. Along the analysis of this model, we will prove some general results that were used in the main body of the chapter. There will also be a difference with the LQC analysis regarding the saddle point approximation, Section 5.A.3. The simplicity of the model allows one to directly compute the  $\hbar \rightarrow 0$  asymptotics of the transition amplitude by means of a standard, one-dimensional saddle point approximation. Instead of reproducing the analysis we did in the LQC case, Section 5.3, we will directly evaluate the  $\hbar \rightarrow 0$  limit and then verify the result is in agreement with the expected one from path integrals.

Let us now specify the model. Starting with the classical free particle phase space  $(x, p)$ , we consider a ‘polymer’ quantization given by a Hilbert space of wave functions  $\psi(x)$  with inner product,

$$\|\psi\|^2 = \sum_{x \in \mathbb{R}} |\psi(x)|^2. \quad (5.60)$$

The classical Hamiltonian  $H = p^2/2m$  has to be regularized in order to admit a quantization on this Hilbert space. One possible regularization can be obtained by introducing a momentum cutoff  $\Lambda$  and defining

$$H_\Lambda := \frac{\Lambda^2}{m} [1 - \cos(\frac{p}{\Lambda})] = p^2/2m + O(\Lambda^{-2}). \quad (5.61)$$

For fixed  $\Lambda$ , the resulting quantum theory corresponds to a particle on a lattice  $a\mathbb{Z} \subset \mathbb{R} + \epsilon$ , with  $a = \hbar/\Lambda$  and  $0 \leq \epsilon < a$ . This is the system we will focus on.

One may argue whether such system should be regarded as a genuine ‘polymer’ system, since issues of non-separability of the Hilbert space can be sidestepped by restricting oneself to independent lattices. We note however that the same property holds for the LQC system we studied, and so it will suffice for our purposes. We should also point out that, from the two path integrals –configuration and phase space– it is the second one that makes heavily use of this lattice property. The formulation of the first one is completely general, although the lattice property does simplify the computations.

In the polymer Hilbert space given by (5.60), the Hamiltonian (5.61) has a



straightforward quantization given by

$$(\hat{H}_\Lambda \psi)(x) = \Lambda^2/m \left( \psi(x) - \frac{\psi(x+a) + \psi(x-a)}{2} \right), \quad (5.62)$$

which can be thought of as a discretization of the standard operator  $-\hbar^2/(2m)\nabla^2$ . Our object of interest will be the transition amplitude, defined by the matrix element of the evolution operator:

$$U(x_f, x_i; t) := \langle x_f | e^{-\frac{i}{\hbar} t \hat{H}_\Lambda} | x_i \rangle. \quad (5.63)$$

Our objective is to find the path integral descriptions for this transition amplitude, following the standard Feynman prescription. We will discuss two possible path integrals, one in configuration space and the other one in phase space. The first construction is general and holds for any discrete basis, not just for systems on a lattice like the present one. On the other hand, the phase space path integral does rely on the ability to restrict oneself to a lattice.

### 5.A.1 Configuration space path integral

The first step is to express the transition amplitude (5.63) as a composition of infinitesimal evolutions. Dividing the total time  $t$  in  $N$  time intervals of length  $\epsilon = t/N$ , one has

$$U(x_f, x_i; t) = \sum_{\bar{x}_{N-1}, \dots, \bar{x}_1} \langle x_f | e^{-\frac{i}{\hbar} \epsilon \hat{H}_\Lambda} | \bar{x}_{N-1} \rangle \langle \bar{x}_{N-1} | e^{-\frac{i}{\hbar} \epsilon \hat{H}_\Lambda} | \bar{x}_{N-2} \rangle \dots \langle \bar{x}_1 | e^{-\frac{i}{\hbar} \epsilon \hat{H}_\Lambda} | x_i \rangle \quad (5.64)$$

where we have first split the exponential into  $N$  identical terms and then introduced a decomposition of the identity operator at each intermediate time  $t_n = n\epsilon$ ,  $n = 1, 2, \dots, N-1$ . Equation (5.64) can be thought of as a sum over ‘discrete-time’ paths. Notice that, even though initially each sum ranges over all reals,  $x_n \in \mathbb{R}$ , only countably number of terms are non-vanishing, namely those where  $x_n - x_i \in a\mathbb{Z}$ .

The next step in the standard path integral construction is to take the ‘continuum time’ limit,  $N \rightarrow \infty$ , of the skeletonization. Here is where the difference with the ordinary case comes into play, since we have sums over  $x_n$  as opposed to

integrals.

The idea is to rearrange the sum (5.64) according to paths that are piecewise constant, with a given number of transitions. A path with  $M$  transitions corresponds to a discrete-time path of the form,

$$(x_M, \dots, x_M; x_{M-1}, \dots, x_{M-1}; \dots \dots; \overbrace{x_1, \dots, x_1}^{N_2}; \underbrace{x_0, \dots, x_0}_{N_1}), \quad (5.65)$$

where  $N_m$  denotes the time-step at which the  $m$ -th transition takes place. For fixed  $N$ , all paths take this form, with  $0 \leq M \leq N$ . Thus, the total sum in (5.64) can be reorganized as

$$\sum_{\bar{x}_{N-1}, \dots, \bar{x}_1} = \sum_{M=0}^N \sum_{N_M=M}^{N-1} \sum_{N_{M-1}=M-1}^{N_M-1} \dots \sum_{N_1=1}^{N_2-1} \sum_{\substack{x_{M-1}, \dots, x_1 \\ x_m \neq x_{m+1}}}, \quad (5.66)$$

where a path on the right hand side is labeled by its transition number  $M$ , the ‘transition times’  $N_m$ , and the intermediate positions  $x_{M-1}, \dots, x_1$ , corresponding to a discrete-time path of the form (5.66).

As shown in [42], this rearrangement allows one to take the  $N \rightarrow \infty$  limit, where one obtains

$$U(x_f, x_i; t) = \sum_{M=0}^{\infty} \int_{t > t_M > \dots > t_1 > 0} dt_M \dots dt_1 \sum_{\substack{x_{M-1}, \dots, x_1 \\ x_m \neq x_{m+1}}} A(x_M, \dots, x_0; t_M, \dots, t_1) \quad (5.67)$$

where the amplitude of each ‘continuous-time’ path is given by

$$A(x_M, \dots, x_0; t_M, \dots, t_1; ) = e^{-\frac{i}{\hbar}(t-t_M)H_{x_M x_M}} \left(-\frac{i}{\hbar}H_{x_M x_{M-1}}\right) \times \dots e^{-\frac{i}{\hbar}(t_2-t_1)H_{x_1 x_1}} \left(-\frac{i}{\hbar}H_{x_1 x_0}\right) e^{-\frac{i}{\hbar}t_1 H_{x_0 x_0}}, \quad (5.68)$$

where,

$$H_{yx} \equiv \langle y | \hat{H}_\Lambda | x \rangle. \quad (5.69)$$

We now provide a proof of equation (5.67), which does not involve the ‘continuous-time’ limiting procedure. Expression (5.67) is reminiscent of a perturbative expansion

sion, with the number of transitions playing the role of the order of the perturbation. The transitions are being weighted by off-diagonal matrix elements  $H_{yx}$  with  $y \neq x$ . This motivates to consider a splitting of the Hamiltonian into its diagonal and off-diagonal parts:

$$\hat{H}_\Lambda = \hat{D} + \hat{K}, \quad (5.70)$$

where the matrix elements of  $\hat{D}$  and  $\hat{K}$  are given by:

$$D_{yx} = H_{xx} \delta_{yx}, \quad K_{yx} = \begin{cases} H_{yx} & y \neq x \\ 0 & y = x. \end{cases} \quad (5.71)$$

We now consider expressing the evolution operator  $U(t) = e^{-\frac{i}{\hbar}\hat{H}_\Lambda t}$  using perturbation theory, with  $\hat{D}$  playing the role of unperturbed Hamiltonian and  $\hat{K}$  the perturbation. Following the textbook procedure, we define the interaction Hamiltonian as

$$\hat{H}_I(t) := e^{\frac{i}{\hbar}t\hat{D}} \hat{K} e^{-\frac{i}{\hbar}t\hat{D}}. \quad (5.72)$$

Then the evolution in the interaction picture is dictated by the operator

$$\tilde{U}(t) = e^{\frac{i}{\hbar}t\hat{D}} e^{-\frac{i}{\hbar}t\hat{H}_\Lambda}, \quad \text{satisfying} \quad \frac{d\tilde{U}(t)}{dt} = -\frac{i}{\hbar}\hat{H}_I(t)\tilde{U}(t). \quad (5.73)$$

The solution of this equation is given by a time-ordered exponential:

$$\begin{aligned} \tilde{U}(t) &= \mathcal{T} e^{-\frac{i}{\hbar}\int_0^t \hat{H}_I(t') dt'} \\ &= \sum_{M=0}^{\infty} \int_0^t dt_M \int_0^{t_M} dt_{M-1} \dots \int_0^{t_2} dt_1 [-\frac{i}{\hbar}\hat{H}_I(t_M)] \dots [-\frac{i}{\hbar}\hat{H}_I(t_1)]. \end{aligned} \quad (5.74)$$

Upon inserting a complete basis in between each product  $[\hat{H}_I(t_{m+1})][\hat{H}_I(t_m)]$ , one recovers (5.67).

So far we have not referred to the particular form of the Hamiltonian (5.61), and the result (5.67) is very general. In particular it applies to the  $\Theta$  operator of the LQC example, providing the proof of equations (5.9) and (5.10).

We now specialize to the polymer free particle case. The matrix elements of

the Hamiltonian (5.61) are given by

$$\langle y | \hat{H}_\Lambda | x \rangle = \begin{cases} \frac{\Lambda^2}{m} & \text{if } y = x \\ -\frac{\Lambda^2}{2m} & \text{if } y - x = \pm a \\ 0 & \text{otherwise} \end{cases} \quad (5.75)$$

Thus, the only non-trivial amplitudes are the ones given by sequences

$$(x_M, \dots, x_m, x_{m+1}, \dots, x_0) \quad (5.76)$$

such that  $x_{m+1} - x_m = \pm a$ . From the form of the matrix elements (5.75), it is easy to verify that such amplitudes only depend on the total number of transitions  $M$ , and are given by

$$A_{\text{path with } M \text{ transitions}} = \left( \frac{i\Lambda^2}{2m\hbar} \right)^M e^{-\frac{it\Lambda^2}{m\hbar}}. \quad (5.77)$$

The sum over different paths in (5.67) is then given by a combinatorial factor that we now compute. Let

$$n := (x_f - x_i)/a, \quad (5.78)$$

with  $n \in \mathbb{Z}$  (for otherwise the total amplitude is zero). The combinatorial factor is given by the number of ways of going from 0 to  $n$  by  $\pm 1$  transitions, with  $M$  total transitions. Let  $M_+$  and  $M_-$  be the number of  $+1$  and  $-1$  transitions respectively, so that  $M = M_+ + M_-$  and  $n = M_+ - M_-$ . For concreteness let us take  $n \geq 0$ . The possible values  $M$  can take are then given by

$$M = 2M_- + n, \quad M_- = 0, 1, \dots \quad (5.79)$$

and the total number of paths with given  $M_-$  is  $\binom{M}{M_-}$ . The remaining piece of the total amplitude (5.67) is given by the time integrals. Since the amplitudes are independent of the transitions time, this simply gives a  $\frac{t^M}{M!}$  overall factor. Thus

(5.67) reduces to

$$U(x_f, x_i; t) = e^{-\frac{it\Lambda^2}{m\hbar}} \sum_{M_-=0}^{\infty} \frac{1}{(M_- + n)!M_-!} \left(\frac{it\Lambda^2}{2m\hbar}\right)^{2M_-+n}. \quad (5.80)$$

A Bessel function can be recognized in the sum, and the total amplitude is given by

$$U(x_f, x_i; t) = i^{|n|} e^{-\frac{it\Lambda^2}{m\hbar}} J_{|n|} \left(\frac{t\Lambda^2}{m\hbar}\right) \quad (5.81)$$

where we now wrote the final result for arbitrary sign of  $n = (x_f - x_i)/a$ . One can verify that (5.81) satisfies the Schrodinger equation<sup>3</sup> with respect to the Hamiltonian (5.61) with initial condition  $U(x_i, x_f; 0) = \delta_{x_i x_f}$ , and so it represents the correct expression for the matrix elements of the evolution operator  $U(t) = e^{-\frac{i}{\hbar}\hat{H}\Delta t}$ .

This type of expansion shares some of the expected properties of spin foam-type path integrals, where paths are given by sequences of spin-network, but at the same time it is completely different from standard path integrals, where amplitudes are weighted by the classical action. In particular, it does not seem to be suited for semiclassical analysis. In the next section, we will see how, for the polymer free particle model, it is possible to construct an alternative path integral of the ‘standard’ form, that among other things allows one to extract the semiclassical approximation.

## 5.A.2 Phase space path integral

The special property that  $\hat{H}_\Lambda$  only involves shifts of constant lengths  $a$ , allows one to restrict attention to a lattice  $a\mathbb{Z} \subset \mathbb{R}$  and thus work in the now separable Hilbert space of sequences  $\psi_n \equiv \psi(an)$ . This space admits a momentum basis given by

$$\langle an|p\rangle = \frac{e^{inp/\Lambda}}{\sqrt{2\pi\Lambda}}, \quad (5.82)$$

with  $p \in (-\pi\Lambda, \pi\Lambda)$ . Further simplification of this model, which is absent in the LQC case, is that the Hamiltonian (5.61) is diagonal in this basis, and so the

---

<sup>3</sup>This follows from the property of the Bessel function:  $2dJ_n/ds(s) + J_{n+1}(s) - J_{n-1}(s) = 0$ .

evolution operator can be written as

$$U(an_f, an_i; t) = \frac{1}{2\pi\Lambda} \int_{-\pi\Lambda}^{\pi\Lambda} dp e^{i(n_f - n_i)p/\Lambda - i\frac{\Lambda^2}{m\hbar}(1 - \cos p/\Lambda)}. \quad (5.83)$$

Let us now go back to the ‘discrete-time’ sum over paths (5.64), and use (5.83) to express each of the ‘infinitesimal’ evolutions. The result is a ‘discrete-time’ phase-space path integral:<sup>4</sup>

$$U(x_f, x_i; t) = (2\pi\Lambda)^{-N} \sum_{x_{N-1}, \dots, x_1} \int dp_N \dots dp_1 e^{\frac{i}{\hbar} S_N}, \quad (5.84)$$

where  $x_k \in a\mathbb{Z}$ ,  $p \in (-\pi\Lambda, \pi\Lambda)$ , and

$$S_N = \epsilon \sum_{k=0}^{N-1} \left( p_k \frac{x_{k+1} - x_k}{\epsilon} - \frac{\Lambda^2}{m} (1 - \cos \frac{p_k}{\Lambda}) \right). \quad (5.85)$$

This now resembles a more standard path integral, except for the fact that the paths being integrated are not the standard ones. Similar situation occurs in the construction of the path integral for a particle in a circle [58], where by means of the identity

$$\sum_{m \in \mathbb{Z}} \int_0^{2\pi} d\theta f(\theta, m) e^{im\theta} = \int_{-\infty}^{\infty} dx \int_{-\infty}^{\infty} d\theta f(\theta, x) e^{ix\theta}, \quad (5.86)$$

which holds for any continuous  $f(\theta, x)$  with a  $2\pi$  period in  $\theta$ , one can obtain the usual paths. Applying this in (5.84), one obtains

$$U(x_f, x_i; t) = (2\pi)^{-N} \int dx_{N-1} \dots dx_1 \int dp_N \dots dp_1 e^{\frac{i}{\hbar} S_N}, \quad (5.87)$$

where the integrals are over all reals, except for the  $p_N$  one that remains with the original domain. The formal  $N \rightarrow \infty$  limit of expression (5.87) defines the

---

<sup>4</sup>Unlike the LQC case, we do not need to use small  $\epsilon$  approximations, since  $|p\rangle$  diagonalizes the Hamiltonian, compare with equation (5.24).

standard phase space path integral:

$$U(x_f, x_i; t) = \lim_{N \rightarrow \infty} \text{RHS of (5.87)} =: \int \mathcal{D}x \mathcal{D}p e^{\frac{i}{\hbar} S}, \quad (5.88)$$

with

$$S = \int_0^t dt' (p \dot{x} - H_\Lambda), \quad (5.89)$$

$H_\Lambda = \frac{\Lambda^2}{m} (1 - \cos \frac{p}{\Lambda})$ , and the integral is over phase space paths with fixed configuration endpoints  $x_i$  and  $x_f$ . Among other things, this path integral can be used to obtain a formal  $\hbar$  expansion, whose leading term is given by the saddle point approximation:

$$U(x_f, x_i; t) \sim (\det \delta^2 S|_{\text{cl}})^{-1/2} e^{\frac{i}{\hbar} S|_{\text{cl}}}, \quad (5.90)$$

where  $S|_{\text{cl}}$  is the action evaluated along the trajectory extremizing the action with initial and final configuration points fixed, and the prefactor  $(\det \delta^2 S|_{\text{cl}})^{-1/2}$  represents a formal infinite dimensional determinant.

We will now study the  $\hbar \rightarrow 0$  behavior of the transition amplitude, directly from expression (5.81), and verify it is given by the saddle point approximation (5.90).

### 5.A.3 Saddle point approximation

The trajectories extremizing the action are those obeying the equations of motion of the Hamiltonian  $H_\Lambda$ . These are given by

$$\begin{aligned} p(t') &= \text{constant} \\ x(t') &= x_i + \frac{\Lambda}{m} \sin(p/\Lambda) t', \end{aligned} \quad (5.91)$$

and represent a particle moving at a velocity  $v = \frac{\Lambda}{m} \sin(\frac{p}{\Lambda})$ . For the saddle point evaluation (5.90), we need to find the trajectory for given initial and final positions  $x_i$  and  $x_f$  and total time  $t$ . This is given by (5.91) with  $p$  determined by

$$\sin(p/\Lambda) = \frac{m}{\Lambda} \frac{x_f - x_i}{t}, \quad (5.92)$$

which has real solutions provided that,

$$\left| \frac{x_f - x_i}{t} \right| \leq \frac{\Lambda}{m}. \quad (5.93)$$

For strict inequality, there exist two trajectories, one with  $|p| < \pi\Lambda/2$  and the other one with  $|p| > \pi\Lambda/2$  (only trajectories with  $|p| \leq \pi\Lambda$  contribute since the final value of  $p$  in the path integral has to be in this range, see Eq. (5.87)). The action evaluated along these trajectories is

$$\begin{aligned} S_+ &= t\Lambda \left( v \arcsin v/v_{\max} + \sqrt{v_{\max}^2 - v^2} - v_{\max} \right), & |p| < \pi\Lambda/2 \\ S_- &= t\Lambda \left( v(\pi - \arcsin v/v_{\max}) - \sqrt{v_{\max}^2 - v^2} - v_{\max} \right), & |p| > \pi\Lambda/2 \end{aligned} \quad (5.94)$$

where

$$v := (x_f - x_0)/t \quad (5.95)$$

$$v_{\max} := \Lambda/m. \quad (5.96)$$

When  $|v| = \Lambda/m$ , the two solutions collapse to a single one. The region  $|v| > \Lambda/m$  represents ‘classically forbidden’ configurations, which will correspond to exponentially suppressed amplitudes. For  $|v| < \Lambda/m$ , the saddle point approximation will then involve the two terms (5.94). Each term will contain the  $(\det \delta^2 S|_{\text{cl}})^{-1/2}$  pre-factor, which can be calculated by the WKB method as we did in Section 5.3. Instead of repeating that procedure, we will now directly compute the  $\hbar \rightarrow 0$  asymptotics of  $U(x_i, x_f; t)$  and verify it reproduces the expected saddle point/WKB approximation. To this end, we start by the integral representation (5.83). Defining

$$z := e^{-ip/\Lambda} \quad (5.97)$$

$$s := \frac{t\Lambda^2}{m\hbar} = t\Lambda v_{\max}/\hbar \quad (5.98)$$

we obtain the following contour integral representation,

$$U(x_f, x_i; t) = \frac{e^{-is}}{2\pi i} \oint z^{-(n+1)} e^{i\frac{s}{2}(z+z^{-1})} dz, \quad (5.99)$$



where the contour is the counterclockwise unit circle, and as before  $n = (x_f - x_i)/a \in \mathbb{Z}$ . Bringing the  $\hbar$  factors explicitly, (5.99) reads,

$$U(x_f, x_i; t) = \frac{e^{-it\Lambda v_{\max}/\hbar}}{2\pi i} \oint z^{-1} e^{f(z)/\hbar} dz, \quad (5.100)$$

with

$$f(z) = t\Lambda \left( i v_{\max} (z + z^{-1})/2 - v \ln z \right). \quad (5.101)$$

We now apply the standard, one-dimensional,  $\hbar \rightarrow 0$  saddle-point approximation to the integral (5.100):

$$\oint z^{-1} e^{f(z)/\hbar} dz = \sum_k \sqrt{2\pi\hbar/|f''(z_k)|} z_k^{-1} e^{f(z_k)/\hbar} e^{i\alpha_k}, \quad (5.102)$$

where  $\alpha_k = (\pi - \arg f''(z_k))/2$  and one is summing over points  $z_k$  such that  $f'(z_k) = 0$ , see for instance [59]. The solutions of  $f'(z) = 0$ , given by

$$z_{\pm} = (-iv \pm \sqrt{v_{\max}^2 - v^2})/v_{\max}, \quad (5.103)$$

divide into two classes, depending whether  $|v|$  is smaller or greater than  $v_{\max}$ . They will correspond respectively to oscillatory and damped behavior. We now study each case separately.

In the  $|v| < v_{\max}$  case,  $|z_{\pm}| = 1$  and the integration contour picks up both solutions.  $f(z_{\pm})$  is purely imaginary and given by

$$f(z_+) = it\Lambda \left( v \arcsin v/v_{\max} + \sqrt{v_{\max}^2 - v^2} \right), \quad (5.104)$$

$$f(z_-) = it\Lambda \left( v(\pi - \arcsin v/v_{\max}) - \sqrt{v_{\max}^2 - v^2} \right), \quad (5.105)$$

and corresponds to the two solutions (5.94). This can also be seen by writing  $v = v_{\max} \sin(p/\Lambda)$  then  $z_+ = e^{-ip/\Lambda}$  and  $z_- = e^{-i(\pi-p/\Lambda)}$ . In terms of these quantities, we have

$$f''(z_{\pm}) = \pm i e^{\pm i2p/\Lambda} t\Lambda \sqrt{v_{\max}^2 - v^2}. \quad (5.106)$$

Combining all the elements and using formula (5.102) we obtain

$$U(x_f, x_i; t) \approx \sqrt{\frac{\hbar}{2\pi it\Lambda\sqrt{v_{\max}^2 - v^2}}} (e^{iS_+/\hbar} + ie^{iS_-/\hbar}), \quad (5.107)$$

with  $S_{\pm}$ ,  $v$  and  $v_{\max}$  given by Eqs. (5.94), (5.95), (5.96).

For the  $|v| > v_{\max}$  case, let us assume for simplicity that  $v > 0$  and write  $v = v_{\max} \cosh q$  with  $q > 0$ . The solutions are then given by  $z_{\pm} = -ie^{\pm q}$ . The contour of integration can now be moved such that it goes to either  $z_+$  or  $z_-$ . The correct asymptotics is the one giving the exponential decay. For  $t > 0$ , this is given by  $z_-$ , with  $f(z_-) = t\Lambda(-qv + v_{\max} \sinh q + iv\pi/2)$  and  $f''(z_-) = -t\Lambda v_{\max} e^{-2q} \sinh q$ . This leads to the following asymptotic formula ( $v > 0$ ,  $t > 0$  case)

$$U(x_f, x_i; t) \approx -\sqrt{\frac{\hbar}{2\pi t\Lambda\sqrt{v^2 - v_{\max}^2}}} e^{\frac{t\Lambda}{\hbar} (v(i\pi/2 - \operatorname{arccosh} v/v_{\max} + \sqrt{v^2 - v_{\max}^2} - iv_{\max}))}, \quad (5.108)$$

and can be interpreted as the action along a path with imaginary momentum, as in the LQC example. Furthermore, one can verify the prefactors in (5.107) and (5.108) satisfy the analogue of the WKB equation (5.116).

To summarize, the saddle point approximation provides the following picture for the behavior of the transition amplitude  $U(x_i, x_f; t)$ , depending on whether the velocity (5.95) is greater or smaller in absolute value to the maximum velocity (5.96). For  $|v| < |v_{\max}|$  there exist two trajectories connecting the endpoints yielding real actions and an oscillatory amplitude.  $|v| > |v_{\max}|$  is ‘classically forbidden’ yielding a complex action and an exponentially damped amplitude. The saddle point approximation breaks down as  $|v| \rightarrow |v_{\max}|$ . These features are illustrated in Figures 5.5 and 5.6 where we compare the exact transition amplitude (5.81) with its saddle point approximation (5.107) and (5.108) for some particular values of the variables.

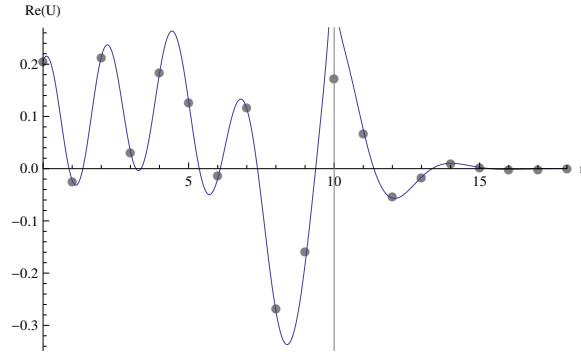


**Figure 5.5.** Real part of transition amplitude (5.81) as a function of  $n = (x_f - x_i)/a$  for  $s = t\Lambda^2/(m\hbar) = 10$  (dots) and its saddle point approximation (solid line).  $n = 10$  marks the transition between real and complex actions.

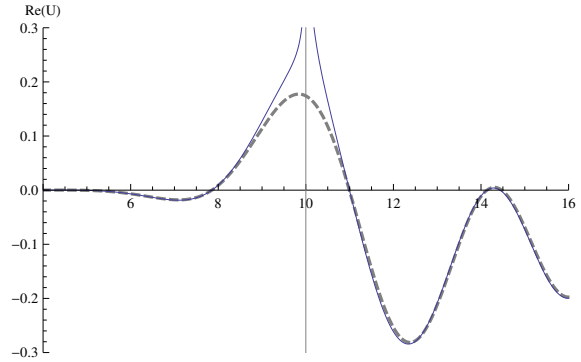


**Figure 5.6.** Real part of transition amplitude (5.81) as a function of  $s = t\Lambda^2/(m\hbar)$  for  $n = 10$  (dashed line) and its saddle point approximation (solid line).  $s = 10$  marks the transition between real and complex actions.

## 5.B Appendix: WKB approximation for constrained systems

Let us consider a system with phase space  $\mathbb{R}^{2n}$  and a single constraint  $C(q, p) = 0$ , to be thought of as the Hamiltonian constraint. We will assume that the  $C(q, p)$  can be written as a Taylor expansion in the  $p$ , as is the case for a large class of physically interesting systems.

The kinematic Hilbert space is  $L^2(\mathbb{R}^n)$  of normalizable wave functions  $\Psi(q) \equiv \Psi(q^1, \dots, q^n)$ . The elementary operators are the usual  $\hat{q}^j$  and  $\hat{p}_j$  which act by

multiplication and derivation respectively:

$$\hat{q}^j \Psi(q) = q^j \Psi(q) \quad (5.109)$$

$$\hat{p}_j \Psi(q) = -i\hbar \frac{\partial \Psi}{\partial q^j}(q). \quad (5.110)$$

The physical states are then solutions to the quantum constraint:

$$\hat{C} \Psi = 0, \quad (5.111)$$

where  $\hat{C}$  is an operator analog of  $C(q, p)$ , obtained by replacing  $q, p$  with  $\hat{q}^j$  and  $\hat{p}_j$  with a suitable choice of factor ordering. As is standard in the group averaging procedure, we will assume that  $\hat{C}$  is self-adjoint. For unconstrained systems, the WKB ansatz provides approximate solutions to the Schrödinger equation. In this Appendix we will extend that method to obtain approximate solutions of (5.111) where, again,  $\hbar$  plays the role of small parameter governing the expansion. As one might expect, the main idea is to write both  $\hat{C}$  and  $\Psi$  in (5.111) as expansions in  $\hbar$ , and to collect terms having the same  $\hbar$  power. Let us now explicitly calculate the zeroth and first order terms.

The construction is as follows. First, the constraint operator  $\hat{C}$  is written as a sum of ‘normal ordered’ operators, in which all  $\hat{q}$ ’s appear to the left of the  $\hat{p}$ ’s:

$$\hat{C} = \sum_{n=0}^{\infty} (\hbar/i)^n C_n(\overset{\text{L}}{\hat{q}}, \overset{\text{R}}{\hat{p}}). \quad (5.112)$$

Here the  $C_n$ ’s are functions on the classical phase space—for instance,  $C_0$  will typically be the classical constraint function—which are now ‘evaluated’ on the operators  $\hat{q}$  and  $\hat{p}$  according to the ‘normal ordered’ prescription indicated by the superscripts. Second, the unknown state  $\Psi(q)$  is written as the exponential

$$\Psi(q) = e^{\frac{i}{\hbar} S(q)} \quad (5.113)$$

where the exponent is written as a power series in  $\hbar$ :

$$S(q) = \sum_{n=0}^{\infty} (\hbar/i)^n S_n(q). \quad (5.114)$$

Since  $C(q, p)$  is assumed to admit a Taylor expansion in the  $p$ , so do  $C_n(q, p)$ . Imposition of the quantum constraint (5.111) now leads to the following zeroth and first order equations:

$$C_0(q, \partial_q S_0) = 0, \quad (5.115)$$

$$\frac{1}{2} \frac{\partial^2 C_0}{\partial p_i \partial p_j} \Big|_{p=\partial_q S_0} \frac{\partial^2 S_0}{\partial q^i \partial q^j} + \frac{\partial C_0}{\partial p_i} \Big|_{p=\partial_q S_0} \frac{\partial S_1}{\partial q^i} + C_1(q, \partial_q S_0) = 0 \quad (5.116)$$

The zeroth order equation (5.115) can be recognized as the Hamilton-Jacobi equation. The first order one, (5.116), can be rewritten as follows. If we use the fact that  $\widehat{C}$  is self-adjoint, the condition  $\widehat{C}^\dagger = \widehat{C}$ , when applied to (5.112) implies

$$C_1 = \frac{1}{2} \frac{\partial^2 C_0}{\partial q^j \partial p_j}. \quad (5.117)$$

Using (5.117), and writing  $a(q) := e^{S_1(q)}$ , Eq. (5.116) can be written as a derivative of the function  $a$  along the vector field

$$X := \frac{\partial C_0}{\partial p_j} \Big|_{p=\partial_q S_0} \frac{\partial}{\partial q^j} \quad (5.118)$$

as

$$X(a) + \frac{1}{2} a \operatorname{div} X = 0. \quad (5.119)$$

The divergence term in (5.119) suggest one to interpret  $a$  and  $\Psi \sim a e^{\frac{i}{\hbar} S_0}$  as half densities on  $\mathbb{R}^n$ . Then (5.119) is just the Lie derivative of  $a$  along  $X$ :

$$\text{Eq. (5.116)} \iff \mathcal{L}_X a = 0. \quad (5.120)$$

These are the equations used in Sec. 5.3.2.

## 5.C Appendix: Exact Amplitude

In Sec.5.3.3 we compared the exact extraction amplitude with the WKB approximation. In this Appendix we recall from [41] the expression that was used in the numerical evaluation of the exact amplitude.

The first step in the calculation is to find the eigenvectors of  $\Theta$ . They are given

by  $|k\pm\rangle$ , with  $k > 0$ , satisfying the eigenvalue equation

$$\Theta|k\pm\rangle = 12\pi Gk^2\hbar^2|k\pm\rangle. \quad (5.121)$$

These vectors are not normalized; the decomposition of the identity reads

$$\mathbf{I} = \int_0^\infty \frac{dk}{2\pi k \sinh(\pi k)} (|k+\rangle\langle k+| + |k-\rangle\langle k-|). \quad (5.122)$$

In terms of the ‘volume basis’  $|4n\ell_o\hbar\rangle$  used in the main body of this paper, the vectors  $|k\pm\rangle$  are given by

$$\langle 4n\ell_o\hbar|k\pm\rangle = \begin{cases} \sqrt{4|n|\pi ik}P_{\pm n}(k) & \pm n \geq 0 \\ 0 & \pm n < 0 \end{cases}, \quad (5.123)$$

where  $P_n(k)$  is the following  $(2n-1)$ -degree polynomial in  $k$ :

$$P_n(k) := \frac{1}{ik(2n)!} \left. \frac{d^{2n}}{ds^{2n}} \right|_{s=0} \left( \frac{1-s}{1+s} \right)^{ik} = \sum_{m=0}^{2n} \frac{1}{m!(2n-m)!} \prod_{l=1}^{2n-1} (ik+m-l). \quad (5.124)$$

We are now ready to present the expression of the extraction amplitude. For this, it is convenient to work in the deparameterized framework. In [41] it was shown that the extraction amplitude in the timeless framework coincides with the transition amplitude of the deparameterized theory:<sup>5</sup>

$$A(\nu_f, \phi_f; \nu_i, \phi_i) = \langle \nu_f | e^{\frac{i}{\hbar} \sqrt{\Theta}(\phi_f - \phi_i)} | \nu_i \rangle. \quad (5.125)$$

Let us take  $\nu_i = 4\ell_o\hbar n_i$  and  $\nu_f = 4\ell_o\hbar n_f$  with  $n_i$  and  $n_f$  positive integers, and define  $t := \sqrt{12\pi G}(\phi_f - \phi_i)$ .

By inserting the complete basis (5.122) in the right hand side of (5.125), we

---

<sup>5</sup>Equality (5.125) holds for the extraction amplitude with a normalization given by  $A_+(\nu_f, \phi_f; \nu_i, \phi_i) = (2 \int d\alpha \langle \nu_f, \phi_f | e^{i\alpha \hat{C}} | p_\phi | \nu_i, \phi_i \rangle)_+$ , and where one further selects the positive  $p_\phi$  part (indicated by the +).

obtain

$$A(\nu_f, \phi_f; \nu_i, \phi_i) = -2\sqrt{n_i n_f} \int_0^\infty \frac{dk}{\sinh(\pi k)} P_{n_f}(k) P_{n_i}(k) k e^{ikt} \quad (5.126)$$

$$= -2\sqrt{n_i n_f} P_{n_f}(-i\partial_t) P_{n_i}(-i\partial_t) \int_0^\infty \frac{dk}{\sinh(\pi k)} k e^{ikt} \quad (5.127)$$

$$= -\frac{\sqrt{n_i n_f}}{\pi^2} P_{n_f}(-i\partial_t) P_{n_i}(-i\partial_t) \psi^{(1)}\left(1/2 - i\frac{t}{2\pi}\right) \quad (5.128)$$

where  $\psi^{(1)}(z) = d \log \Gamma(z)/dz$ , and  $\Gamma(z) = (z-1)!$  is the Gamma function.

This last expression (5.128) was the one used to numerically compute the exact extraction amplitude for the plots in Sec. 5.3.3.

# Bibliography

- [1] WALD, R. (1984) *General Relativity*, University of Chicago Press.
- [2] KOKKOTAS, K. D. and B. SCHMIDT (1999) “Quasi-Normal Modes of Stars and Black Holes,” *Living Reviews in Relativity*, **2**(2).
- [3] PRETORIUS, F. (2007) “Binary Black Hole Coalescence,” 0710.1338.
- [4] CENTRELLA, J., J. G. BAKER, B. J. KELLY, and J. R. VAN METER (2010) “Black-hole binaries, gravitational waves, and numerical relativity,” *Rev. Mod. Phys.*, **82**, pp. 3069–3119.
- [5] ASHTEKAR, A. and B. KRISHNAN (2004) “Isolated and dynamical horizons and their applications,” *Living Rev.Rel.*, **7**, p. 10, gr-qc/0407042.
- [6] BUONANNO, A., G. B. COOK, and F. PRETORIUS (2007) “Inspirals, merger and ring-down of equal-mass black-hole binaries,” *Phys.Rev.*, **D75**, p. 124018, gr-qc/0610122.
- [7] SCHNETTER, E., B. KRISHNAN, and F. BEYER (2006) “Introduction to dynamical horizons in numerical relativity,” *Phys.Rev.*, **D74**, p. 024028, gr-qc/0604015.
- [8] OWEN, R. (2009) “The Final Remnant of Binary Black Hole Mergers: Multipolar Analysis,” *Phys.Rev.*, **D80**, p. 084012, 0907.0280.
- [9] POISSON, E. (2004) *A Relativist’s Toolkit: The Mathematics of Black-Hole Mechanics*, Cambridge University Press.
- [10] KURODA, Y. (1984) “Naked Singularities in the Vaidya Spacetime,” *Prog. Theor. Phys.*, **72**, pp. 63–72.
- [11] BOOTH, I. (2005) “Black hole boundaries,” *Can.J.Phys.*, **83**, pp. 1073–1099, gr-qc/0508107.



- [12] ASHTEKAR, A., J. ENGLE, T. PAWLOWSKI, and C. VAN DEN BROECK (2004) “Multipole moments of isolated horizons,” *Class.Quant.Grav.*, **21**, pp. 2549–2570, [gr-qc/0401114](#).
- [13] BENTIVEGNA, E. (2008) *Ringing in unison: exploring black hole coalescence with quasinormal modes*, Ph.D. thesis, Penn State University.  
URL <https://etda.libraries.psu.edu/paper/8245/>
- [14] JARAMILLO, J., R. MACEDO, P. MOESTA, and L. REZZOLLA (2011) “Towards a cross-correlation approach to strong-field dynamics in Black Hole spacetimes,” *AIP Conf.Proc.*, **1458**, pp. 158–173, [1205.3902](#).
- [15] BOOTH, I. and S. FAIRHURST (2007) “Isolated, slowly evolving, and dynamical trapping horizons: Geometry and mechanics from surface deformations,” *Phys.Rev.*, **D75**, p. 084019, [gr-qc/0610032](#).
- [16] ASHTEKAR, A., C. BEETLE, and J. LEWANDOWSKI (2002) “Geometry of generic isolated horizons,” *Class.Quant.Grav.*, **19**, pp. 1195–1225, [gr-qc/0111067](#).
- [17] ASHTEKAR, A. and B. KRISHNAN (2003) “Dynamical horizons and their properties,” *Phys.Rev.*, **D68**, p. 104030, [gr-qc/0308033](#).
- [18] FABBRI, A. and J. NAVARRO-SALAS (2005) *Modeling Black Hole Evaporation*, Imperial College Press.
- [19] WALD, R. (1994) *Quantum Field Theory in Curved Spacetime and Black Hole Thermodynamics*, Chicago Lectures in Physics, University of Chicago Press.
- [20] ASHTEKAR, A., C. BEETLE, and J. LEWANDOWSKI (2001) “Mechanics of rotating isolated horizons,” *Phys.Rev.*, **D64**, p. 044016, [gr-qc/0103026](#).
- [21] ASHTEKAR, A., J. C. BAEZ, and K. KRASNOV (2000) “Quantum geometry of isolated horizons and black hole entropy,” *Adv.Theor.Math.Phys.*, **4**, pp. 1–94, [gr-qc/0005126](#).
- [22] LEWANDOWSKI, J. and T. PAWLOWSKI (2003) “Extremal isolated horizons: A Local uniqueness theorem,” *Class.Quant.Grav.*, **20**, pp. 587–606, [gr-qc/0208032](#).
- [23] GOURGOULHON, E. (2007) “3+1 formalism and bases of numerical relativity,” [gr-qc/0703035](#).
- [24] OWEN, R., J. BRINK, Y. CHEN, J. D. KAPLAN, G. LOVELACE, ET AL. (2011) “Frame-Dragging Vortexes and Tidal Tendexes Attached to Colliding Black Holes: Visualizing the Curvature of Spacetime,” *Phys.Rev.Lett.*, **106**, p. 151101, [1012.4869](#).

- [25] NICHOLS, D. A., R. OWEN, F. ZHANG, A. ZIMMERMAN, J. BRINK, ET AL. (2011) “Visualizing Spacetime Curvature via Frame-Drag Vortexes and Tidal Tendexes I. General Theory and Weak-Gravity Applications,” *Phys.Rev.*, **D84**, p. 124014, 1108.5486.
- [26] LEWANDOWSKI, J. and T. PAWLOWSKI (2002) “Geometric characterizations of the Kerr isolated horizon,” *Int.J.Mod.Phys.*, **D11**, pp. 739–746, gr-qc/0101008.
- [27] GUNDLACH, C. and J. M. MARTN-GARCA (2007) “Critical Phenomena in Gravitational Collapse,” *Living Reviews in Relativity*, **10**(5).
- [28] PRICE, R. H., G. KHANNA, and S. A. HUGHES (2011) “Systematics of black hole binary inspiral kicks and the slowness approximation,” *Phys.Rev.*, **D83**, p. 124002, 1104.0387.
- [29] BARTNIK, R. and J. ISENBERG (2006) “Spherically symmetric dynamical horizons,” *Class.Quant.Grav.*, **23**, pp. 2559–2570, gr-qc/0512091.
- [30] NAKAHARA, M. (2003) *Geometry, Topology and Physics, Second Edition*, Graduate Student Series in Physics, Taylor & Francis.
- [31] BOJOWALD, M. (2008) “Loop Quantum Cosmology,” *Living Reviews in Relativity*, **11**(4).
- [32] ASHTEKAR, A. and P. SINGH (2011) “Loop Quantum Cosmology: A Status Report,” *Class.Quant.Grav.*, **28**, p. 213001, 1108.0893.
- [33] ASHTEKAR, A. and J. LEWANDOWSKI (2004) “Background independent quantum gravity: a status report,” *Classical and Quantum Gravity*, **21**, p. 53, arXiv:gr-qc/0404018.
- [34] PEREZ, A. (2004) “Introduction to Loop Quantum Gravity and Spin Foams,” gr-qc/0409061.
- [35] ASHTEKAR, A., M. BOJOWALD, and J. LEWANDOWSKI (2003) “Mathematical structure of loop quantum cosmology,” *Adv.Theor.Math.Phys.*, **7**, pp. 233–268, gr-qc/0304074.
- [36] LEWANDOWSKI, J., A. OKOLOW, H. SAHLMANN, and T. THIEMANN (2006) “Uniqueness of diffeomorphism invariant states on holonomy-flux algebras,” *Commun.Math.Phys.*, **267**, pp. 703–733, gr-qc/0504147.
- [37] FLEISCHHACK, C. (2009) “Representations of the Weyl Algebra in Quantum Geometry,” *Communications in Mathematical Physics*, **285**, pp. 67–140, arXiv:math-ph/0407006.

- [38] ASHTEKAR, A., A. CORICHI, and P. SINGH (2008) “Robustness of key features of loop quantum cosmology,” *Phys.Rev.*, **D77**, p. 024046, 0710.3565.
- [39] ASHTEKAR, A., T. PAWLOWSKI, and P. SINGH (2006) “Quantum Nature of the Big Bang: Improved dynamics,” *Phys.Rev.*, **D74**, p. 084003, gr-qc/0607039.
- [40] MAROLF, D. (1995) “Refined algebraic quantization: Systems with a single constraint,” gr-qc/9508015.
- [41] ASHTEKAR, A., M. CAMPIGLIA, and A. HENDERSON (2010) “Casting Loop Quantum Cosmology in the Spin Foam Paradigm,” *Class.Quant.Grav.*, **27**, p. 135020, 1001.5147.
- [42] ——— (2009) “Loop Quantum Cosmology and Spin Foams,” *Phys.Lett.*, **B681**, pp. 347–352, 0909.4221.
- [43] ASHTEKAR, A. (2008) “Loop Quantum Gravity:. Four Recent Advances and a Dozen Frequently Asked Questions,” in *The Eleventh Marcel Grossmann Meeting On Recent Developments in Theoretical and Experimental General Relativity, Gravitation and Relativistic Field Theories* (H. Kleinert, R. T. Jantzen, and R. Ruffini, eds.), pp. 126–147, 0705.2222.
- [44] SIMON, B. (1971) “Topics in Functional Analysis,” in *Mathematics of Contemporary Physics* (R. F. Streater, ed.), Academic Press, London.
- [45] ASHTEKAR, A., S. FAIRHURST, and J. L. WILLIS (2003) “Quantum gravity, shadow states, and quantum mechanics,” *Class.Quant.Grav.*, **20**, pp. 1031–1062, gr-qc/0207106.
- [46] FEYNMAN, R. and A. HIBBS (1965) *Quantum mechanics and path integrals*, International series in pure and applied physics, McGraw-Hill.
- [47] FEYNMAN, R. (1948) “Space-time approach to nonrelativistic quantum mechanics,” *Rev.Mod.Phys.*, **20**, pp. 367–387.
- [48] HARTLE, J. B. and K. V. KUCHAR (1986) “Path integrals in parametrized theories: The free relativistic particle,” *Phys. Rev. D*, **34**, pp. 2323–2331.
- [49] HALLIWELL, J. J. (1988) “Derivation of the Wheeler-DeWitt equation from a path integral for minisuperspace models,” *Phys. Rev. D*, **38**, pp. 2468–2481.
- [50] MAROLF, D. (1996) “Path integrals and instantons in quantum gravity: Minisuperspace models,” *Phys.Rev.*, **D53**, pp. 6979–6990, gr-qc/9602019.

- [51] HENDERSON, A. (2011) *Loop Quantum Cosmology: A Window Into the Path Integral Representation of Quantum Gravity*, Ph.D. thesis, Penn State University.  
URL <https://etda.libraries.psu.edu/paper/12472/>
- [52] REISENBERGER, M. P. and C. ROVELLI (1997) “‘Sum over surfaces’ form of loop quantum gravity,” *Phys.Rev.*, **D56**, pp. 3490–3508, [gr-qc/9612035](#).
- [53] DEWITT, B. S. (1957) “Dynamical theory in curved spaces. 1. A Review of the classical and quantum action principles,” *Rev.Mod.Phys.*, **29**, pp. 377–397.
- [54] GUILLEMIN, V. and S. STERNBERG (1977) *Geometric asymptotics*, Mathematical surveys, American Mathematical Society.
- [55] BATES, S. and A. WEINSTEIN (1997) *Lectures on the Geometry of Quantization*, Berkeley Mathematics Lecture Notes, American Mathematical Society.
- [56] TAVERAS, V. (2008) “Corrections to the Friedmann Equations from LQG for a Universe with a Free Scalar Field,” *Phys.Rev.*, **D78**, p. 064072, [0807.3325](#).
- [57] CORICHI, A., T. VUKASINAC, and J. A. ZAPATA (2007) “Polymer Quantum Mechanics and its Continuum Limit,” *Phys.Rev.*, **D76**, p. 044016, [0704.0007](#).
- [58] KLEINERT, H. (2009) *Path Integrals in Quantum Mechanics, Statistics, Polymer Physics, and Financial Markets*, World Scientific.
- [59] ARFKEN, G. and H. WEBER (2005) *Mathematical Methods for Physicists*, Elsevier.

## Vita

### Miguel Campiglia

Miguel Campiglia was born in Montevideo, Uruguay on April 29, 1982. He obtained his Bachelor's (2004) and Master's (2007) degrees in Physics from Universidad de la República. In 2007 he started his PhD studies at Pennsylvania State University, working under the supervision of professor Abhay Ashtekar. His works include:<sup>6</sup>

1. M. Campiglia, C. Di Bartolo, R. Gambini and J. Pullin, *Uniform discretizations: a new approach for the quantization of totally constrained systems*, Phys. Rev. D **74**, 124012 (2006)
2. M. Campiglia, C. Di Bartolo, R. Gambini and J. Pullin, *Uniform discretizations: A quantization procedure for totally constrained systems including gravity*, J. Phys. Conf. Ser. **67**, 012020 (2007)
3. M. Campiglia, R. Gambini and J. Pullin, *Loop quantization of spherically symmetric midi-superspaces*, Class. Quant. Grav. **24**, 3649 (2007)
4. M. Campiglia, R. Gambini and J. Pullin, *Loop quantization of spherically symmetric midi-superspaces: the interior problem*, AIP Conf. Proc. **977**, 52 (2008)
5. A. Ashtekar, M. Campiglia and A. Henderson, *Loop Quantum Cosmology and Spin Foams*, Phys. Lett. B **681**, 347 (2009)
6. A. Ashtekar, M. Campiglia and A. Henderson, *Casting Loop Quantum Cosmology in the Spin Foam Paradigm*, Class. Quant. Grav. **27**, 135020 (2010)
7. M. Campiglia, A. Henderson and W. Nelson, *Vertex Expansion for the Bianchi I model*, Phys. Rev. D **82**, 064036 (2010)
8. A. Ashtekar, M. Campiglia and A. Henderson, *Path Integrals and the WKB approximation in Loop Quantum Cosmology*, Phys. Rev. D **82**, 124043 (2010). (**Chapter 5**)
9. M. Campiglia, *Polymer representations and geometric quantization*, arXiv:1111.0638
10. A. Ashtekar, M. Campiglia and S. Shah, *Multipole moments of dynamical horizons*, in preparation, based on **Chapter 2**.
11. A. Ashtekar, M. Campiglia and A. Henderson, *Uniqueness of LQC kinematics*, in preparation, based on **Chapter 4**.

---

<sup>6</sup>Works 4 to 11 were realized during my PhD studies at Penn State.